The Thesis Committee for Richard Cain Casteel
Certifies that this is the approved version of the following thesis:

The modern assessment of climate, calcite growth, and the geochemistry of cave drip waters as a precursor to paleoclimate study

APPROVED BY
SUPERVISING COMMITTEE:

Supervisor:

Jay L. Banner

John M. Sharp, Jr.

Terrence M. Quinn

The modern assessment of climate, calcite growth, and the geochemistry of cave drip waters as a precursor to paleoclimate study

by

Richard Cain Casteel B.S., M.A.

Thesis

Presented to the Faculty of the Graduate School of

The University of Texas at Austin

in Partial Fulfillment

of the Requirements

for the Degree of

Master of Science in Geological Sciences

The University of Texas at Austin

August 2011

Acknowledgements

I would like to acknowledge the Jackson School of Geosciences, the Geological Society of America, the National Science Foundation, and the Guadalupe Blanco River Authority for funding and financial support; Jay Banner, Corinne Wong, Weimin Feng, Jud Partin, Jack Sharp, Terry Quinn, Brian Cowan, Larry Mack, Nate Miller, and Eric James for suggestions and assistance with analytical and research questions; all past and current members of Jay Banner ‘s research group for field assistance, especially Ashley Quinn; the staff at Inner Space Cavern and Westcave Preserve for allowing me access to their caves and facilities; and the staff at the Jackson School of Geosciences for administrative support and all around pleasantness. I would like to thank Jay Banner for finding me and bringing me to Austin, TX. His guidance and support has made it possible for me to complete this MS degree.

Abstract

The modern assessment of climate, calcite growth, and the geochemistry of cave drip waters as a precursor to paleoclimate study

Richard Cain Casteel, M.S. Geo. Sci.

The University of Texas at Austin, 2011

Supervisor: Jay L. Banner

The overall goal of this study is to determine the resolution and type of proxy that any one drip site can provide for the determination of past climate. The study examines surface conditions (effective rainfall, temperature, PDSI), cave characteristics (cave geometry, cave air CO2, location), drip site characteristics (drip rate, drip rate response to rainfall), and drip water characteristics (pH, trace element ratios, alkalinity, temperature). The study encompasses two distinctly different caves, Inner Space Cavern (Chapter 2) and Westcave (Chapter 3).

A goal of Chapter 2 is to identify drip sites where there is an intra-annual climate signal, which can assist with high resolution paleo-drought reconstructions when extended to speleothem studies. To be considered an intra-annual climate sensitive drip site, a site should display statistically significant correlations between (1) effective rainfall and drip rate; (2) effective rainfall and Mg/Ca; (3) drip rate and Mg/Ca; (4) Palmer Drought Severity Index (PDSI) and drip rate; and (5) PDSI and Mg/Ca. These relationships can be explained by the extent to which water flux in the karst overburden influences flow path characteristics, water residence time, and water-rock interactions.

The data in Chapter 3 will indicate that (1) variations in trace element/Ca values in cave drip waters are temperature dependent and vary on a seasonal time scale, (2) the

standardization of trace element/Ca values allows for between drip site comparisons, (3) the standardization of trace element/Ca values can add statistical power to statistical analyses by increasing the sample size, (4) calcite growth rates follow a seasonal pattern based on variations in surface temperature, (5) a regional drought indicator provides correlation with trace element/Ca values at some drip sites and this relationship is most likely dependent upon temperature.

Table of Contents

List of Tables

List of Figures

Chapter 1: Introduction to the paleoclimate history and modern day climate of central Texas

This study compares the modern hydrologic system, cave environment, and cave drip trace element/Ca values of two distinct caves in central Texas: Inner Space Cavern (Chapter 2) and Westcave (Chapter 3). The study of modern climate and cave drip waters is an important intermediary that must be understood prior to application to the paleoclimate study of speleothems. The strengths of this study include (1) a rigorous assessment of the climate factors influencing cave drip water trace element/Ca values and (2) statistical methods for the application of drip water trace element/Ca variations to the study of paleoclimate.

1.1 Introduction

The climate of central Texas has undergone rainfall and temperature variations on millennial as well as annual time scales. Mechanisms for these changes include millennial scale variations in the Earth's orbital cycles to variations in annual sea surface temperature. The majority of paleoclimate reconstructions for central Texas rely on data that allow for lower than annual resolution inferences of climate variability (i.e., scales ranging from thousands to hundreds of years). One difficulty of paleoclimate reconstructions for the region is finding proxies that are able to relate climate variability on annual scales. Of importance to this region is the extent to which drought occurs on an annual scale because annual rainfall variability has significant impact on water resources. A more highly resolved regional understanding of past climate variability can: (1) determine the severity of past drought; (2) assist in refining the inputs for climate models and thus enhance their predictive capabilities; (3) help identify the mechanisms that control regional climate change; and (4) help policy makers plan for the future. Prior to a discussion of possible high resolution proxies (speleothems and tree rings) this introduction reviews the existing lower resolution paleoclimate reconstructions for the region.

Several central Texas studies have reconstructed paleoclimate for the last 24,000 yBP (e.g., Toomey et al., 1993). Reconstruction proxies have included floral and faunal fossils, pollen, Sr isotopes, C isotopes, magnetic susceptibility, speleothems, and tree rings. The general trend has been a warming and drying of the climate of central Texas since ~24,000 before present but there have also been higher frequency oscillations of warmer/drier to cooler/wetter conditions. There is general agreement between many of the proxies as far as lower resolution climate trends are concerned (Toomey et al., 1993). A lack of higher resolution proxies (i.e., decadal to annual resolution) leads to inexact temporal matching between proxies and limited knowledge of short term trends in rainfall variation, both of which are important to determining the drought history of central Texas.

1.2 Central Texas Paleoclimate Overview

Several central Texas studies have reconstructed paleoclimate for the last 24,000 before present (e.g., Toomey et al., 1993). Reconstruction proxies have included floral and faunal fossils, pollen, Sr isotopes, C isotopes, magnetic susceptibility, speleothems, and tree rings. The general trend has been a warming and drying of the climate of central Texas since ~24,000 yBP but there have also been higher frequency oscillations of warmer/drier to cooler/wetter conditions. There is general agreement between many of the proxies as far as lower resolution climate trends are concerned (Toomey et al., 1993). A lack of higher resolution proxies (i.e., decadal to annual resolution) leads to inexact temporal matching between proxies and limited knowledge of short term trends in rainfall variation, both of which are important to determining the drought history of central Texas.

1.2.1 24,000 to 14,000 yBP

During the Last Glacial Maximum (LGM), approximately 20,000 to 18,000 years ago, low-latitude glaciers were present in many regions of the world (Porter, 1983). In

North America, the Laurentide and Cordilleran ice sheets covered the northern third of the United States (Porter, 1983). The climate of central Texas at this time is inferred to be cooler with more effective moisture (effective moisture = rainfall-potential evapotranspiration).

In central Texas, the increased rate of calcite growth of cave deposits is associated with the onset of the LGM (Musgrove et al., 2001). Fossil evidence indicates that: (1) large mammals once present in the region are now extinct (Lundelius, 1967; Graham, 1976); (2) animals once living in this region migrated to regions that are cooler and wetter (Toomey et al., 1993); and (3) $^{87}Sr/^{86}Sr$ ratios of fossil Hackberry aragonite and vole/pocket gopher tooth enamel suggest that 20,000 yBP there were thicker soils and this thickness has since decreased (Cooke et al., 2003). Increased calcite growth, larger mammals, and thicker soils are all associated with cooler temperatures and increased moisture availability.

Pollen data from ~15,590 yBP suggest the presence of deciduous woodlands (Bryant, 1977), with trees that grow in cooler summer temperatures (~21° C) in the region (Bryant, 1969, 1977; Camper, 1991). Higher elevations once dominated by woodlands are now inhabited by desert vegetation (Spaulding et al., 1983). $\delta^{13}C$ values of alluvium deposited ca. 15,000 yBP also suggests abundant trees and C3 grasses (40-50%) in the region (Nordt et al., 1994). Magnetic susceptibility (MS) analysis from Hall's Cave, TX indicates the lowest value of the 19,000 years of analysis (Ellwood and Gose, 2006). These factors are all interpreted to indicate a cooler/wetter climate.

1.2.2 14,000 to 10,500 yBP

During this time period it is inferred that temperatures warmed and rainfall decreased as glaciers receded to higher latitudes. The abundant evidence is marked by the disappearance of the masked shrew *(Sorex cinerus/haydeni)* that prefers cooler temperatures and the appearance of the cotton rat, which can live in temperatures of more than 24°C (Hall, 1981). There also appears to be an increase in grass pollen that suggests higher temperatures and less effective moisture that occurred in the glacial period

(Toomey et al., 1993; Bryant, 1977; Hall, 1991, 1992). Alluvium deposited 11,000-8,000 yBP is inferred to be composed of 50-60% of C4 grasses and, thus, represents a shift to drier and warmer conditions (Nordt et al., 1994).

This is not a time period where the shift in effective moisture followed a unidirectional decrease. Instead there appears to be some variation from 14,000 to 10,500 yBP (Toomey et al., 1993). These inferences are marked by: (1) the loss of the bog lemming (*Synaptomys cooperi*; ca. 14,000 yBP) indicating decreased effective moisture (Toomey et al., 1993); (2) the appearance of a drier weather shrew (*Notiosorex crawfordi),* and emigration of a shrew (*Cryptotis parva),* requiring wetter conditions; and (3) then a decrease in the drier weather shrew from 12,500 to 10,500 suggesting alternating drier and wetter time periods (Toomey et al., 1993).

Magnetic susceptibility data describe this as a time period of continued warming and drying (Ellwood and Gose, 2006). Oscillations in the MS data also indicate periods of warming intermingled with periods of cooling. The data imply a slight cooling trend from the warmest period ending the LGM to 10,500 yBP. This coincides with the proposed Younger Dryas event from 12,900-10,700 yBP (Dansgaard et al., 1989).

1.2.3 10,500 to 5000 yBP

The early Holocene continued the warming and drying trend of the previous 4,000 years with a retreat from glacial conditions. This trend is inferred by the loss of vertebrate fauna with a preference for wetter conditions and the emergence of species adapted to drier conditions (Toomey, 1991, 1992). Pollen records also indicate an increase in grass species beginning 10,500 yBP while 8,700-6,000 yBP pollen records indicate a larger abundance of taxa favoring drier conditions near Hinds Cave (Toomey et al., 1993; Bryant and Holloway, 1985). Two sites, Hershop and Boriack Bog, have pollen records which indicate a loss of trees and increase in grasses between 7,000 and 4,500 yBP (Bryant, 1977). Included in this is evidence of a shift of tree populations away from this region and into wetter regions (Bryant and Holloway, 1985).

Sedimentary records suggest "eolian sedimentation" between 6,500-4,500 yBP due to drier conditions (Holliday, 1989) and after 8,000 yBP the rate of deposition of soil in Hall's Cave doubled, clay deposition decreased, and limestone clast deposition increased (Toomey et al., 1993). Vertebrate fossils indicate the disappearance of prairie dogs which need thicker soils in which to reside (Toomey et al., 1993). Additional sedimentary evidence from the Fort Hood alluvium deposited between 8,000-5,000 yBP indicates that C4 grasses comprise 65 to 70% of the fauna, which represents a warming and drying of the climate (Nordt et al., 1994).

Magnetic susceptibility data from this time period indicate a general warming trend with a pronounced, extreme period of warming beginning around 8,400 yBP and peaking at 8200 yBP (Ellwood and Gose, 2006). After this event it appears that temperatures cooled to reflect conditions that were present prior to this warming period. The timing of this cooling event coincides with a decrease in global temperatures termed as the 8.2 ka event (Ellison, 2006). This was followed by a pronounced period of drying that lasted from 8,000 yBP to ca. 5,900 yBP. The data suggest an oscillating cooling and warming from until slightly after 5,000 yBP (Ellwood and Gose, 2006).

1.2.4 5000 to 2500 yBP

Nordt (1994) contends that the drying of the central Texas climate reaches a peak around 5,000 yBP and the time period between 6,000 to 4,000 yBP is the driest of the Holocene. The carbon isotopic composition of the shell of the *Rabdotus alternates* provide evidence that the driest climate occurs at 4,600 yBP and that dry conditions reach a maximum at 3,500 yBP (Goodfriend and Ellis, 2000). A sample from 4,600 yBP has a $\delta^{13}C$ value of -4.7‰. This reflects an abundance of C4 grasses and agrees with other paleoclimate proxies that around 5,000 yBP was the warmest and driest of the Holocene (Goodfriend and Ellis, 2000). In the same locale 4,300 to 4,100 yBP, four samples have an average $\delta^{13}C$ value of -6.5‰ and a range of -6.9 to -6.1‰ (Goodfriend and Ellis, 2000). This represents a cooler/wetter environment than 4,600 yBP and agrees with $\delta^{13}C$ values of stream alluvial and soil in three separate streams in central Texas that point to a

reduction in C4 grasses to approximately 65 to 70% ca. 4,000 yBP (Nordt, 1994). However, warmer/drier conditions appear to return as snail shell (*Rabdotus alternates*) samples dated between 3,600 and 3,100 yBP reveal average $\delta^{13}C$ values of -4.5‰. Magnetic susceptibility data from this time period point towards significant warming events ca. 4,400 yBP, 3,200 yBP, and 2,900 yBP (Ellwood and Gose, 2006). This provides agreement with ^{13}C indicators of a significantly drier climate during this time period.

Lower resolution paleoclimate proxies indicate that between 5,000 and 2,500 yBP was the driest and warmest period of climate in the last 20,000 years. This is evidenced by the regional extinction of taxa requiring large amounts of moisture such as the pipistrelle bat (*Pipistrellus subflavus*) and the woodland vole (*Microtus pinetorum*; Toomey, 1990, 1992). It is also represented at Schulze Cave by the absence or minimum of wet weather shrew (*Cryptotis*) and the abundance of a dry weather shrew (*Notiosorex,*) population ca. 3,800 yBP (Dalquest et al., 1969). Gastropod samples from Bering Sinkhole suggest the driest conditions occurred between ca. 4,000 and 2,700 yBP (Toomey et al., 1993).

1.2.5 2500 to 1000 yBP

Fossil evidence indicates a return to cooler/wetter conditions with the return of the woodland vole and pipistrelle bat to the Hall's cave area as well as a significant increase in the abundance of the least shrew (*Cryptotis,* a wetter condition species) around 2,500 yBP (Toomey et al., 1993). Additionally, pollen records indicate cooler conditions or more moisture through an increase in pine trees and grasses (Bryant and Holloway, 1985) and an increase in oak-woodland in east-central Texas between 2,500-1,500 yBP (Holloway et al., 1987). Increasingly negative average $\delta^{13}C$ values (-6.5‰) of snail shells, dating from 2,700 to 1,500 yBP, suggest that conditions were moving towards cooler/wetter (Goodfriend and Ellis, 2000). These trends indicate a cooler and wetter environment than the dry conditions represented in the previous ~3,500 years.

1.2.6 1000 yBP to present

There appears to be some conflicting evidence as to the climatic conditions during the last 1,500 to 1,000 years. Four main pieces of evidence from surrounding regions (Oklahoma, New Mexico, and Arizona) suggest that drier conditions emerged after 1,000 yBP; (1) the emergence of a dominating shrew fauna (*Notiosorex*) after 1,430 yBP represents a shift to drier conditions that favors the species, (2) a large increase in the amount of bison fossils suggesting a shift to more open grasslands and drier conditions (Huebner, 1991), (3) shift to a snail species that is favored by drier conditions (Oklahoma; Hall, 1988; 1990), (4) and pollen records from surrounding regions that suggest a decrease in large trees and an increase in grasses (Hall, 1985; 1988; 1990). It seems unlikely that this climate pattern did not affect central Texas but the only evidence from this region suggests that conditions during the last 1,000 are cooler/wetter than the previous 1,500 years. By 1,000 yBP $\delta^{13}C$ values of snail shells become more negative (-8.0‰) and thus represent a continued cooler/wetter trend. A live sample of the same snail species obtained from the cave in 1890 has a similar value, which supports the notion that the last 1,000 years are representative of today's climate (Goodfriend and Ellis, 2000). There are little data for central Texas for the last 1,000 years. Were climate conditions similar to the surrounding regions or was there a cooling trend in central Texas? Possible resolution to this issue may reside in using tree rings and/or speleothems as proxies.

1.3 Reconstructed drought variability

The studies discussed above reconstruct climate at lower than annual to decadal resolution and yield little data to determine the occurrence of drought for the region. Drought is a common occurrence in central Texas and is predicted to occur with increased intensity and periodicity as current climate models indicate Texas as a "hot spot" for adverse effects of climate change (IPCC, 2007). Dendrochronology for the region provides annual drought data but only extends to the 16th century. The high resolution tree ring signal indicates decadal droughts periodically occurring at least once per century since the 1500s, with the early 1700s being particularly dry (Stahle and

Cleaveland, 1988; Cleaveland et al., in prep). What remains unknown is the magnitude and frequency of occurrence of droughts prior to the 16th century. It is difficult to determine the periodicity and/or cyclicity of severe droughts with a truncated annual record lasting ~500 years. Therefore, a longer record of the drought history of central Texas is needed to: (1) gain insight into the future of water resources; (2) understand past climate conditions; and (3) help verify the validity of climate model predictions. A possible high resolution extension to the paleoclimate records for the region exists in speleothems (i.e. cave calcite deposits). Speleothems can potentially provide paleoclimate data for tens of thousands of years. One difficulty in deciphering paleoclimate is understanding the relationship between water flux, the karst system, and geochemical variations in cave drip waters. A second difficulty is high resolution dating of speleothems in this region as there is a lack of visible annual banding. These issues can potentially be resolved through assessment of the modern day climate, cave drip waters, and cave atmosphere, which is a goal of this study.

Speleothems have proven to be useful paleoclimate indicators due to their expansive geographic distribution, extensive temporal range (Fairchild et al., 2006), and high preservation potential. Past research using speleothems as paleoclimate proxies has been useful in determining residence time of groundwater and relative changes in rainfall amount (e.g. Banner et al., 1996; Musgrove et al., 2001). Central to the current study, trace element variations can reflect variations in rainfall (Fairchild and Treble, 2009). The present study is taking a systematic approach to selecting speleothems for paleoclimate study. This involves assessing the geochemistry of drip waters at multiple drip sites and comparing it to the modern hydrologic response to climate variations.

1.4 Modern-day Texas climate

The modern day climate of central Texas ranges from subtropical-subhumid to semiarid (Larkin and Bomar, 1983). In terms of temperature and precipitation this amounts to dry, hot summers, wet springs and falls, and dry, mild winters (Larkin and Bomar, 1983). The coldest month is January with an average temperature of 9° C while

the warmest average temperature of 27° C occurs in July and August (Larkin and Bomar, 1983). A pronounced west to east precipitation gradient across the state creates arid conditions in western Texas and wetter conditions towards the east (Figure 1).

The physiological province of south central Texas (the location of the study sites) lies in a zone where average precipitation is between 68 and 104 cm per year (Figure 1; Larkin and Bomar, 1983). The bulk of precipitation occurs in the spring and fall while the lowest amounts of precipitation occur in the winter, July, and August (Larkin and Bomar, 1983). Year to year variability in rainfall is high with intermittent droughts dispersed amongst wetter periods. An important aspect of this region is that potential evapotranspiration (PET) exceeds rainfall for nearly every month of the year and the discrepancy is especially pronounced between May and September (Larkin and Bomar, 1983). This creates a moisture deficit that is exacerbated during periods of below average rainfall. Thus, effective rainfall is an important variable to be considered as a measure of water flux.

The most likely and most devastating extreme weather event to impact central Texas is drought. Summer drought is more likely to occur in the region when "subtropical high pressure cells in the upper atmosphere" are formed over the Southern States (USGS WSP, 1801-1804). This acts to inhibit moist air flowing from the Gulf of Mexico and encourages hotter, drier air to flow from the southwestern United States (USGS WSP, 1801-1804). Drought during the winter and fall are associated with high pressure cells above the Great Basin in the western US (USGS WSP, 1801-1804). This acts to spread dry air from the interior of the US to other regions, including Texas (USGS WSP, 1801-1804).

Drought occurrence. In central Texas serious drought has been present at least once every decade of the 20th century (Riggio et al., 1987). The instrumental record indicates that the most severe deficit in precipitation occurred during the drought of record in the 1950s (1950-1956). Towards the end of this drought in 1956, 96% of the counties (244 out of 254) in Texas were considered disaster areas by the federal government (Hatfield, 1964). This was also a time where temperatures increased, thus

increasing PET and magnifying the effect of decreased precipitation. It is important for water planners as well as citizens to understand that the drought of the 1950s is most likely not an aberration and can return. This was brought into the forefront of many individual's minds as the region has experienced extreme drought conditions from 2008-2009 (Figure 2). However, this is easily forgotten as the region also experiences abnormally wet periods that ease the ill effects of drought (Figure 3).

1.5 Summary

Paleoclimate proxies for central Texas indicate a general trend of warming and drying since the Last Glacial Maximum. The majority of data are of lower than annual resolution and do not reflect variations in rainfall. Instrumental records extend to the late 19th century and do not allow for determination of trends or long term cycles in precipitation. To determine drought periodicity, it is important to find adequate paleoclimate proxies that extend the record of rainfall for central Texas. There are tree ring data for the region that provides annual resolution; although the extent of the data only reaches the mid 16th century (Stahle and Cleaveland, 1988; Cleaveland et al., in prep). Thus, there is a need for paleoclimate proxies that extend back in time and are of annual resolution. Speleothems can provide insight into the climate history of central Texas. An assessment of variations in the modern climate system and the subsequent variations in cave drip waters is needed: (1) as cave drip waters are an intermediary between climate and speleothems; (2) to determine the resolution trace element proxies can provide; and (3) selectively and conservatively sample speleothems for climate reconstructions.

This study takes a conservative approach to sampling stalagmites for paleoclimate research. It does so by sampling cave drip waters above actively growing stalagmites and comparing the cave drip waters to modern day surface conditions (air temperature, effective rainfall, PDSI). This approach allows for one to gain an understanding of the climate resolution for which each drip site represents. For example, some of the sites display intra-annual variability in drip water trace element/Ca values and others display

longer term variability. The knowledge of the modern geochemical response allows for the selective sampling of stalagmites by allowing a priori assessment of the best speleothem candidate for paleoclimate study.

The overall goal of this study is to determine the resolution and type of proxy that any one drip site can provide for the determination of past climate. The study examines surface conditions (effective rainfall, temperature, PDSI), cave characteristics (cave geometry, cave air CO2, location), drip site characteristics (drip rate, drip rate response to rainfall), and drip water characteristics (pH, trace element ratios, alkalinity, temperature). The study encompasses two distinctly different caves, Inner Space Cavern (Chapter 2) and Westcave (Chapter 3). Inner Space Cavern is a larger, deeper, seasonally ventilated cave, whereas Westcave is smaller, shallower, and maintains near atmospheric conditions year round. The results indicate that there are distinct controls over trace element/Ca values and calcite growth in each cave.

A goal of Chapter 2 is to identify drip sites where there is an intra-annual climate signal, which can assist with high resolution paleo-drought reconstructions when extended to speleothem studies. To be considered an intra-annual climate sensitive drip site, a site should display statistically significant correlations between (1) effective rainfall and drip rate; (2) effective rainfall and Mg/Ca; (3) drip rate and Mg/Ca; (4) Palmer Drought Severity Index (PDSI) and drip rate; and (5) PDSI and Mg/Ca. These relationships can be explained by the extent to which water flux in the karst overburden influences flow path characteristics, water residence time, and water-rock interactions. Each drip site is subject to variations in the proportion of conduit and diffuse flowpaths, thus multiple drip sites should be studied in order to determine the most appropriate site for later paleoclimate study.

Chapter 3 takes a systematic approach to selecting drip sites with actively growing speleothems for paleoclimate study. This involves assessing the geochemistry of cave drip waters at multiple drip sites and comparing it to the modern hydrologic response to climate variations. The data in Chapter 3 indicate that (1) variations in trace element/Ca values in cave drip waters are temperature dependent and vary on a seasonal

time scale, (2) the standardization of trace element/Ca values allows for between drip site comparisons, (3) the standardization of trace element/Ca values can add statistical power to statistical analyses by increasing the sample size, (4) calcite growth rates follow a seasonal pattern based on variations in surface temperature, (5) a regional drought indicator provides correlation with trace element/Ca values at some drip sites and this relationship is most likely dependent upon temperature.

Chapter 2: The assessment of modern-day drought variability using Mg/Ca values of cave drip waters as a precursor to paleoclimate study

2.0 Abstract

Drought is a common occurrence in central Texas. The highest resolution records of past droughts for the region are reconstructed from tree-ring studies, which extend back to the 1400's. Speleothems offer a potential extension to the regional paleoclimate record. To maximize the applicability of speleothem proxies in this region, this study monitored cave air, drip rates, calcite growth, and drip water geochemical composition at Inner Space Cavern in central Texas. These data allow assessment of the degree of correspondence between surface conditions, cave atmospheric and hydrologic variability, and cave drip water geochemistry. The drip sites were divided into two groups based on the resolution of climate data that can potentially be procured from each site.

Group 1 drip sites (n = 2) reflect an intra-annual climate signal in that they exhibit: (i) positive correlations between effective rainfall and drip rates, (ii) negative correlations between drip rates and drip water Mg/Ca values, (iii) negative correlations between effective rainfall and Mg/Ca values, and (iv) negative correlations between the Palmer Drought Severity Index (PDSI) and Mg/Ca values. These correlations are clearest when applying a standardization approach to comparing different drip sites with climate variables such as the PDSI. Group 2 drip sites (n = 6) do not display a clear intra-annual climate signal, possibly due to: (i) flowpath type that constrains the variability of Mg/Ca values and/or (ii) seasonal cave air CO_2 variations that alter drip water geochemistry due to prior calcite precipitation. A lower resolution climate signal can be gained from Group 2 sites as more extended droughts and/or longer-term fluctuations in Mg/Ca values may be detectable. This highlights the importance of targeting multiple drip sites for paleoclimate application as only a certain percentage of sites will yield an intra-annual climate signal. Also important to studying the modern system is the *a priori* assessment of cave drip water geochemistry, which can strengthen the validity of the inferred paleoclimate from a corresponding speleothem.

2.1 Introduction

The climate of central Texas has undergone precipitation and temperature changes on millennial as well as annual time scales (Banner et al., 2010). Mechanisms for these changes have ranged from Milankovitch cycles to annual sea surface temperatures. On a shorter time

scale, intermittent and perhaps unpredictable periods of drought are a cause for concern for policy makers as water resources are limited in this region. In order to plan for future needs, a more accurate and extensive climate history for central Texas is required. A possible climate proxy exists in cave calcite deposits (speleothems).

Speleothems have proven to be useful paleoclimate indicators due to their expansive geographic distribution, extensive temporal range (Fairchild et al., 2006), and high preservation potential. Past research using speleothems as paleoclimate proxies has been useful in determining residence time of groundwater and relative changes in rainfall amount (e.g. Banner et al., 1996; Musgrove et al., 2001). Central to the current study, trace element variations can reflect variations in rainfall (Fairchild and Treble, 2009). The present study is taking a systematic approach to selecting speleothems for paleoclimate study. This involves assessing the geochemistry of drip waters at multiple drip sites and comparing it to the modern hydrologic response to climate variations. Without assessing the modern system there is no information to the correspondence between the modern climate system and speleothems, which can lead to erroneous paleoclimate interpretations as speleothem geochemistry is not a 1 to 1 relationship with surface climate. Furthermore, drip waters are an important intermediary between surface conditions and what is recorded in a speleothem. Understanding the modern response of drip waters to surface conditions allows for climate trends to be more readily detected in a speleothem. The study offers the opportunity to determine the difference in geochemical signal from drip waters collected during a period of drought and drip waters collected as conditions become wetter. It also offers a unique opportunity for high

frequency sampling to assess the impact of a large scale rain event (Tropical Storm Hermine from 9/7/10 to 9/8/10) on the cave system flow path and geochemical response.

Previous studies at the current study site, Inner Space Cavern, have established a broad knowledge base of the controls on drip water geochemistry. In twelve years of monitoring cave atmosphere and drip water several key results have emerged: (1) seasonal CO_2 fluctuations influence calcite growth (Banner et al., 2007) and drip water geochemistry (Guilfoyle, 2006); (2) at drip sites where drip rate variations are related to effective rainfall (effective rainfall = rainfall – potential evapotranspiration) variations, $^{87}Sr/^{86}Sr$ in cave drip water acts as a tracer for effective rainfall variations (Pierson, 2005; Duran, 2010); (3) carbon and oxygen isotopes appear to be influenced by non-equilibrium processes during calcite precipitation (Guilfoyle, 2006; Feng et al., in prep); and in (4) drip water $\delta^{18}O$ values for all sites studied to date appear to be derived from a well mixed reservoir in the vadose zone and are similar to the mean annual rainfall $\delta^{18}O$ value for the region (Pape et al., 2010). This study is an extension of the time series analysis of drip sites ISST and ISLM from Guilfoyle (2006) and establishes six new drip sites.

A goal of the study is to identify drip sites where there is an intra-annual climate signal, which can assist with high resolution paleo-drought reconstructions when extended to speleothem studies. To be considered an intra-annual climate sensitive drip site, a site should display statistically significant correlations between: (1) effective rainfall and drip rate; (2) effective rainfall and Mg/Ca; (3) drip rate and Mg/Ca; (4) Palmer Drought Severity Index (PDSI) and drip rate; and (5) PDSI and Mg/Ca. These relationships can be explained by the extent to which water flux in the karst overburden influences flow path characteristics, water residence time, and water-rock interactions. Each drip site is subject to spatial and temporal variations in the proportion of fracture and diffuse flowpaths (as defined by Halihan et al., 2000), thus multiple drip sites should be studied to determine appropriate sites for subsequent paleoclimate study. In this respect, the majority of drip sites chosen for the study have actively growing stalagmites.

Furthermore, this study highlights the importance of understanding and assessing the modern system prior to analyzing the geochemistry of a stalagmite.

Water flux and air temperature are two overarching controls on the processes in the cave environment that determine the extent to which we can decode past climate change (e.g., Banner et al., 2007; Fairchild and Treble, 2009). Air temperature acts to control cave air CO_2 ventilation and thus calcite deposition at Inner Space Cavern (Banner et al., 2007). In warmer months, less dense surface air will not exchange as readily with the cooler, denser cave air. This decreases the ventilation of cave air CO_2 and allows for an increase in cave air CO_2. In cooler months, the denser surface air exchanges more readily with the less dense cave air and ventilation of cave air CO_2 occurs. Water flux is related to rainfall variability, flow path characteristics, and drip rate response to varying surface moisture conditions. At some drip sites (Group 1) in Inner Space Cavern water flux parameters (effective rainfall, PDSI, and drip rate) can be traced through Mg/Ca variations and linked to intra-annual surface climate changes. At other sites (Group 2) it appears that Mg/Ca values vary on a longer time scale.

During times of lower rainfall (i.e., drought) larger, fracture flow routes are more likely to be exhausted and a larger proportion of water will enter cave drip sites through matrix flow; which draws from a reservoir of water stored in the subsurface for a longer period of time (e.g., Fairchild and Treble, 2009). During periods of higher rainfall, infiltrating water will preferentially flow through fracture flow routes. Thus, at sites where there is a larger influence of fracture flow, vadose water will more quickly reach a drip site and produce an increase in drip rate. A schematic of the karst system and flow path response to variation in rainfall can be found in Figure 4. The degree to which any drip site is subject to drip rate variations has implications for water residence time above the cave, the extent of water-rock interaction, Mg/Ca variations in the drip water, and thus the extent to which a drip site will yield an intra-annual climate signal. It is expected that at sites where variations in drip rate are positively correlated with rainfall variability there will be negative correlations with Mg/Ca values.

It has been widely documented, on a variety of time scales in both laboratory experiments and the natural environment, that varying residence times of water in a karst setting alter Mg/Ca ratios of water (Plummer, 1977; Roberts, 1998; Fairchild and Treble, 2009). Two distinct mechanisms, changing water residence time and prior calcite precipitation (PCP), act to produce variations in the Mg/Ca values of cave drip waters (Fairchild and Treble, 2009; Wong et al., 2011). The exchange reaction distribution coefficient of Mg ($K_D < 1$) is also important as it dictates the ratio of Mg to Ca that is dissolved or precipitated as water infiltrates to the drip site (Banner and Hanson, 1990; Fairchild and Treble, 2009). Water residence time influences the extent of water-rock interaction with longer residence times increasing Mg/Ca ratios and shorter residence times decreasing Mg/Ca ratios. PCP can also be influenced by water residence times, the amount of air versus water in pore spaces, and the type of flowpath water takes prior to drip.

Both mechanisms result in variations in the calcite dissolution/precipitation process that is partly driven by CO_2 degassing. During times of lower rainfall, water drains from vadose zone pore spaces and allows for more air to enter the pore spaces. This allows for CO_2 to degas more readily and calcite to precipitate from the infiltrating drip water (Fairchild and Treble, 2009). The exchange reaction distribution coefficient of Mg is less than 1, meaning that it will prefer the aqueous phase relative to Ca. Thus, as drier conditions and calcite precipitation persist, cave drip water decreases in Ca relative to an increase in Mg. A second process relates to the proportion of younger, fracture flow water versus the proportion of more evolved matrix water reaching a drip site (Fairchild and Treble, 2009). During drier time periods, as fractures dry, a higher proportion of more evolved matrix water can dominate the drip water geochemical signal and lead to higher Mg/Ca values.

During periods of higher rainfall there is less calcite precipitation as vadose zone pore spaces are more likely to be fluid filled and have less of an opportunity for CO_2 degassing. Additionally, the residence time during periods of higher rainfall is shorter, which allows for water to reach the drip site faster (at more fracture dominated sites) and

decreases the amount of time for the processes of calcite dissolution/precipitation to be influenced by K_D values of carbonate species. This can be applied to determining the extent to which variations in rainfall will be reflected as geochemical variations in cave drip waters. This is useful in paleoclimate study in that during times of lower rainfall residence time will increase when compared to periods of higher rainfall. However, there is not a direct relationship between rainfall amount and residence time of water above a cave. Each drip site is subject to different flow path regimes, which range from completely fracture dominated to completely diffuse dominated. Flowpaths can also vary temporally; however, the magnitude of this variation acts on a timescale of hundreds to thousands of years and is not of concern for a short term project such as this study. A goal of this study is to determine appropriate characteristics of drip sites for which to use Mg/Ca ratios as inter-annual paleoclimate proxies. This will also enable the characterization of less responsive drip sites that are potential lower temporal resolution paleoclimate proxies.

2.1.2 Sampling of multiple drip sites

Due to the complexities of the karst system the proximity of one drip site to the next is not a determining factor in the correspondence of the between site drip water geochemistry (Baldini, 2006). The present study is unique in that it employs a relatively simple statistical methodology of standardizing Mg/Ca values to each drip site's mean Mg/Ca value. This allows Mg/ Ca values to be equated on similar scales in order to compare multiple drip sites to each other and to water flux parameters. This can statistically strengthen paleoclimate interpretations by increasing the number of samples that can be compared to each other. Some drip sites will be suitable for longer-term climate analysis whereas others may reflect intra- annual variability. Thus the intensive and long-term sampling of multiple drip sites will allow for a better assessment of the modern system. Once the modern system is understood it can be applied to assess paleoclimate. This study systematically assesses the relationship of the modern climate system and modern drip waters as a precursor for paleoclimate analysis using stalagmites

and allows for the determination of the drip rate characteristics (i.e., maximum drip rate, drip rate variability) that would be expected to yield climate information on a variety of timescales. This knowledge can be applied to other drip sites in the cave and/or other caves in the region.

2.1.3 Drought measurement: Palmer Drought Severity Index.

The Palmer Drought Severity Index (PDSI) was developed as a measure of the moisture deviation from "normal" (Palmer, 1965). To assess the severity of drought the index calculates a weighted average of temperature, rainfall, and soil moisture for the current and preceding 12 months to determine the dryness of the system. The scale ranges from extremely moist (+4 or above) to extreme drought (-4 or below) with divisions for severe wet/dry (+/-3-3.99), moderate wet/dry (+/-2-2.99), and mid-range wet/dry (1.99 to -1.99). The PDSI is a widely accepted drought measure as it provides: (1) a measure of abnormal weather; (2) allows for comparison of current and historic conditions; and (3) gives a regional perspective of drought (Alley 1984). It is frequently used in tree ring studies to reconstruct climate and appears to provide a measurement of regional drought conditions as it correlates very well with historic rainfall records (Stahle and Cleaveland, 1988). PDSI appears to be a more robust indicator of water flux versus effective rainfall as it factors in antecedent moisture conditions from previous months (temperature, rainfall, soil moisture), whereas effective rainfall is a measure more rooted in current, daily conditions.

2.2 Hydrogeologic setting

Inner Space Cavern is located on the eastern edge of the Edwards Plateau in central Texas, approximately 42 km north of Austin, TX (Figure 5). The Edwards Plateau is composed of Cretaceous carbonates, and subsequent uplift led to the development of this karst region composed of numerous caves (Banner et al., 2007). The soils above Inner Space Cavern are thin (5 to 90 cm) and consist of Crawford stony clay and Denton stony clay (Godfrey et al., 1973). Detailed descriptions of the soils, geology,

and hydrogeology of the region can be found in Kastning (1983), Veni (1994), Musgrove (2000), and Guilfoyle (2006).

Inner Space Cavern was formed in the Edwards Limestone (Figure 5) and reaches a maximum depth of ~25 meters with the majority of the cave residing ~13-20 meters below the surface (Kastning, 1983). The length of the cave is 4600 meters with an internal relief of 25 meters (Kastning, 1983). The overburden is primarily composed of limestone with the occasional local unit of dolomite (Kastning, 1983).

Ventilation of cave air is a significant control on the precipitation of calcite at Inner Space Cavern. In the cooler months, cave air CO_2 is lower as a result of a temperature/density gradient between the cooler/denser surface air and the warmer/less dense cave air. This allows for ventilation of the cave air as it exchanges with the surface air. Thus, as the higher CO_2 drip waters enter the cave atmosphere they degas to reach equilibrium with the cave air and deposit calcite. As the temperature gradient between the surface air and the cave air becomes less pronounced and reverses during the warmer months the degassed CO_2 builds up in the cave atmosphere. Over time the cave air CO_2 reaches high enough concentrations to inhibit drip water CO_2 degassing and calcite precipitation. Regionally, in the majority of the caves studied (Banner et al., 2007; Wong, 2008; Cowan, 2010) , cave air temperature varies by less than 5° C while average surface air temperature varies seasonally by ~25° C. This process has been well documented at the current study location by Banner et al. (2007).

The modern day climate of central Texas ranges from subtropical-subhumid to semiarid (Larkin and Bomar, 1983). In terms of temperature and precipitation this amounts to dry, hot summers, wet springs and falls, and dry, mild winters (Larkin and Bomar, 1983). The physiological province south central Texas (the location of the study sites) lies in a zone where average precipitation is between 68 and 104 cm per year (Larkin and Bomar, 1983). The bulk of precipitation occurs in the spring and fall while the lowest amounts of precipitation occur in the winter, July, and August (Larkin and Bomar, 1983). Interannual variability in rainfall is high with intermittent droughts dispersed amongst wetter periods. An important aspect of this region is that potential

evapotranspiration (PET) exceeds rainfall for nearly every month of the year and the discrepancy is especially pronounced between May and September (Larkin and Bomar, 1983). This creates a moisture deficit that is exacerbated during periods of below average rainfall.

In central Texas serious drought has been present at least once every decade of the 20th century (Riggio et al., 1987). The instrumental record indicates that the most severe deficit in precipitation occurred during the drought of record in the 1950s (1950-1956). Towards the end of this drought in 1956, 96% of the counties (244 out of 254) in Texas were considered disaster areas by the federal government (Hatfield, 1964). Dendrochronology for the region suggests that severe drought occurs at least once a century and there have been longer drier periods, or megadroughts, in the past compared with what is reflected in the instrumental record (Stahle and Cleaveland, 1988; Cleaveland et al., in prep.).

2.3 Methods

For this study eight drip sites were monitored on approximately monthly time intervals. Drip site locations and descriptions are given in Appendix A. Data analysis for two sites encompasses the time period from 5/4/00 to 9/26/10. For one site data collection began in January of 2007, while the remainder of the sites were sampled beginning in February 2009. All data collection for this project ended in September 2010. Sampling included measurement of cave air parameters, cave water drip rates, collection of drip water, and collection of calcite on glass substrates. Field data collection methods and sample preparation methods mimic those developed over a 12-year period of cave monitoring (Musgrove and Banner, 2004; Guilfoyle, 2006; Banner et al., 2007; Wong, 2008; Wong et al., 2011) and closely follow the methods outlined in Wong (2008).

Surface and cave air relative humidity, CO_2 concentration, and temperature were recorded for each sampling trip. Surface measurements were taken at the onset of each trip while cave air measurements occurred at each drip site. Relative humidity was measured using a Digital Psychrometer (+/- 5% error above 90%). Cave air CO_2 was

measured using a TelAire 7001 meter (+/- 5% error). The CO_2 meter was calibrated using a nitrogen gas source with 0 ppm CO_2.

At each drip site a one liter polypropylene bottle was placed to collect water. Time intervals for collection ranged from 10 minutes to 4-5 hours depending on the drip rate. Ideally, ~150 ml of water was needed to completely fill smaller sample bottles designated for analysis for Sr isotopes, cations, anions, oxygen isotopes, hydrogen isotopes, alkalinity, field pH, and field conductivity. Each sample bottle was wrapped with Parafilm. Sr isotope and cation samples were acidified in the laboratory with 2% HNO_3 to prevent plating of calcite on the collection bottle walls. Anion, oxygen isotope, and hydrogen isotope samples were kept refrigerated until analysis. Conductivity, pH, and water temperature were measured using a Myron L Company Ultrameter II in the field. Alkalinity samples were analyzed less than 24 hours after collection to limit any effects associated with degassing. Replicate alkalinity samples reveal an average percent difference of 1.2% (n = 12). Alkalinity pairs (n = 4) measured (1) in cave by hand show an average percent difference of 4.9% versus those analyzed (2) less than 24 hours later by an autotirator. Replicate alkalinity samples analyzed (1) less than 24 hours after collection versus those analyzed (2) 48 hours after collection show an average difference of 3.8% (n = 3), where alkalinity decreases with increased time from collection.

Cation analyses were performed at The University of Texas at Austin using an Agilent 7500ce quadruple ICP-MS in the Department of Geological Sciences. Samples were diluted 10:1 with 2% HNO_3 prior to analysis. NIST 1643e was used as an external standard (measured 3 times throughout each run) and reveals an accuracy of 3.8% for Ca, 2.8% for Mg, 2.9% for Sr, 6.1% for Ba, 3.8% for Na, and 2.5% for K. This accuracy was determined by measuring the NIST 1643e standard and comparing the measurement difference to the known value. Each unknown sample was measured three times during a run (i.e., duplicate analyses) and the relative standard deviation between measurements reveals an analytical precision of 1.7% for Ca, 1.0% for Mg, 1.4% for Sr, 3.4% for Ba, 1.8% for Na, and 3.8% for K. Replicate analyses (i.e., splits of the same water sample followed by dilution) on 15 unknown samples reveal an average percent difference

between a sample and its replicate of 2.9% for Ca, 4.4% for Mg, 2.9% for Sr, 5.2% for Ba, 3.3% for Na, and 4.1% for K, 3.2% for Mg/Ca, 3.1% for Sr/Ca, and 4.2% for Ba/Ca. Field blanks for Ca, Mg, Sr, Ba, Na, and K are below the detection limit of 1.9, 0.80, 0.01, 0.01, 0.65, and 1.9 ppb, respectively.

Anion analyses were performed at the Bureau of Economic Geology Pickle Research Center at The University of Texas at Austin using a Dionex Ion Chromotography System-2000. The RSD for eight internal standards are as follows: F = 7%, Cl = 2%, Br = 8%, NO_2 = 4%, NO_3 = 4%, SO_4 = 4%, and PO_4 = 9%. The RSD values are calculated by dividing the standard deviation of internal anion instrument standards (1-10 ppm), measured eight times throughout the run, by the average of the standard measurements. Three unknown replicates reveal an average percent difference as follows: F = 0.56%, Cl = 0.62%, Br = 0.57%, NO_2 = 0.51%, NO_3 = 0.51%, SO_4 = 0.59%, and PO_4 = below detection limit. Spike recovery for the anions is as follows: F = 106%, Cl = 100%, Br = 98%, NO_2 = 99%, NO_3 = 92%, SO_4 = 99%, and PO_4 = 94%. Charge balances were performed on 26 samples. Twenty five samples had a charge balance that ranged from -1.28% to 5.1% while one sample had a charge balance of 6.3% (sample ISSR 3 from 7/17/09).

Calcite was collected by placing 10 x 10 cm glass plates under each drip site and collecting them during the subsequent cave trip. Prior to deployment, the glass plates were sanded on one side to increase nucleation sites for calcite growth. In order to measure monthly calcite growth (expressed in units of mg/day), plates were weighed prior to deployment and after collection. A standard plate was repeatedly weighed and reveals a standard deviation of 0.0002 g. This approach follows the methods described in Banner et al. (2007).

2.4 RESULTS

All data are compiled in Appendix B2. These data include effective rainfall, PDSI values, drip rate, pH, alkalinity, Ca, Mg, Sr, Ba, N, K, anions, charge balances,

cave air CO_2, cave air temperature, calcite growth. This results section highlights the most pertinent data for the study.

Vadose drip waters at Inner Space Cavern plot as Ca-HCO_3 waters on a Stiff diagram. Conductivity ranges from 390 to 630 µS (mean = 460 µS) while pH ranges from 7.0 to 8.5 (mean = 7.9) and of HCO_3 ranges from 200 to 325 ppm. Ca values (n = 261) range from 58.8 to 140 ppm (mean = 85.0 ppm), Mg values (n = 261) range from 3.6 to 14.1 ppm (mean = 5.9 ppm), Sr values (n = 261) range from 0.07 to 0.16 ppm (mean = 0.11 ppm), Ba values (n = 261) range from 0.015 to 0.062 ppm (mean = 0.024 ppm), Na values range from 2.77 to 8.23 ppm (mean = 4.5 ppm), and K values range from 0.85 to 2.46 ppm (mean = 1.1 ppm). The Mg, Ca, Sr, Ba, Na, K, Mg/Ca, Sr/Ca, and Ba/Ca values fall within the range of drip waters from previous study of Inner Space Cavern and are similar to the values of another regional cave, Natural Bridge Caverns (Musgrove and Banner, 2004; Guilfoyle, 2006; Wong et al., 2011). The drip water Mg/Ca and Sr/Ca values are more similar to measured soil values above the cave than to limestone values (Musgrove and Banner, 2004).

2.4.1 Rainfall and Palmer Drought Severity Index

Rainfall data were procured from www.weatherunderground.com from a NOAA station located at Lake Georgetown, which is 10.8 km from the cave. Effective rainfall was calculated using the monthly totals from the nearest NOAA weather station at Lake Georgetown. Rainfall for the study period of 2007-2010 ranged from abnormally wet conditions in 2007 to drought conditions from 2008 to September of 2009. The average yearly rainfall for the region is 85.6 cm (1895-2010) and the average for the study period was 70.4 cm. The highest single day rainfall during the study period occurred on 9/8/10 as a result of tropical storm Hermine and was 13.5 cm. The highest monthly total was 25 cm for the month of July in 2007. The driest months were July of 2009 and August of 2010 when the site received no rainfall (Figure 6).

The Palmer Drought Severity Index for a given month uses a weighted average of temperature, precipitation, and soil moisture conditions over the previous 12 months,

with the most recent months more heavily weighted. The most positive PDSI value was 6.54 and occurred in August 2007 and the most negative value of -6.51 occurred in August 2009. The PDSI indicates that drought occurred in the region from May 2008 to August 2009 and PDSI values during this time ranged from -6.51 to -2.42 (Figure 6).

2.4.2 Drip rate, Mg/Ca, effective rainfall, and PDSI relationships

Drip sites were grouped according to the extent to which a given site's physical and geochemical characteristics provide an intra-annual climate signal. Group 1 drip sites display a clear intra-annual climate signal, which is evident through significant correlations ($p < 0.05$) between effective rainfall/PDSI and drip rate as well as effective rainfall/PDSI and Mg/Ca values (Table 1). Group 2 drip sites have a less clear intra-annual climate signal (Table 2) and have the potential to reflect climate signals at a greater than intra- annual resolution.

Group 1 drip sites ($n = 2$) display statistically significant correlations between (1) effective rainfall and drip rate; (2) effective rainfall and Mg/Ca; (3) drip rate and Mg/Ca; (4) PDSI and drip rate; and (5) PDSI and Mg/Ca (Table 1). Group 1 have the highest maximum drip rate; 0.29 – 0.51 ml/sec, which distinguishes them from the lower maximum drip rate of Group 2 drip sites; 0.007 – 0.06 ml/sec (Figure 7).

The relationship between water flux and Sr/Ca is less clear. Sr/Ca does not correlate with water flux at ISSR 3 and it correlates with only PDSI at ISSR 5. Furthermore, Mg/Ca and Sr/Ca do not correlate at ISSR 5 and have a significant inverse correlation at ISSR 3. This is in contrast to the expected positive correlation between Mg/Ca and Sr/Ca at Group 1 drip sites. It is possible that $^{87}Sr/^{86}Sr$ analyses of drip waters can provide insight into the vadose zone processes contributing to the differences between Mg/Ca and Sr/Ca (Wong et al., 2011). A table of correlations between Mg/Ca and Sr/Ca and water flux is located in Appendix B2.

The relationship between water flux and Ba/Ca is also not as clear as the relationship between Mg/Ca and water flux. Ba/Ca does not correlate with water flux at ISSR 3 and it correlates with drip rate and PDSI at ISSR 5. Furthermore, Mg/Ca and

Ba/Ca as well as Sr/Ca and Ba/Ca do not correlate at ISSR 3 but they are significantly correlated at ISSR 5. It is expected that Sr/Ca and Ba/Ca will be correlated; however, this is only true at one of two Group 1 drip sites. A table of correlations between Ba/Ca, Sr/Ca, Mg/Ca and water flux is located in Appendix B2.

At Group 1 drip sites the relationship between water flux and K and Na is less clear than it is with Mg/Ca values. Na correlates with drip rate, effective rainfall, and PDSI at ISSR 3 while K significantly correlates with only PDSI. At site ISSR 5 Na and K correlate with only drip rate. A table of correlations can be found in Appendix B2.

Assessing correspondence of Mg/Ca values and PDSI. The low regression coefficient between Mg/Ca and PDSI was interpreted to be a consequence of Mg/Ca varying on a higher frequency scale than PDSI. Therefore, it is necessary to assess the correspondence of Mg/Ca and PDSI on similar frequency scales. Thus, for specific time periods, average values of PDSI and the corresponding average Mg/Ca values were calculated and compared (Figures 8a-b). These averages were based on time periods when PDSI was wetter than normal (+2 and above), near normal but positive (between 0 and 2), near normal but negative (between 0 and -2) and drier than normal (-2 and below). On these time scales the two variables have a much higher correlation, with PDSI significantly correlating with Mg/Ca at ISSR 3 ($r^2 = 0.81$, $p < 0.01$). A limited temporal extent of data prevents similar analyses at ISSR 5.

Between site comparison of Mg/Ca and PDSI. In order to make between-site comparisons at Group 1 drip sites, the average Mg/Ca and average PDSI values were standardized to each drip site's mean. The results indicate that there is a significant correlation between standardized Mg/Ca values and standardized PDSI values when all Group 1 sites are compared ($r^2 = 0.71$; $p < 0.01$; Figure 8b).

Group 2 drip sites (n = 6) have a less clear intra-annual climate signal in that there are no significant correlations between effective rainfall and drip rate. Additionally, the correlations between effective rainfall and Mg/Ca, PDSI and drip rate, and PDSI and Mg/Ca are inconsistent across the sites (Table 2; Figure 6). Group 2 sites appear to have relatively lower maximum drip rates when compared to Group 1 drip sites (Figure 7).

These sites appear to be better candidates to display correspondence between longer term variations in water flux and drip water Mg/Ca values.

At Group 2 sites the relationship between water flux and Sr/Ca is limited as well. Sr/Ca does not correlate with water flux at any Group 2 drip site except for ISST where it significantly correlates with drip rate and PDSI. Furthermore, Mg/Ca and Sr/Ca positively correlate at ISST and ISLM and inversely correlate at ISSR 9. There are no other significant relationships between Mg/Ca and Sr/Ca. At Group 2 sites the relationship between water flux and Ba/Ca does not exist for effective rainfall or drip rate. However, at all Group 2 drip sites there is a significant correlation between Ba/Ca and PDSI. At Group 2 drip sites there is a similar inconsistency (to that which is seen with Mg/Ca, Sr/Ca, and Ba/Ca values versus water flux) in significant correlations between Na and K and measures of water flux. All correlations can be found in Appendix B2.

2.4.3 High frequency sampling of ISSR 3 and ISSR 5

High frequency sampling coincided with a time period before and after Tropical Storm Hermine, which passed through the region from 9/7/10 to 9/8/10. The tropical storm resulted in 18.8 cm of rain for the study area. At drip site ISSR 3, the event appears to have increased drip rates from 0.07 ml/sec on 8/31/10 to a maximum of 0.22 ml/sec on 9/17/10. Mg/Ca ratios had a corresponding change from 89.1 mmol/mol on 8/31/10 to a minimum of 77.9 mmol/mol on 9/17/10 (Figure 9). At drip site ISSR 5, drip rates increased from 0.27 ml/sec on 8/31/10 to a maximum of 0.48 ml/sec on 9/17/10. Mg/Ca ratios had a corresponding change from 96.3 mmol/mol on 8/31/10 to a minimum of 81.6 mmol/mol on 9/13/10 (Figure 10).Over the sampling interval drip rate is significantly correlated with Mg/Ca at ISSR 3 ($r^2 = 0.89$, $p < 0.005$) and at ISSR 5 ($r^2 = 0.91$, $p < 0.005$).

2.4.4 Calcite growth and cave air CO_2

Calcite growth at all sites studied (n = 7) reflects a seasonal growth pattern in which higher cave air CO_2 concentrations will inhibit CO_2 degassing from cave drip water and thus inhibit calcite precipitation (Figure 10). This process is driven by a varying temperature gradient between surface air and cave air, which drives the ventilation of caves (Banner et al., 2007). Cave air CO_2 concentrations range from 457 to 11,900 ppm over the study period, which are consistent with concentrations for previous time periods in this cave (Banner et al., 2007). For all drip sites there is a period of calcite non-deposition each year, usually occurring between late June and late October when CO_2 concentrations are the highest; above ~5,000 ppm (Figure 10). The other months each year are highlighted by between-site variations in the amount of calcite deposited, which do not appear to be related to drip rate variations. Calcite deposition at all sites ranges from 0 mg/day to 35.7 mg/day (mean = 5.27 mg/day). All drip sites display a negative correlation between cave air CO_2 concentration and calcite growth.

2.5 Discussion

The overarching goal of the study is to determine the extent to which intra-annual climate variability is reflected by the intra-annual variability in Mg/Ca values of cave drip water. The main results that will be used in this discussion include the comparison of Mg/Ca variations to drip rates, effective rainfall, and PDSI. Drip sites have been grouped according to the extent to which they display an intra-annual climate signal. Group 1 sites consist of two sites, ISSR 3 and ISSR 5, for which the intra-annual climate signal is most clearly reflected in the relationships between drip rates, effective rainfall, PDSI, and Mg/Ca values. Group 2 drip sites do not display as clear of an intra-annual climate signal between the same variables. The extent to which climate information of varying timescales can be gleaned from Group 2 drip sites is discussed as well.

2.5.1 Intra-annual climate sites (Group 1)

At Group 1 drip sites an intra-annual climate signal is initially identified through a positive correlation between water flux parameters (both effective rainfall and PDSI) and

drip rate (Figure 6; Table 1). This signifies that flowpaths to the drip site are responsive to variations in surface water flux, making it more likely that the inverse correlations between (1) drip rate and Mg/Ca, (2) effective rainfall and Mg/Ca, and (3) PDSI and Mg/Ca at Group 1 sites are related to climate and not an artifact of other cave processes. As effective rainfall increases, drip rates increase on the timescale of a few days as there is an influx of water entering the system. The responsiveness of drip rates to effective rainfall indicates that Group 1 drip sites have a larger component of fracture flow (compared to Group 2 sites) that is activated during wetter times. Another commonality between Group 1 sites is a relatively higher maximum drip rate compared to the other sites studied (Figure 7). It appears that this is the type of hydrologic system and response needed to produce an intra-annual climate signal in Mg/Ca values. As effective rainfall and drip rates increase, Mg/Ca values decrease and as effective rainfall and drip rates decrease, Mg/Ca values increase. This indicates that in times of higher rainfall less evolved water is delivered through fractures and dominates the geochemical input, which results in decreased Mg/Ca values. During drier time periods more evolved water (i.e., increase in residence time and/or prior calcite precipitation) supplies a larger proportion of water to a drip site, which results in higher Mg/Ca values.

The relationship between water flux and Mg/Ca values discussed above is explainable within the theories of water flux through karst and its impact on the processes of calcite precipitation and dissolution. It has been well documented that varying (1) water residence times and (2) prior calcite precipitation act together to determine this relationship, which is controlled by the K_D values of Ca and Mg (e.g., Fairchild et al., 1996; Fairchild et al., 2000; Fairchild and Treble, 2009). It is also possible to delineate between the two mechanisms of water residence time and prior calcite precipitation by integrating Sr isotopes into trace element studies (Wong et al., 2011). While delineating between the two mechanisms is important, it is outside the scope of the present study. The relationship of Mg/Ca to an intra-annual climate signal is influenced by the type of flow path above a drip site, which determines the drip rate response to water flux. A higher proportion of fracture dominated flowpaths will display higher resolution climate

fluctuations due to more frequent variations in water storage and thus drip rates. A higher proportion of diffuse controlled flowpaths will display lower resolution climate fluctuations due to a larger storage reservoir and less frequent variations in water storage and drip rates.

To be sensitive to intra-annual Mg/Ca variations, it appears that a drip site is required to have (1) a certain proportion of fracture dominated flow paths in which the response to rain events is fairly quick (within a few days) and (2) an ample supply of diffuse flow water to sustain drip rates during drier times. During wetter time periods, as more water enters the limestone overburden, larger flow paths are activated as water preferentially flows through larger fractures. These fractures more quickly transmit water to the drip site, which increases drip rates. This has two effects: (1) lower Mg/Ca water, which is younger and less evolved through water-rock interaction/PCP, reaches the drip site in a higher proportion to older, more evolved, higher Mg/Ca diffuse flowpath generated water; (2) the amount of air in pore spaces decreases and the amount of water increases (Figure 4). This acts to limit CO_2 degassing, which decreases prior calcite precipitation of water reaching the drip site (Fairchild and Treble, 2009). Decreased PCP acts to keep more Ca ($K_D \sim 1$) in solution relative to Mg ($K_D < 1$).

During drier times less water enters the karst system from the surface; causing fractures to dry and allowing more air in pore spaces. This will have two effects: (1) degassing of CO_2 from pore spaces will increase, causing PCP and higher Mg/Ca values in cave drip waters (Fairchild and Treble, 2009); and (2) the proportion of less evolved (lower Mg/Ca values) fracture water will decrease, as fractures are the quickest to transmit water and also the quickest to decrease in saturation when there is no influx of water from the surface. Higher Mg/Ca waters will then have a more dominant effect on the input into the drip water geochemistry as diffuse dominated pore spaces will contribute a higher proportion of matrix water, which is more evolved and has higher Mg/Ca values, compared to the less evolved fracture generated drip water. Thus, a larger proportion of drip waters during dry periods will be under the influence of diffuse generated waters that have had a longer residence time/more PCP and higher Mg/Ca

values. These processes are depicted in Figure 4, a vadose zone and cave schematic showing the effects of periods of higher versus lower rainfall.

A question then arises as to what makes Group 1 sites distinct from the other less sensitive climate sites studied, Group 2 sites. This relationship is illustrated in Figure 7 using a parsimonious model graphically depicting the maximum drip rate and the drip rate coefficient of variation (see Smart and Friederich, 1987; Wong, 2008). The main differentiating characteristic in Figure 7 is that Group 1 sites have a higher maximum drip rate than the Group 2 sites. Thus, it appears that a higher maximum drip rate relates to Group 1 sites having more fracture controlled pathways. A higher proportion of fracture pathways allow Group 1 drip sites to exhibit a quicker and more uniform response to variations in water flux and Mg/Ca values. Perhaps sites with higher coefficients of variation but those for which drip rates do not cease during times of drought would display higher correlations between measures of water flux and Mg/Ca values. Sites with this characteristic have been located in another cave in the region- Natural Bridge Caverns (Figure 5; Wong et al., 2011).

Sr/Ca correlations. It is expected that Mg/Ca and Sr/Ca will behave in a similar manner (e.g., Fairchild and Treble, 2009; Wong et al., 2011). However, the correlations indicate that Sr/Ca does not positively correlate with Mg/Ca at Group 1 drip sites. Furthermore, Sr/Ca does not correlate with water flux parameters at Group 1 drip sites. To better determine the mechanisms controlling this behavior it is plausible to use $^{87}Sr/^{86}Sr$ values (Wong et al., 2011).

Ba/Ca correlations. It is expected that Sr/Ca and Ba/Ca will be significantly correlated. This is the case only at one Group 1 drip site, ISSR 5. The relationship between Ba/Ca and water flux also appears more complicated than that of Mg/Ca and water flux. There are limited correlations between Ba/Ca and water flux. At site ISSR 3 Ba/Ca is not correlated with any water flux parameter and it is only correlated with PDSI at ISSR 5. It appears that Ba/Ca is not a strong climate indicator at Group 1 sites.

N and K correlations. At Group 1 drip sites, similar to Sr/Ca and Ba/Ca, Na and K variations do not correspond to water flux variations in the same manner as Mg/Ca. At

one site, ISSR 3, Na is correlated with drip rate, effective rainfall, and PDSI, thus indicating that it may be useful as a climate proxy. At ISSR 3 K is only correlated with PDSI and thus is not expected to be a very robust climate proxy. At ISSR 5 Na and K correlate only with drip rate and are not very robust measures of climate.

2.5.2 Palmer Drought Severity Index

A second and possibly more robust measure of water flux is a drought indicator most commonly used in dendrochronology, the Palmer Drought Severity Index (PDSI). PDSI appears to be a more robust indicator of water flux versus effective rainfall as it factors in antecedent moisture conditions from previous months (temperature, rainfall, soil moisture), whereas effective rainfall is a measure more rooted in current, daily conditions. PDSI has a significant negative correlation with Mg/Ca values and drip rates at all Group 1 drip sites (Table 1; Figure 6). During drier time periods (PDSI < 0) Mg/Ca values increase and they decrease during wetter periods (PDSI > 0). When conditions are abnormally wet (PDSI > 2) or abnormally dry (PDSI < -2) there is a higher correspondence between PDSI and Mg/Ca values compared to when PDSI values are closer to 0. While PDSI is not commonly used in cave climate studies, this study highlights the usefulness of a regional drought indicator such as the PDSI to correlate with the geochemistry of cave drip waters.

Although significant, the correlation between Mg/Ca values and PDSI is fairly low at Group 1 drip sites ($r^2 = 0.19 – 0.28$). This can be attributed to Mg/Ca ratios varying on a higher frequency scale (compared to PDSI) as drip waters are subject to shorter term variations through the processes of precipitation and dissolution of limestone/dolomite as they infiltrate through the vadose zone. The karst system is a complex interaction of water, varying flow routes, and varying degrees of calcite dissolution and precipitation, all of which vary on the timescale of seasons, months, weeks, days, and hours. The low correlation between Mg/Ca and PDSI is most likely a product of the heterogeneous nature of the karst system with respect to the complexities of interconnected and varying flowpaths. One must also consider that the heterogeneities

of CO_2 concentrations in the soil zone and degassing of CO_2 at varying rates in the karst overburden can produce high frequency variations in Mg/Ca values, which are independent of water flux.

PDSI is reflective of lower frequency variations (compared with Mg/Ca values) as it is comprised of current and antecedent monthly assessments of rainfall, temperature, and soil moisture, all of which are subject to lower frequency variations compared to the highly variable hydrologic response of the karst system. At Group 1 drip sites, when PDSI and Mg/Ca were compared on more similar temporal frequencies, PDSI is significantly correlated with Mg/Ca with a much higher regression coefficient (Figure 8a-b).

The difficulty of making between-site comparisons has previously been documented (Baldini, 2006). To make comparisons between all Group 1 drip sites, PDSI and Mg/Ca averages were standardized to each Group 1 drip site's mean. The significant relationship between standardized PDSI and standardized Mg/Ca at Group 1 drip sites provides a method for comparing multiple drip water sites with varying concentrations of Mg/Ca (Figure 8c). Standardizing values offers the advantage of comparing multiple drip sites, which can be applied to compare multiple speleothem samples. This can strengthen the statistical power of paleoclimate interpretations by increasing the sample size in a similar manner to the comparison of multiple samples in dendrochronology studies. This is the first cave study to make these statistical comparisons and their utility can be applied to studies other cave systems.

2.5.3 High frequency variations in response to Tropical Storm Hermine

If there is a component of fracture flow that is activated quickly after a rain event and is a determining factor in detecting an intra-annual climate signal, then a large influx of water in a short time period should provide a strong correlation between Mg/Ca and drip rate. This is due to limiting the noise associated with the drying/wetting cycle of intermittent periods of rainfall and subsequent high frequency variations in Mg/Ca.

The influx of water from Tropical Storm Hermine on 9/7/10 to 9/8/10 indicates that large scale events more directly influence the Mg/Ca ratios in a manner that is more related to water flux than any other factor (Figure 9). The increase in drip rates within a day of the event indicates that infiltrating water is reaching the Group 1 drip sites fairly quickly through fracture flow and is the primary factor controlling Mg/Ca ratios. This implies that when the system is under the influence of an extreme event it is more well behaved versus when there are oscillations between wetter and drier periods. This highlights the complexities of the karst system with respect to intermittent periods of rain and drying out, which can cause variations in drip water geochemistry that are not necessarily reflective of an uncomplicated climate signal devoid of noise from the complicated processes of calcite dissolution and precipitation.

A similar high frequency sampling during a drought period is also expected to yield similar high correlations between drip rate and Mg/Ca. It appears that drip rate is a better correlate with higher frequency variations in Mg/Ca values and PDSI of lower frequency variations as PDSI does not correlate with Mg/Ca during the time period in which Tropical Storm Hermine occurred. However, PDSI is predicted to be a better paleoclimate proxy than rainfall because speleothem calcite is not likely to record individual tropical storms in this cave due to the low rate of calcite growth relative to some fast-growing speleothems in other regions (see Frappier et al., 2007). On longer time scales, even relatively slow-growing speleothems may record periods of higher vs. lower numbers of tropical storms.

2.5.4 Less climate sensitive drip sites (Group 2 sites)

At Group 2 drip sites the interaction of effective rainfall, drip rates, PDSI, and Mg/Ca is not as clearly indicative of intra-annual variations in water flux as Group 1 sites. No Group 2 sites have a significant correlation between effective rainfall and drip rate (Table 2; Figure 6). This is indicative of a smaller component of fracture flow as the drip sites do not appear to be responsive on the same timescale as the more climate sensitive (i.e. responsive to PDSI and effective rainfall on an intra-annual timescale)

Group 1 sites. In as much, the drip site characterization model (Figure 7; Smart and Friederich, 1987) offers between-group distinctions with respect to a lower maximum discharge for Group 2 sites. Thus, it appears that maximum discharge is a more important variable than the coefficient of variation when detecting intra-annual climate variations.

There are some statistically significant relationships between water flux indicators and Mg/Ca at some of the less sensitive Group 2 drip sites (Table 2). However, without the significant relationship between effective rainfall and drip rate it is difficult to determine the extent to which these relationships are valid. Perhaps droughts or abnormally wet periods occurring on a longer timescale will be reflected in Group 2 drip sites. This is related to diffuse flowpaths being slower to react to variations in water flux as it takes a longer time for the infiltrating (or the non-infiltration in drought) rainfall to reach the drip site.

Also included in Group 2 drip sites are those sites for which seasonal CO_2 fluctuations exhibit control on drip water Mg/Ca values. There are statistically significant relationships between cave air CO_2 and Mg/Ca values for four Group 2 drip sites; ISSR 6, ISSR 8, ISSR 9, and ISST. The possibility of seasonal cave air CO_2 fluctuations to obscure a climate signal due to water flux arises.

Site ISST is a prime example of how a long, exposed flowpath can obscure a significant relationship between Mg/Ca and water flux. It is expected that drip waters at ISST would have higher correlations between Mg/Ca and water flux as previous studies show a strong correlation between $^{87}Sr/^{86}Sr$ values and water flux at this site (Pierson et al., 2004, Duran et al., 2010). The non-significant correlations between water flux and Mg/Ca values are hypothesized to be a result of the flow path of the drip waters. At ISST infiltrating water is exposed to the cave atmosphere as it flows down the surface of a large flowstone. This long flowpath would engender extensive prior calcite precipitation, which acts to produce variations in Mg/Ca independent of water flux. However, $^{87}Sr/^{86}Sr$ values are potentially more useful at ISST as they are more directly controlled by water flux and not subject to the effects of PCP (Pierson, 2005; Duran, 2010; Wong et al.,

2011). Knowledge of this interaction would not have been possible without a modern day assessment of the cave system. Sampling a stalagmite without knowledge of the surface climate - karst system - drip water interaction provides little a priori information on the controls on Mg/Ca fluctuations. This may lead to inaccurate interpretations of paleoclimate from Mg/Ca fluctuations.

Sr/Ca correlations. It is expected that Mg/Ca and Sr/Ca will behave in a similar manner (e.g., Fairchild and Treble, 2009; Wong et al., 2011). However, the correlations indicate that Mg/Ca and Sr/Ca positively correlate at only two of seven Group 2 drip sites. To better determine the mechanisms controlling this behavior it is plausible to use $^{87}Sr/^{86}Sr$ values (Wong et al., 2011). This has been done at one site, ISST, and it appears that prior calcite precipitation controls the behavior of Sr/Ca and Mg/Ca at this drip site (Pierson, 2005; Duran, 2010).

Ba/Ca correlations. It is expected that Ba/Ca and Sr/Ca will behave in a similar manner. However, Ba/Ca and Sr/Ca only significantly correlate at one Group 2 drip site. Ba/Ca presents a limited relationship with water flux parameters at Group 2 drip sites. This is similar to the relationship that Mg/Ca and Sr/Ca values have with water flux measures except that Ba/Ca correlates with PDSI at all Group 2 drip sites.

N and K correlations. Na and K inconsistently correlate with measures of water flux at Group 2 drip sites. This is an expected result as elements at these sites do not appear to change on an annual timescale. Perhaps longer term fluctuations in climate will be recorded by Na and K.

2.5.5 Paleoclimate interpretation

This discussion has centered on the response of the modern hydrologic system and drip water geochemistry to variations in water flux (effective rainfall, PDSI, and drip rate). It is important to make assessments of how variations in the modern system relate to variations in drip water geochemistry in order to: (1) select appropriate speleothem samples for paleoclimate analysis as speleothems may need to be conserved for aesthetic purposes and (2) gain *a priori* knowledge of the expected geochemical signal of a

speleothem because drip waters act as an intermediary between surface conditions and deposited calcite. Having *a priori* knowledge of the drip water geochemical input to a speleothem strengthens the accuracy of interpretations of the climate signal within a speleothem. An assumption behind this approach is that the modern drip water response is similar to the paleo-drip water response.

The extent to which Mg/Ca values vary from peak values to low values has implications for the interpretation of paleoclimate when a stalagmite is sampled. By using the modern day differences in Mg/Ca values during drought vs. wetter time periods, we can infer drought periods in a speleothem. Periods for which Mg/Ca varies by at least as large as the values found in this study (+/- 2 standard deviations from the Mg/Ca mean) can be inferred as droughts as severe as the drought period in this study (~2 years). Time periods with lower or higher magnitude shifts in Mg/Ca values can be interpreted as wetter or drier periods. This information can be used to calibrate modern climate and extend the paleoclimate record further into the past.

There is also an extensive reconstructed regional PDSI paleoclimate record from tree rings (Stahle and Cleaveland, 1988; Banner et al., 2010; Cleaveland et al., in prep.). This is useful information when attempting to reconstruct paleoclimate from a stalagmite as PDSI: (1) is a commonly used measure in dendrochronology reconstructions; (2) correlates with Group 1 Mg/Ca drip water values; and (3) might be a useful calibration tool in speleothems. Reconstructing climate on an annual resolution using a speleothem is more problematic than dendrochronology reconstructions as speleothems do not commonly have visible annual layers (Baker, 2006). At the current study site, modern day assessment of the cave-drip water system has yielded important considerations when interpreting the geochemistry of speleothems, including the following: (1) the truncation of calcite deposition by seasonal cave air CO_2 variations, which can obscure an annual climate signal; (2) the rate of deposition of calcite, which can limit high resolution sampling if deposition is slow; (3) relating variations in the geochemistry of cave drip waters to speleothems on an interpretable timescale.

The seasonal deposition of calcite due to cave air CO_2 ventilation at Inner Space Cavern has been well documented (Banner et al., 2007; Figure 10). This creates a seasonal truncation in the calcite record. The period of non-deposition, due to high cave air CO_2, usually lasts ~4 months. This indicates that periods of drought lasting longer than four months can still be captured in the speleothem record. Figure 11 depicts the occurrences of calcite non-deposition at drip site ISSR 3. Although the Mg/Ca signal is truncated during the warmer months, a climate signal still appears for each year of the 3-year record. This includes the wet time period of 2007, the drying that occurred in 2008, the drought of 2009, and the break from the drought in 2009-2010. There have been recent attempts to forward model the appearance of seasonal truncations in the calcite record (Wong et al., 2011). The models are useful in (1) demonstrating an expected high resolution climate signal in speleothems prior to analysis and (2) application to cave systems where multi-year drip water monitoring studies cannot be conducted.

It can be inferred that the length of most droughts in central Texas (greater than four months) are temporally extensive enough to be recorded in a speleothem regardless of periods of non-deposition of calcite. A slow rate of calcite deposition may prevent sub-annual to annual sampling resolution while a lack of annual banding may inhibit high resolution climate reconstructions. However, there is evidence for decadal or longer regional "megadroughts" in the tree ring record over the past 700 years (e.g., Stahle and Cleaveland, 1988; Banner et al., 2010; Cleaveland et al., in prep). These long-term droughts may appear as markers in the speleothem record with which to more precisely date samples. Furthermore, megadroughts are predicted to be more noticeable in the speleothem record as they are more severe and longer lived.

2.6 Implications and Conclusions

This study supports the approach of the extended monitoring of cave drip water from multiple drip sites and making comparisons to modern surface conditions as a precursor to understanding the extent to which a drip site can be used to decipher paleoclimate. Drip sites were grouped according to the resolution of the climate signal

that can be procured. Group 1 drip sites display intra-annual correlations between water flux and Mg/Ca values, whereas Group 2 drip sites do not display as clear of a correspondence between water flux and Mg/Ca values. A main distinction between the two groups is an overall higher maximum drip rate at Group 1 sites. It can be concluded that speleothem Mg/Ca values following similar patterns through time to those in this study can indicate the similar occurrences of droughts. Those with smaller/larger differences in Mg/Ca values can be interpreted as wetter/drier time periods. Furthermore this study highlights using a more robust climate measure, PDSI, to compare to drip water geochemistry. This is important as it is a commonly used measure in dendrochronology and thus regional tree ring climate records can possibly be used as a calibration tool when examining speleothems. This may add a higher degree of certainty to the validity of central Texas climate reconstructions.

The results of this study suggest that vadose water Mg/Ca values at drip sites with an influence of both fracture flow and diffuse flow are influenced by water flux and thus time periods of higher or lower Mg/Ca may be equated to varying surface moisture conditions. Increased temperatures and increased rates of evaporation during drought periods exacerbate the drying of the karst system. Subsequent degassing of the system occurs, which is why a more robust measure of water flux that includes temperature, evaporation, and soil moisture as parameters, such as the PDSI, is appropriate. This appears to make sense when looking at the relationships of Mg/Ca and PDSI with drip site characteristics. Fractures would lose water from pore spaces more readily and thus be affected by a larger proportion of air in the pore spaces and subject to increased water input from adjacent matrix waters. Thus, drip sites with adequate fracture flow are more ideal sites for intra-annual climate analysis, but an ample amount of diffuse flow to the drip sites is also needed to prevent periods of inactive drip and growth hiatuses. Group 1 sites fit this mold as their drip rate is not only variable but also rapid and responsive enough to water flux. Group 2 sites have lower maximum drip rates thus indicating a larger component of diffuse flow, which would dry up at a slower rate compared to fractures. It is hypothesized that drip sites with lower maximum drip rates would be

more apt predictors of larger scale droughts. A lower maximum drip rate suggests more diffuse flow, which would be affected by drought on a longer timescale as it will take the reservoir in diffuse storage longer to significantly dry. Thus, it would take a more severe drought over a longer period of time to cause similar Mg/Ca variations in Group 2 sites as seen in Group 1 sites.

The correspondence between PDSI and Group 1 Mg/Ca values has implications for the ability of a single drip site in a specific location to provide regional climate data. The interpretation of Mg/Ca from drip waters is significantly different than the interpretation of Mg/Ca of calcite. This is due to the uncertainty of defining the timescale at which calcite grows and more importantly is limited by the rate of calcite growth. Conversely, we know when drip waters were collected, thus constraining ages of drip waters is a simple process. Regardless of timescale and the rate of calcite growth, the mechanisms that operate at Group 1 drip sites to yield correlations between Mg/Ca values and PDSI variations are hypothesized to also operate on longer timescales, at lower resolutions, and at different caves with similar drip site characteristics. The ability to identify commonalities in intra-annually sensitive drip sites is key when attempting to apply this information to other caves where long term monitoring is not possible.

The results of this study have implications for methodologies to reconstruct climate by first studying drip waters and the modern system, and then applying that knowledge to speleothems. Drip waters act as an intermediary between surface conditions and the climate signal preserved in speleothems. Understanding the relationship between drip waters and the modern hydrologic and geochemical response lends the advantage of a priori knowledge of the expected geochemical signal in a speleothem. This strengthens any paleoclimate interpretation procured from a speleothem.

Chapter 3: Speleothem calcite deposition rates and cave drip water trace element variations as a function of seasonal temperature variability: Westcave Preserve, central Texas, USA

3.0 Abstract

A 1.5-year cave monitoring study at Westcave Preserve in central Texas provides insight on the controls of the rate of speleothem calcite deposition and drip water Mg/Ca, Sr/Ca, and Ba/Ca values. The geometry of the cave appears to play a significant role in this regard in that there is a relatively large cave opening area to cave volume ratio (~0.02 m^{-1}). Deeper, more seasonally ventilated caves have a significantly smaller cave opening area to cave volume ratio (e.g., Inner Space Caverns ~ 0.0004 m^{-1}), which acts to create a seasonal ventilation regime, where cave air CO_2 concentrations peak in the summer and inhibit calcite deposition. Conversely, at Westcave, cave air CO_2 concentrations are near atmospheric throughout the year and thus not a limiting factor in calcite deposition. Instead, seasonal temperature variations appear to drive changes in the rate of calcite deposition.

Temperature also appears to be the predominant control on seasonal variations in drip water trace-element/Ca variations, as average monthly surface air temperature and water temperature are significantly correlated with Mg/Ca (at three of six drip sites), Sr/Ca (at five of six drip sites), and Ba/Ca (at six of six drip sites). Drip water Mg/Ca, Sr/Ca, and Ba/Ca follow a similar pattern as calcite deposition in that the values increase in warmer months and decrease in cooler months. The increase in trace-element/Ca values as temperatures warm can be explained by the exchange reaction distribution coefficient (K_D) values for Mg, Sr, and Ba ($K_D < 1$), which dictates these elements will prefer the aqueous phase. Understanding drip water seasonal trace-element/Ca variations has implications for paleoclimate studies as these variations can translate to geochemical laminae in speleothems, which may provide seasonal age-constraints in speleothems.

By standardizing trace-element/Ca values to each drip site's mean we can compare multiple drip sites to each other and add statistical power to our analyses by increasing the sample size. Modeling of trace-element/Ca values using historic average monthly surface air temperature and PDSI as independent variables yields a multiple regression equation explaining 73% of the variance in Ba/Ca values. Predicted drip water trace-element/Ca values can then be applied to understand trends in trace-element/Ca values in stalagmites for calibration to the modern system and reconstruction of paleoclimate. This study highlights the usefulness of modern day assessment of climate and cave drip waters to provide a realm in which one can begin to decode the past.

3.1 Introduction

The climate of central Texas has undergone rainfall and temperature changes on millennial as well as annual time scales (e.g. Toomey et al., 1993; Banner et al., 2010). On shorter time scales, intermittent and perhaps unpredictable periods of drought are a concern for policy makers as water resources are a limiting resource in this region. In order to more appropriately plan for the future needs the climate history of central Texas should be better understood. A potential proxy exists in cave calcite deposits (speleothems).

Past research using speleothems as paleoclimate proxies has been useful in determining residence time of groundwater, relative changes in rainfall amount, and the response of trace elements to variations in climate (e.g. Banner et al., 1996; Musgrove et al., 2001; Fairchild and Treble, 2009). An important aspect of the present study is the a priori assessment of geochemical and drip rate variations in cave drip waters in order to determine the response of drip waters to variations in surface climate. This is important because cave drip waters are an intermediary between surface climate and speleothem geochemical composition. Thus, cave drip waters provide a means to ground truth the geochemical results from speleothems. The geochemical ratios of Mg/Ca, Sr/Ca, and Ba/Ca (collectively referred to hereafter as trace-element/Ca values) in drip waters can be altered by a number of factors: Soil composition, bedrock composition, and variations in

rainfall, flow path characteristics, temperature, and seasonal cave air CO_2 concentrations (Fairchild and Treble, 2009; Wong et al., 2011). An understanding of the drip water trace-element/Ca response to climate is essential for the most accurate inferences to be made when interpreting speleothem geochemistry.

This study takes a systematic approach to selecting drip sites with actively growing speleothems for paleoclimate study. This involves assessing the geochemistry of cave drip waters at multiple drip sites and comparing it to the modern hydrologic response to climate variations. Results of this study indicate that (1) variations in trace-element/Ca values in cave drip waters are temperature dependent and vary on a seasonal time scale, (2) the standardization of trace-element/Ca values allows for between-site comparisons, and add rigor to statistical analyses by increasing the sample size, (3) calcite growth rates follow a seasonal pattern based on variations in surface temperature, and (4) a regional drought indicator provides correlation with trace-element/Ca values at some drip sites and this relationship is most likely dependent upon temperature. Such results provide a valuable framework for selecting speleothems for analysis in future studies.

Air temperature and water flux are two overarching controls on processes in the cave environment that determine the geochemical response of cave drip waters, speleothem geochemistry, and calcite growth rates (e.g., Banner et al., 2007; Fairchild and Treble, 2009; Wong et al., 2011). Water flux is related to drip rates, effective rainfall, Palmer Drought Severity Index (PDSI), flow path characteristics (diffuse versus fracture dominated), and flow path response to varying surface moisture conditions. Surface temperature variations can influence cave air CO_2 ventilation, drip water temperature, soil zone CO_2 concentrations, calcite deposition, and trace-element/Ca values (e.g., Banner et al., 2007; Fairchild and Treble, 2009; Wong et al., 2011). As stated earlier it is important to study the modern system to determine the influence of surface water flux, flow path characteristics, and cave atmosphere on trace-element/Ca variations in cave drip waters. In this study it appears that seasonal surface air temperature is the primary control on seasonal cave drip water trace-element/Ca

variations. Water flux shares a somewhat obscure relationship with trace-element/Ca values and is most clearly related to PDSI variations.

Whereas drip water geochemistry is quite variable between drip sites, seasonal cave air CO_2 concentration variations appears to be more of a ubiquitous factor in the seasonal deposition of calcite in deeper, seasonally ventilated caves in the region (e.g., Banner et al., 2007, Wong, 2008). Seasonal variations in CO_2 ventilation allows calcite deposition in cooler months and inhibits calcite deposition in warmer months. The current study location, Westcave Preserve, is distinct in that the cave air CO_2 concentration is similar to atmospheric levels year round and thus does not inhibit calcite growth like in seasonally ventilated caves. Instead, surface air temperature variations appear to affect the rate of calcite deposition. Temperature can act to affect calcite deposition at Westcave in two ways. Generally, an increase in temperature and soil moisture will increase the concentration of CO_2 in the soil through increased microbial, root, and faunal respiration (Rastogi et al., 2002; Edward, 1975; Wiant, 1967). In central Texas, the amount of moisture in soil is an important variable in determining the productivity of soil CO_2 (Kjelgaard et al., 2008). If soils become too dry, CO_2 productivity will decrease while an influx of water will increase soil CO_2 productivity (Kjelgaard et al., 2008). Therefore, when temperatures are warmer and soils wet enough, infiltrating vadose waters will absorb more CO_2 thus lowering the pH and increasing the ability of the water to dissolve carbonate. This should act to increase the SI of carbonate species in the drip waters during warmer months, which will increase the amount of calcite that can be precipitated from cave drip waters. A second factor relates to the retrograde solubility of calcite, in which calcite is more likely to precipitate out of solution when temperatures are warmer. Thus, it is proposed that in a well-ventilated cave such as Westcave calcite growth will be driven by seasonal temperature fluctuations as there are not strong seasonal cave air CO_2 variations.

If temperature is a dominant factor in carbonate dissolution and calcite precipitation at Westcave then it is possible that the trace-element/Ca values of cave drip waters will vary as temperature and the rate of calcite precipitation varies (e.g., Lorens,

1981; Stoll et al., 2002). This temperature dependence has been applied to Sr/Ca values of coral (e.g., Beck, 1992; Shen, 1996; Beck, 1997; Correge, 2000). The majority of cave drip water/speleothem research that relates trace-element/Ca variations to temperature variations uses Mg/Ca and notes that water flux can obscure the temperature signal (e.g., Katz, 1973; Gascoyne, 1983; Roberts et al., 1998; Huang and Fairchild, 2001). The present study, by contrast, provides evidence that cave drip water Mg/Ca, Sr/Ca, and Ba/Ca values can act as a proxy for relative seasonal surface temperature variations. Seasonal temperature variations can produce seasonal patterns in trace-element/Ca values, which can produce chemical laminae in speleothems and can be used to provide high resolution age constraints (Wong et al., 2011).

3.1.1 Sampling of multiple drip sites

Due to the complexities of the karst system the proximity of one drip site to the next is not a determining factor in the degree to which drip water trace-element/Ca values correspond between drip sites (Baldini, 2006). Thus the intensive, long term analysis of multiple drip sites will allow for a rigorous assessment of the modern system (e.g., Wong et al., 2011). Once the mechanisms that control the modern system are understood this knowledge can be applied to improve the accuracy of paleoclimate data as drip waters act as an intermediary between surface climate variations and the information preserved in a speleothem (e.g., Fairchild and Treble, 2009) This study draws from the field methods of previous research (e.g., Guilfoyle, 2006; Banner et al., 2007; Cowan, 2010; Wong et al., 2011) and systematically assesses the relationship between the modern climate system and modern drip waters.

The comparison of multiple drip sites has been cited as a difficulty by previous researchers (e.g., Baldini, 2006). A unique aspect of this study is the statistical treatment of the data, which places the trace-element/Ca values of multiple drip sites, each with widely varying trace-element/Ca values, on similar scales. Placing the trace-element/Ca values on similar scales enables the comparison of multiple drip sites. This is accomplished by standardizing trace-element/Ca values for multiple drip sites to each

drip site's mean. This method can potentially improve statistical rigor by increasing the sample size when performing a regression analysis. A larger sample size increases the likelihood that the observed effects reflect a valid relationship (Cohen, 1998). The method in this study is similar to dendrochronology studies in that numerous trees are sampled to ensure statistical rigor (e.g., Cook and Pederson, 2011). This knowledge can be applied to other drip sites in the cave and/or caves in this region or other regions.

3.1.2 Drought measurement: Palmer Drought Severity Index

The Palmer Drought Severity Index (PDSI) was developed as a measure of the moisture deviation from normal (Palmer, 1965). The index considers temperature, rainfall, and soil moisture of the current and preceding 12 months to determine the dryness of the system. The scale ranges from extremely moist (+4 or above) to extreme drought (-4 or below) with divisions for severe wet/dry (+/-3-3.99), moderate wet/dry (+/-2-2.99), and mid-range wet/dry (1.99 to -1.99). The PDSI is a widely accepted drought measure as it provides a measure of abnormal weather and gives a regional perspective of drought (Alley 1984). It is frequently used in tree ring studies to reconstruct climate and appears to provide a robust measurement of regional drought conditions as it correlates very well with historic rainfall records (Stahle and Cleaveland, 1988).

3.2 Hydrogeologic setting

Westcave Preserve is located in the Balcones Canyonlands of central Texas on the eastern edge of the Edwards Plateau; approximately 32 miles west of Austin, TX (Figure 12). The regional climate ranges from subtropical/sub-humid to semi-arid (Larkin and Bomar, 1983). In terms of temperature and precipitation this amounts to dry, hot summers, wet springs and falls, and dry, mild winters. Average rainfall is between 68 and 104 cm per year while average temperature ranges from 9° C to 27° C. Annual and monthly variability in rainfall is high with intermittent droughts dispersed amongst wetter periods (Larkin and Bomar, 1983).

Westcave is located in the Heinz Branch Watershed, which has a drainage area of 1,660 acres (LCRA, 2007). The soils of the area are Volente Series (alluvial), Brackett Series (shallow gravelly clay loam), and Hensell sand, all of which support pasture grasses, ashe juniper trees and shrubs, and oaks (LCRA, 2007). Westcave resides in the highly porous Cow Creek Formation, which is composed of Lower Cretaceous limestone (Caran, 2004a; Figure 13). Westcave has an approximate volume of 2,000 m^3 with a large opening at the entrance and smaller openings at the rear. It has a relatively large ratio of its opening area to the cave volume of 0.02 m^{-1}. This allows for Westcave to be well ventilated and have an internal atmosphere similar to surface conditions. Seasonally ventilated caves in central Texas, such as Inner Space Cavern and Natural Bridge Caverns, tend to be deeper and have much larger cave volumes (> 100,000 m^3) that prevent them from being well ventilated during the warmer months of the year (Cowan, 2010). Inner Space Cavern and Natural Bridge Caverns have an approximate opening area to the cave volume of 0.0004 m^{-1}.

The cave is located ~7 meters above the valley floor of a 30m deep canyon on Westcave Preserve (Figure 13; Reddell and Smith, 1961; Fieseler et al., 1972; Caran, 2004a). The overburden above the drip sites is ~20 -25 meters. The drips feeding the stalagmites at sites WC-1, WC-3, WC-4, WC-5, and WC-7 emanate from soda straws (2.5 – 20 cm in length) while the drip for WC-6 flows down a 30 cm drapery prior to drip. Appendix A contains more detailed cave and drip site descriptions.

3.3 Methods

Six drip sites were monitored (WC-1, WC-3, WC-4, WC-5, WC-6, and WC-7; Figure 13) from July 2009 to September 2010. Sampling trips were conducted at least every 4-5 weeks. Sampling included measurement of cave air parameters, cave water drip rates, collection of drip water, and collection of calcite on glass plate substrates. Field data collection methods and sample preparation methods follow those developed over a 12-year period of cave monitoring (Musgrove and Banner, 2004; Guilfoyle, 2006; Banner et al., 2007; Wong, 2008; Wong et al., 2011) and those outlined in Wong (2008).

Rainfall data was measured on site daily by Westcave Preserve staff using a rain gauge. Daily surface air temperature data was collected from www.wunderground.com using the closest NOAA weather station located in Bee Caves, TX, which is 11.3 km from Westcave Preserve. How does rainfall compare between on site and at the NOAA station?

Surface and cave air relative humidity, CO_2 concentration, and temperature were recorded for each sampling trip. Surface measurements were taken at the onset of each trip while cave air measurements occurred at each drip site. Relative humidity was measured using a Digital Psychrometer (+/- 5% error above 90%). Cave air CO_2 was measured using a TelAire 7001 meter (+/- 5% error). The CO_2 meter was calibrated using a nitrogen gas source with 99.9% pure nitrogen.

At each drip site a one liter polypropylene bottle was placed to collect water. Time intervals for collection ranged from 10 minutes to 4-5 hours depending on the drip rate. Ideally, ~150 ml of water was needed to completely fill smaller sample bottles designated for analysis for Sr isotopes, cations, anions, oxygen isotopes, hydrogen isotopes, alkalinity, field pH, and field conductivity. Each sample bottle was wrapped with Parafilm. Sr isotope and cation samples were acidified in the laboratory with 2% HNO_3 to prevent plating of calcite on the collection bottle walls. Anion, oxygen isotope, and hydrogen isotope samples were kept refrigerated until analysis. Conductivity, pH, and water temperature were measured using a Myron L Company Ultrameter II in the field less than twenty minutes after collection. Water temperature was also measured with a hand held Hannah thermometer directly from the tip of the drapery that feeds drip site WC-6. Alkalinity samples were analyzed less than 24 hours after collection to limit any effects associated with degassing. Replicate alkalinity samples reveal an average percent difference of 1.2% (n = 12). Alkalinity pairs (n = 4) measured (1) in cave by hand show an average percent difference of 4.9% versus those analyzed (2) less than 24 hours later by an autotirator. Replicate alkalinity samples analyzed (1) less than 24 hours after collection versus those analyzed (2) 48 hours after collection show an average

difference of 3.8% (n = 3), where alkalinity decreases with increased time from collection.

Measured water temperature of drip site WC-6 is used as a proxy for all drip sites as (1) not all sites have measured water temperatures due to the limited amount of drip water; (2) drip water temperature at WC-6 can be measured directly prior to drip; and (3) collection bottles at the other sites are left open to the atmosphere for 4-6 hours as water collection proceeds slowly. This may allow for drip water temperature to equilibrate to atmospheric temperature at the time of collection and thus not accurately reflect drip water temperature. Drip water temperature at WC-6 was measured directly prior to drip with a hand-held temperature probe. There is, on average, a 4°C difference from site WC-6 drip water temperature and the other sites in the study. A handheld temperature probe also measured WC-6 drip water temperature, yielding, on average a 0.5°C difference between direct temperature measurement and temperature measurement 30-60 minutes later. It is expected that drip water temperature between each drip site is very similar, thus adding credence to this method of using WC-6 drip water temperature as a proxy for all drip sites.

Cation analyses were performed at The University of Texas at Austin using an Agilent 7500ce quadruple ICP-MS in the Department of Geological Sciences. Samples were diluted 10:1 with 2% HNO_3 prior to analysis. NIST 1643e was used as an external standard (measured 3 times throughout each run) and reveals an accuracy of 3.8% for Ca, 2.8% for Mg, 2.9% for Sr, and 6.1% for Ba. This accuracy was determined by measuring the NIST 1643e standard and comparing the measurement difference to the known value. Each unknown sample was measured three times during a run (i.e., duplicate analyses) and the relative standard deviation between measurements reveals an analytical precision of 1.7% for Ca, 1.0% for Mg, 1.4% for Sr, and 3.4% for Ba, 1.8%. Replicate analyses (i.e., splits of the same water sample followed by dilution) on 10 unknown samples reveal an average percent difference between a sample and its replicate of 2.3% for Ca, 3.6% for Mg, 1.9% for Sr, 3.4% for Ba, 3.6% for Mg/Ca, 0.80% for Sr/Ca, and 1.5% for Ba/Ca. Field blanks for Ca, Mg, Sr, and Ba are below the detection limit of 1.8, 0.83, 0.012, and

0.011 ppb, respectively. Field blanks were treated the same as collection bottles in that they were uncapped and exposed to the cave atmosphere during drip water collection. Field blanks are deionized water and are placed where no drip water can enter them.

Anion analyses were performed at the Bureau of Economic Geology at The University of Texas at Austin using a Dionex Ion Chromotography System-2000. Analytical uncertainty for eight external standards are as follows: F = 7%, Cl = 2%, Br = 8%, NO_2 = 4%, NO_3 = 4%, SO_4 = 4%, and PO_4 = 9%. Replicates reveal an average percent difference as follows: F = 0.56%, Cl = 0.62%, Br = 0.57%, NO_2 = 0.51%, NO_3 = 0.51%, SO_4 = 0.59%, and PO_4 = below detection limit. Charge balances were performed on six samples. The samples had charge balances that ranged from 2.7% to 5.9% with an average of 4.3%. A limited number of charge balances can be performed due to the lack of enough water for alkalinity analyses.

Calcite was collected by placing 10 x 10 cm glass plates under each drip site and collecting them during the subsequent cave trip. Prior to deployment, the glass plates were sanded on one side to increase nucleation sites for calcite growth. In order to measure monthly calcite growth (expressed in units of mg/day) plates were weighed prior to deployment and after collection. A standard plate was repeatedly weighed and reveals a standard deviation of 0.0002 g. This approach follows the methods described in Banner et al. (2007).

3.4 Results

All data can be found in Appendix B. These data include effective rainfall, PDSI, drip rate, pH, alkalinity, Ca, Mg, Sr, Ba, anions, charge balances, cave air CO_2, cave air temperature, calcite growth, and the statistical relationships between these variables. This section highlights the most pertinent data and statistical relationships for the study. A p-value must be less than or equal to 0.05 in order for statistical significance to be achieved.

The study period at Westcave (7/3/09 to 9/26/10) began while the region was in a period of drought, which ended in September of 2009. The study period drought

variability was characterized by a Palmer Drought Severity Index minimum of -6.57 at the height of the drought in August of 2009 and a maximum wetness value of 3.66 in February of 2010. The drought subsided in September of 2009 (PDSI = 0.58) and the region experienced non-drought conditions until the end of the study period in September of 2010 (Figure 14).

The average yearly rainfall for Westcave Preserve is 90.2 cm (1974-2009). Effective rainfall was calculated using rainfall and evaporation data (NOAA, 2010b). The range of average monthly surface air temperature during the study period was 9.05° C to 32.29° C (Figure 14).

Vadose drip waters at Westcave Preserve plot as Ca-HCO_3 waters on a Stiff diagram. Conductivity ranges from 462 to 768 µS while pH ranges from 8.0 to 8.7. Ca concentrations (n = 72) range from 66.8 to 113 ppm with an average of 93.9 ppm, Mg concentrations (n = 72) range from 29.3 to 47.7 ppm with an average of 37.0 ppm, Sr concentrations (n = 72) range from 0.26 to 1.1 ppm with an average of 0.41 ppm, Ba concentrations (n = 72) range from 0.05 to 0.09 ppm with an average of 0.07 ppm. The range of HCO_3 is 359 to 434 ppm. The Ca, Mg, HCO_3, and conductivity values are similar to values from a well sampled from a Cretaceous aquifer 85 m in depth (Caran, 2004b). The ranges for cations, anions, and HCO_3 are also similar to previously published values for other regional caves (Musgrove and Banner, 2004; Guilfoyle, 2006; Wong et al, 2011).Seasonal variations in trace-element/Ca values range from a high of 717 mmol/mol for Mg/Ca, 2.4 mmol/mol for Sr/Ca, and 0.23 mmol/mol for Ba/Ca in the late spring/summer to a low of 662 mmol/mol for Mg/Ca, 2.0 mmol/mol for Sr/Ca, and 0.18 mmol/mol for Ba/Ca in the fall/winter.

Calcite growth rates range from 2.8 to 67 mg/day with an average growth rate of 18 mg/day and are similar compared to other caves studied in the region (Guilfoyle, 2006; Banner et al., 2007; Wong et al., 2011). On average, calcite growth is highest in August, ~ 25 mg/day, and lowest in the January, ~ 6 mg/day. Calcite growth rates for each site can be found in Appendix B. Cave-air CO_2 concentrations do not appear to inhibit calcite growth as they are near atmospheric throughout the year (394-638 ppm;

Figure 14). The average amount of calcite growth from all sites is not correlated with cave-air CO_2 concentrations; $r^2 = 0.02$; $p = 0.33$. Drip rate is correlated with calcite growth at four of six sites, WC-1, WC-5, WC-6, and WC-7. However, temperature explains the majority of the variance in calcite growth. The average amount of calcite growth from all sites is significantly related to the average monthly temperature, $r^2 = 0.84$; $p < 0.001$. Measured monthly cave drip water temperature is also significantly related to the average calcite growth rate at all sites, $r^2 = 0.42$; $p < 0.01$ (Table 3). These relationships are also present at each individual drip site (Figure 14).

Temperature also appears to have a significant effect on Mg/Ca, Sr/Ca, and Ba/Ca values. All drip sites at Westcave provide a significant positive correlation between average monthly surface air temperature and at least one of the following: Mg/Ca, Sr/Ca, and Ba/Ca (Table 3; Figure 15). This amounts to temperature being significantly correlated at three of six sites for Mg/Ca, five of six sites for Sr/Ca, and six of six sites for Ba/Ca. Similar trends are revealed when comparing measured drip water temperature to trace-element/Ca values (Table 4; Figure 15).

For drip sites where air and water temperatures are significantly correlated with Mg/Ca (n = 3), Sr/Ca (n = 5), and Ba/Ca (n = 6), these values were standardized to each drip site's Mg/Ca, Sr/Ca, and Ba/Ca mean. Standardization allows for drip sites with varying concentrations of trace-element/Ca values to be compared on the same scale. The results indicate that standardized trace-element/Ca values follow similar trends at each drip site (Figure 15). When the standardized Sr/Ca and Ba/Ca values from all sites combined are compared to average monthly surface air temperature there is a significant correlation between standardized Sr/Ca and average monthly surface air temperature, $r^2 = 0.80$ (Figure 16a) and a significant correlation between the average of all drip sites standardized Sr/Ca values and average monthly surface air temperature, $r^2 = 0.61$ (Figure 16b). There is also a significant correlation between standardized Ba/Ca and average monthly surface air temperature, $r^2 = 0.53$ (Figure 17a) and a significant correlation between the average of all drip sites standardized Ba/Ca values and average monthly surface air temperature, $r^2 = 0.65$ (Figure 17b).

Inconsistent correlations exist between Westcave drip site trace-element/Ca values and two measures of water flux, effective rainfall and drip rate. More consistent correlations appear between trace-element/Ca values and PDSI as the correlations appear for Mg/Ca at one of six drip sites, for Sr/Ca at three of six drip sites, and for Ba/Ca at four of six drip sites.

For drip sites where PDSI and trace-element/Ca values were significantly correlated (WC-1, WC-3, WC-4, WC-7), trace-element/Ca values and PDSI values were separately averaged for time periods when PDSI was wetter than normal (+2 and above), near normal (between -2 and 2), and drier than normal (-2 and below). Regression analyses were conducted by comparing the average PDSI values versus average trace-element/Ca values. The results can be found in Table 6 and Figure 18. For these same drip sites where trace-element/Ca values and PDSI were correlated, PDSI were standardized to their mean and trace-element/Ca values were standardized to each drip site's mean trace-element/Ca value. Standardized trace-element/Ca values and standardized PDSI values were separately averaged for time periods when PDSI was wetter than normal (+2 and above), near normal (between -2 and 2), and drier than normal (-2 and below). This method allows for comparison of all drip site's trace-element/Ca values at once to PDSI, thus strengthening statistical power by increasing sample size. When all drip sites are compared there appear to be significant correlations between PDSI and Sr/Ca ($r^2 = 0.49$; Figure 18) as well as significant correlations between PDSI and Ba/Ca ($r^2 = 0.73$; Figure 19).

There are three drip sites (WC-1, WC-4, and WC-7) where Ba/Ca is significantly correlated to both average monthly surface air temperature and PDSI. To determine the extent to which average monthly surface air temperature and PDSI are simultaneously correlated with Ba/Ca a multiple regression (step wise) was conducted for each site. The results indicate that at WC-1 Ba/Ca is significantly related to both average monthly surface air temperature ($\beta = 0.694$; $p < 0.001$) and PDSI ($\beta = -0.304$; $p < 0.05$); $r^2 = 0.73$ (Figure 20). Of the 73% of the variability in Ba/Ca that is explained by average monthly surface air temperature and PDSI, average monthly surface air temperature shares 65% of

the variance in Ba/Ca values while PDSI shares 18% of the variance. The multiple regression analysis allows the construction of a model equation to predict Ba/Ca values using both average monthly surface air temperature and PDSI; Ba/Ca = 0.161 + 0.001*(average monthly surface air temperature) – (0.001*(PDSI)). Similar results occur when conducting a multiple regression using WC-1 Sr/Ca values; however, these results will not be discussed. At WC-4 and WC-7 only average monthly surface air temperature is correlated with Ba/Ca when a multiple regression is conducted. Therefore, WC-1 was chosen to model Ba/Ca values.

5.0 Discussion

This discussion will center on assessing the controls on calcite growth and drip water trace-element/Ca values. A statistical methodology for comparing multiple drip sites to each other will be discussed as well. Temperature variations are correlated with calcite growth at all drip sites. The effect of temperature variations on trace-element/Ca values is strong as well, with average monthly surface air temperature and drip water temperature both correlating with Mg/Ca at three of six sites, with Sr/Ca at five of six sites, and with Ba/Ca at six of six sites. The processes to explain the temperature dependence of calcite growth and trace-element/Ca values appear to be driven by thermodynamic principles - the exchangeable reaction distribution coefficient of Mg, Sr, and Ba as well as the retrograde solubility of calcite. The relationship between water flux (drip rate, effective rainfall, PDSI) and trace-element/Ca variations is inconsistent between drip sites and water flux parameters. The strongest relationship is between PDSI and trace-element/Ca variations and it is hypothesized that this relationship is temperature driven as well.

It appears common in this region that calcite growth rate variability is either a direct or indirect result of seasonal changes in surface air temperature. In deeper, seasonally ventilated caves the density difference between cave air and atmospheric air is the driving force behind cave air CO_2 buildup and ventilation (e.g., Banner et al., 2007). This creates the seasonal deposition of calcite, where deposition is inhibited during

warmer months. In caves where the seasonal deposition of calcite occurs there is generally a relatively large cave volume compared to the area of the openings to the surface (e.g., Inner Space Cavern cave volume/area of openings to surface = ~0.0004 m^{-1}). The geometry at Westcave is distinct in its shallow depth and short length. It has a significantly larger opening area to cave volume ratio of ~0.02 m^{-1}. Therefore, in smaller, more open air caves such as Westcave, ventilation should occur year-round rather than seasonally. This should result in near atmospheric levels of cave air CO_2 year-round, as observed at Westcave (Figure 15), and allow for continuous calcite growth (Figure 15). Westcave is distinct from seasonally ventilated caves in this region in that calcite deposition (1) is not inhibited by CO_2, (2) is driven by surface air temperature variations, (3) is highest in warmer months, and (3) is lowest in cooler months. Considering that cave air CO_2 concentrations are near atmospheric year round and do not reach levels high enough to inhibit calcite deposition, variations in surface air temperature can explain the seasonal calcite growth variations. The relationship to temperature is strongest when calcite growth is compared to the average monthly air temperature but is also present when calcite growth is compared to measured water temperature (Table 3; Figure 14). The relationship between temperature and calcite growth at Westcave is theorized to be controlled by soil zone CO_2 processes and the retrograde solubility of calcite.

Other studies have linked increased soil zone CO_2 to temperature and soil moisture increases (Kjelgaard et al., 2008; Rastogi et al., 2002; Edward, 1975; Wiant, 1967), which will increase the concentration of CO_2 and decrease the pH in vadose zone waters. These more acidic waters will be able to dissolve an increased amount of carbonate minerals as they infiltrate through the karst overburden and to drip sites. It appears likely that the retrograde solubility of calcite assists in driving the positive relationship between temperature and calcite growth – as temperatures warm there is increased calcite precipitation due to retrograde solubility. Thus, at Westcave seasonal temperature variations drive seasonal calcite deposition where more calcite will be precipitated during warmer months. This relationship between calcite deposition and

temperature coincides with the relationship between trace-element/Ca values in cave drip waters, temperature, and the exchangeable reaction distribution coefficient (K_D) values of the carbonate minerals.

Thermodynamic principles can also explain the correlation between seasonal surface/ water temperature variations and trace-element/Ca values. For three of six drip sites there is a significant correlation between temperature and Mg/Ca values, for Sr/Ca this occurs at five of six drip sites, and for Ba/Ca this occurs at all drip sites (Table 3; Figure 15). The relation between Mg/Ca, Sr/Ca, and Ba/Ca and average monthly air temperature/water temperature appears to be dependent upon the exchangeable reaction distribution coefficient of each element. The K_D values of Mg, Sr, and Ba are less than 1, indicating that the elements prefer the aqueous phase relative to the solid phase. A likely scenario to explain the increase in drip water trace-element/Ca values, as temperature increases, is increased calcite precipitation prior to drip during warmer months, which leads to higher amounts of Ca leaving solution relative to Mg, Sr, and Ba. In cooler months there is less calcite precipitation prior to drip, which leads to lower Mg/Ca, Sr/Ca, and Ba/Ca values. It appears that temperature predicts trace-element/Ca values the best when the trace element has a lower K_D value. This is evidenced in this study as Ba/Ca at all drip sites (6/6) correlates with temperature and Ba has a lower K_D value versus Mg and Sr (e.g., Tesoriero, 1996). Sr has the second lowest K_D value and Sr/Ca correlates with temperature at 5/6 drip sites. Mg has the highest K_D value of the three elements and Mg/Ca correlates with temperature and the fewest number of drip sites, 3/6.

A difficulty with comparing absolute trace-element/Ca values between drip sites is that each drip site is subject to different flow paths, which produces distinct trace-element/Ca values at each drip site (e.g., Banner et al., 1996; Baldini, 2006). These variations are most likely a result of the heterogeneous distribution of flowpaths connected to each drip site, which will influence drip water residence time in the vadose zone. Therefore the trace-element/Ca values for each site were standardized with respect to the mean value of each drip site in order to make between drip site comparisons (Figure 15). Standardizing the trace-element/Ca values places all of the values on similar

scales. When comparing all drip sites to teach other, standardized trace-element/Ca values show a closer correspondence with temperature compared with non-standardized trace-element/Ca values (Figure 15).

3.5.1 Paleoclimate implications

One challenge with employing any geochemical proxy in stalagmites is defining a timescale with which to construct a geochemical time series. Stalagmites in central Texas do not generally have visible seasonal laminations and do not produce consistent annual bands like tree rings do. As a consequence, age control relies on radiometric ages by U-series methods, which while accurate cannot provide annual resolution (Musgrove et al., 2001). Therefore, the seasonal variations in trace elements/Ca (especially Ba/Ca) provide an opportunity for improving age constraints. This offers an advantage relative to U-series dating as U-series dating (1) requires a larger sample size, which limits the resolution of dates that can be procured from a stalagmite sample; and (2) has a relatively high error, which prevents annual/seasonal age constraints.

At Westcave Mg/Ca values are not as reliable as a temperature proxy (when compared to Sr/Ca and/or Ba/Ca) and this might be attributed to Mg/Ca also being controlled by hydrologic variability (e.g., Fairchild and Treble, 2009; Wong et al., 2011). Sr/Ca values have been widely used in sea surface temperature studies. The Sr/Ca value in seawater is less variable than that of drip waters due to the oceans behaving as a well mixed reservoir relative to Sr and Ca (Beck, 1992). This is contrasted against the varying rates and magnitudes of ion exchange, dissolution and other processes that result in local heterogeneities of trace elements in the soil and limestone overlying a cave. Thus, the accuracy of paleotemperatures in corals is much higher than what can be gleaned from cave drip waters. However, Sr/Ca and Ba/Ca values of cave drip waters at Westcave can provide geochemical laminae, which may enable the constraining of ages at a seasonal resolution in speleothems.

The strong seasonal temperature dependency of Sr/Ca and Ba/Ca values in cave drip waters can potentially produce geochemical laminae in a speleothem. It can then be

possible to constrain the ages of speleothems at Westcave at a seasonal resolution. Seasonal age constraints are advantageous as the high resolution dating of speleothems by radiometric methods is difficult due to the large amount of calcite that must be sampled to provide the most accurate date possible. There is also a relatively high degree of uncertainty of the dates (i.e., +/- 100 years, which limits annual dating). Thus, a limited number of dates can be taken from a single speleothem, which prevents high resolution dating. Furthermore, a low percentage of speleothems have visible annual growth bands, which prevents dating by this method (Baker, 2008). Trace-element/Ca values may provide a means of placing age constraints on speleothems from Westcave. This is due to the correspondence of Sr/Ca and Ba/Ca with seasonal temperature variations, which represents an annual cycle.

The method of seasonally constraining ages in stalagmites using seasonal Sr/Ca and Ba/Ca variations would entail selecting multiple stalagmites and analyzing the trace-element/Ca values along each growth axis. The trace-element/Ca values can then be standardized to equate trace-element/Ca variations on similar scales. Having multiple stalagmite samples strengthens the statistical results through an increased sample sizes. This is a statistical method that has yet to be applied to the comparison of multiple stalagmites. Agreement between multiple stalagmites also strengthens confidence in the reliability of the measured trace-element/Ca values and their preservation of temperature/climatic variations. The statistical method used in this study is similar to the methodology used in dendrochronology studies in that multiple samples are taken at a study site. Multiple samples are required as tree ring growth is predominantly a function of climate but there are other variables that can cause between-tree differences. Collection of multiple samples at one location allows for statistical comparisons to reduce noise associated with variables other than climate. In dendrochronology these variables include nutrient supply, tree genetics, and tree location. In the case of cave drip water studies the pertinent variables are heterogeneities in the soil and limestone composition, the heterogeneous distribution of flowpaths above a drip site and varying rates of the processes of calcite dissolution and precipitation prior to drip. Thus, first assessing the

modern system and standardizing trace elements of drip waters at multiple drip sites offers two advantages; (1) multiple stalagmites from a single cave can be analyzed and compared to each other as standardization reduces between-site trace-element/Ca variations that are not caused by temperature and (2) the correspondence in peaks of standardized trace-element/Ca values can provide seasonal age constraints..

The standardization of multiple samples has the previously discussed advantage of increasing the sample size within a cave. It is feasible that this method can also be used to compare multiple samples from different caves in the same region. It also appears feasible that multiple caves in the same region can be compared to each other assuming that there is a similar trace-element/Ca response to climate conditions at each drip site at each cave. It might also be possible to compare caves from different regions if the climate variable controlling variations in the climate proxy is changing on a similar timescale. For example, the trace-element/Ca response to seasonal temperature variations in Texas will probably not be a good correlate with the response in a region with a different climate (i.e., higher latitudes). However, lower resolution variations or more globally related cycles, such as solar cycles, might provide significant correlations between regions.

3.5.2 Trace elements and water flux

In general, temporal changes in drip rates at Westcave do not appear to be driven by changes in rainfall or effective precipitation (Figure 14). This has implications for the extent to which trace-element/Ca values vary in accordance with rainfall. Instead of being predominantly influenced by water flux, trace-element/Ca values appear to be predominantly controlled by surface air temperature and drip water temperature variations.

The most consistent correlations between water flux and trace-element/Ca variations occur when examining PDSI (Table 6). The relationship between trace-element/Ca values and PDSI is explainable by examination of the inputs to PDSI. The PDSI scale is a combination of water flux and temperature, thus the relationship of PDSI

to trace-element/Ca values is hypothesized to be predominantly driven by temperature variations and not water flux. It is more likely that temperature dictates this relationship as PDSI is comprised of air temperature, soil moisture, and rainfall amount. Thus, there is a large component of temperature and evaporation in the calculation of PDSI, which relates to trace-element/Ca variability as discussed in the previous sections. Ba/Ca values have the strongest correlation with temperature and with PDSI (Tables 3-4, 6; Figures 15, 6, 8-10), which relates to Ba having the lowest K_D value of the three trace elements studied. Thus implying that a lower K_D value will increase the magnitude of response to temperature variations. This assists in reducing noise associated with other variables that interfere with the partitioning of Ba to the solid/aqueous phase. Increasing the magnitude of a signal (in this case Ba/Ca values) will inherently reduce the amount of noise associated with other variables. For example, it's like having a television in a room with other sources of noise. If the television is set at a low volume then the other noises in the room can be heard; if the volume of the television is sufficiently loud, then there will be no detection of noise from the other sources in the room.

Although significant, the correlation between trace-element/Ca values and PDSI is low to moderate. This can be attributed to trace-element/Ca values varying on a higher frequency scale as drip waters are subject to shorter term variations through the processes of precipitation and dissolution of carbonate as they infiltrate through the vadose zone. The low correlation is most likely a product of the heterogeneous nature of the karst system with respect to varying flowpaths on a micro and macro scale as well as varying concentrations of CO_2 in the soil zone and degassing of CO_2 at varying rates in the karst overburden.

PDSI is subject to lower frequency variations as it is comprised of monthly assessments of rainfall, temperature, and soil moisture, which encompass the previous 12 months and are weighted more heavily towards the current month. Monthly variations are subject to lower frequency variations compared to the highly variable hydrologic response of the karst system. At almost all drip sites, when PDSI and trace-element/Ca values are compared on more similar frequencies (by averaging the values during distinct

periods of moisture regimes; refer to Results section), PDSI significantly correlates with trace-element/Ca values at a similar or much higher regression coefficient than when the raw values of PDSI and trace-element/Ca are compared (Figures 19-20).

To equate multiple drip sites on the same scale, Ba/Ca and Sr/Ca were standardized to each drip sites' mean, where Ba/Ca and/or Sr/Ca are significantly correlated with PDSI. The standardized Ba/Ca and Sr/Ca values and PDSI values were then averaged for time periods when PDSI values were wetter than normal (+2 and above), near normal but positive (between -2 and 2), and drier than normal (-2 and below). This approach provides a method for comparing multiple drip water sites with varying concentrations of trace elements (Figures 19-20). Standardizing values offers the advantage of comparing multiple drip sites, which can then be applied to compare multiple speleothem samples. This may strengthen the statistical power of paleoclimate interpretations by increasing the sample size in a similar manner to the comparison of multiple samples in dendrochronology studies.

The relationship between PDSI and trace-element/Ca values is encouraging for paleoclimate reconstruction as PDSI (1) is a regional indicator of climate, (2) has been used in dendrochronology to reconstruct regional PDSI to the 15^{th} century (Stahle and Cleaveland, 1988; Cleaveland et al., in prep), (3) PDSI and trace-element/Ca values of calcite can be averaged/standardized to potentially determine periods of abnormally high or low rainfall, and (4) PDSI is comprised of a large temperature component and temperature appears to control trace-element/Ca values at Westcave Preserve.

It is possible that these methods can also be applied to reconstruct temperature variations at other caves with similar characteristics - relatively large opening area to cave volume ratio and/or well ventilated with an atmosphere similar to surface conditions. It can also be applied to portions of caves near the entrance where CO_2 is closer to atmospheric year round and cave air temperature varies seasonally. The statistical methods outlined in this study can also be applied to any cave to assist in strengthening confidence in the climate signal detected in a speleothem.

3.5.3 Modeling of Ba/Ca at WC-1

A step wise multiple regression using site WC-1 drip water Ba/Ca as the dependent variable and both average monthly surface air temperature and PDSI as predictor variables yields a significant relationship ($r^2 = 0.73$; Figure 20) that can be modeled using the equation: Ba/Ca = 0.161 + 0.001*(average monthly surface air temperature) – (0.001*(PDSI)). This allows for the prediction of past WC-1 drip water Ba/Ca values using historic average surface air temperature and PDSI values (Figure 21). This can be applied to the paleoclimate study of stalagmites by providing a model in which to compare expected calcite Ba/Ca versus measured calcite Ba/Ca values. In a manner similar to dendrochronology, predicted Ba/Ca values can be calibrated with modern day temperature and PDSI to decipher Ba/Ca values in a stalagmite. This has the potential to assist in providing seasonal age constraints and to reconstruct PDSI values. Again, would not it be most useful to use the modern relationship and stalagmite Ba/Ca as a predictor of past PDSI? Why not as a predictor of past temperature? The 20th century model is a good way to ground truth the proxy once a speleothem record for the 20th century is generated.

3.6 Conclusions

This study highlights the utility of a rigorous assessment of the modern hydrologic/climate system and the subsequent response of calcite deposition rates and drip water trace-element/Ca values in a central Texas cave. Variation in the average amount of calcite growth from all sites is significantly related to the seasonal average monthly surface air temperature variations. It appears that the retrograde solubility of calcite has a role in this relationship, where greater amounts of calcite will precipitate when temperatures are warmer. Seasonal temperature variations also affect trace-element/Ca values. All drip sites at Westcave provide a significant positive correlation between average monthly surface air temperature and at least one of the following: Mg/Ca, Sr/Ca, and Ba/Ca. This amounts to temperature being significantly correlated at three of six sites for Mg/Ca, five of six sites for Sr/Ca, and six of six sites for Ba/Ca.

At Westcave, without assessment of the relationship between cave air temperature and drip water trace-element/Ca values it could have been possible to misinterpret the Mg/Ca, Sr/Ca, and Ba/Ca oscillations in drip waters as a water flux proxy. Instead, it appears that seasonal temperature variations drive trace-element/Ca values. The strong temperature dependency of calcite deposition and trace-element/Ca variations is a function of the cave geometry- small size, relatively large cave volume to cave opening ratio. This geometry allows the cave atmosphere to be similar to the surface atmosphere with respect to low, fairly constant CO_2 concentrations and seasonal air temperature variations.

The most consistent correlations between water flux and trace-element/Ca variations occur when examining PDSI. Although significant, the correlation between trace-element/Ca values and PDSI is low to moderate. At almost all drip sites, when PDSI and trace-element/Ca values are compared on more similar frequencies (by averaging the values during distinct periods of moisture regimes; refer to Results section), PDSI significantly correlates with trace-element/Ca values at a similar or much higher regression coefficient than when the raw values of PDSI and trace-element/Ca are compared.

Standardization of trace-element/Ca values allows for drip sites with varying concentrations of trace-element/Ca values to be compared on the same scale. When the standardized Sr/Ca and Ba/Ca values from all sites combined are compared to average monthly surface air temperature there is a significant correlation between the standardized trace-element/Ca values and average monthly surface air temperature. The standardization of trace-element/Ca values has provided an avenue in which we can begin to attempt to interpret the past. This has implications for (1) constraining ages at a seasonal resolution using geochemical laminae produced by variations in trace-element/Ca values; (2) increasing sample size and statistically strengthening interpretations made from calcite trace-element/Ca values by allowing for the comparison of multiple samples; (3) offers a methodology in which to compare multiple drip sites in a single cave and multiple drip sites between caves.

To determine the extent to which average monthly surface air temperature and PDSI are simultaneously correlated with Ba/Ca a multiple regression (step wise) was conducted for each site. The results indicate that at WC-1 Ba/Ca is significantly related to both average monthly surface air temperature and PDSI. The modeling of trace-element/Ca values using a multiple regression equation provides a method in which to compare expected calcite Ba/Ca versus measured calcite Ba/Ca values. In a manner similar to dendrochronology, predicted Ba/Ca values can be calibrated with modern day temperature and PDSI to decipher Ba/Ca values in a stalagmite. This has the potential to assist in providing seasonal age constraints and to reconstruct PDSI values.

Tables

Table 1. Statistical relationships for physical and geochemical parameters for Group 1, ISSR 3 and ISSR 5 drip sites. At both drip sites there are statistically significant correlations between all measures of water flux and Mg/Ca. The sign of β represents the direction of the correlation.

Site	Effective rainfall vs. drip rate	Drip rate vs. Mg/Ca	Effective rainfall vs. Mg/Ca	PDSI vs. drip rate	PDSI vs. Mg/Ca
ISSR 3	$r^2 = 0.23$; $p < 0.005$ ($\beta = +$)	$r^2 = 0.37$; $p < 0.001$ ($\beta = -$)	$r^2 = 0.26$; $p < 0.001$ ($\beta = -$)	$r^2 = 0.28$; $p < 0.001$ ($\beta = +$)	$r^2 = 0.28$; $p < 0.001$ ($\beta = -$)
ISSR 5	$r^2 = 0.47$; $p < 0.001$ ($\beta = +$)	$r^2 = 0.80$; $p < 0.001$ ($\beta = -$)	$r^2 = 0.41$; $p < 0.005$ ($\beta = -$)	$r^2 = 0.26$; $p < 0.005$ ($\beta = +$)	$r^2 = 0.19$; $p < 0.05$ ($\beta = -$)

Table 2. Statistical relationships for physical and geochemical parameters for Group 2 drip sites. Significant correlations denoted by an asterisk. The sign of β represents the direction of the correlation.

Site	Effective rainfall vs. drip rate	Drip rate vs. Mg/Ca	Effective rainfall vs. Mg/Ca	PDSI vs. drip rate	PDSI vs. Mg/Ca
ISSR 6	$r^2 = 0.01$; $p = 0.33$	$r^2 = 0.07$; $p = 0.16$	$r^2 = 0.05$; $p = 0.21$	$r^2 = 0.19$; $p < 0.05$ ($\beta = +$)*	$r^2 = 0.002$; $p = 0.43$
ISSR 7	$r^2 = 0.003$; $p = 0.44$	$r^2 = 0.09$; $p = 0.13$	$r^2 = 0.33$; $p < 0.05$ ($\beta = -$)*	$r^2 = 0.005$; $p = 0.37$	$r^2 = 0.51$; $p < 0.001$ ($\beta = -$)*
ISSR 8	$r^2 = 0.09$; $p = 0.13$	$r^2 = 0.31$; $p = 0.01$ ($\beta = -$)*	$r^2 = 0.002$; $p = 0.44$	$r^2 = 0.07$; $p = 0.13$	$r^2 = 0.10$; $p = 0.10$
ISSR 9	$r^2 = 0.002$; $p = 0.44$	$r^2 = 0.02$; $p = 0.29$	$r^2 = 0.01$; $p = 0.34$	$r^2 = 0.38$; $p < 0.005$ ($\beta = +$)*	$r^2 = 0.22$; $p < 0.05$ ($\beta = -$)*
ISST	$r^2 = 0.003$; $p = 0.26$	$r^2 = 0.19$; $p < 0.001$*	$r^2 = 0.001$; $p = 0.37$	$r^2 = 0.\ 04$; $p < 0.05$ ($\beta = +$)*	$r^2 = 0.04$; $p < 0.05$*
ISLM	$r^2 = 0.01$; $p = 0.16$	$r^2 = 0.002$; $p = 0.34$	$r^2 = 0.04$; $p = 0.10$	$r^2 = 0.01$; $p = 0.11$	$r^2 = 0.00$; $p = 0.29$

Table 3.The number of significant correlations between average monthly surface temperature versus calcite growth, Mg./Ca, Sr/Ca, and Ba/Ca values out of the total number of sites studied. Ranges and means of r^2 values are listed as well.

	Calcite growth vs. average monthly surface air temperature	**Mg/Ca vs. average monthly surface air temperature**	**Sr/Ca vs. average monthly surface air temperature**	**Ba/Ca vs. average monthly surface air temperature**
Sites with significant r^2/Total sites	7/7	3/6	5/6	6/6
Range of r^2	0.25-0.90	0.25-0.40	0.26-0.84	0.30-0.86
Mean of r^2	0.58	0.31	0.48	0.67

Table 4. The number of significant correlations between drip water temperature versus calcite growth, Mg./Ca, Sr/Ca, and Ba/Ca values out of the total number of sites studied. Drip water temperature for site WC-6 was used as a proxy for all drip sites. Ranges and means of the r^2 values are listed as well.

	Calcite growth vs. drip water temperature	**Mg/Ca vs. drp water temperature**	**Sr/Ca vs. drip water temperature**	**Ba/Ca vs. drip water temperature**
Sites with significant r^2/Total sites	5/7	3/6	5/6	6/6
Range of r^2	0.29-0.46	0.21-0.36	0.33-0.73	0.23-0.75
Mean of r^2	0.37	0.29	0.51	0.56

Table 5. Carbonate species SI vs. water temperature regressions. All correlations are positive.

Site	**Calcite SI vs. water temperature**	**Dolomite SI vs. water temperature**	**Strontianite SI vs. water temperature**	**Witherite SI vs. water temperature**
WC-1	$r^2 = 0.74$, $p < 0.05$	$r^2 = 0.87$, $p < 0.05$	$r^2 = 0.57$, $p = 0.07$	$r^2 = 0.78$, $p < 0.05$
WC-6	$r^2 = 0.33$, $p < 0.05$	$r^2 = 0.46$, $p < 0.05$	$r^2 = 0.33$, $p = 0.05$	$r^2 = 0.33$, $p < 0.05$

Table 6. Statistical relationships between average PDSI and average trace-element/Ca values. PDSI and trace-element/Ca values were averaged for time periods when PDSI values were wetter than normal (+2 and above), near normal but positive (between -2 and 2), and drier than normal (-2 and below). Only statistically significant r^2 values are shown.

Site	Average PDSI vs. average Mg/Ca	Average PDSI vs. average Sr/Ca	Average PDSI vs. average Ba/Ca
WC-1	$r^2 = 0.31$	$r^2 = 0.32$	$r^2 = 0.60$
WC-3	xx	$r^2 = 0.95$	xx
WC-4	xx	$r^2 = 0.93$	$r^2 = 0.84$
WC-5	xx	xx	xx
WC-6	xx	xx	xx
WC-7	xx	xx	$r^2 = 0.35$

xx = $p > 0.05$

FIGURES

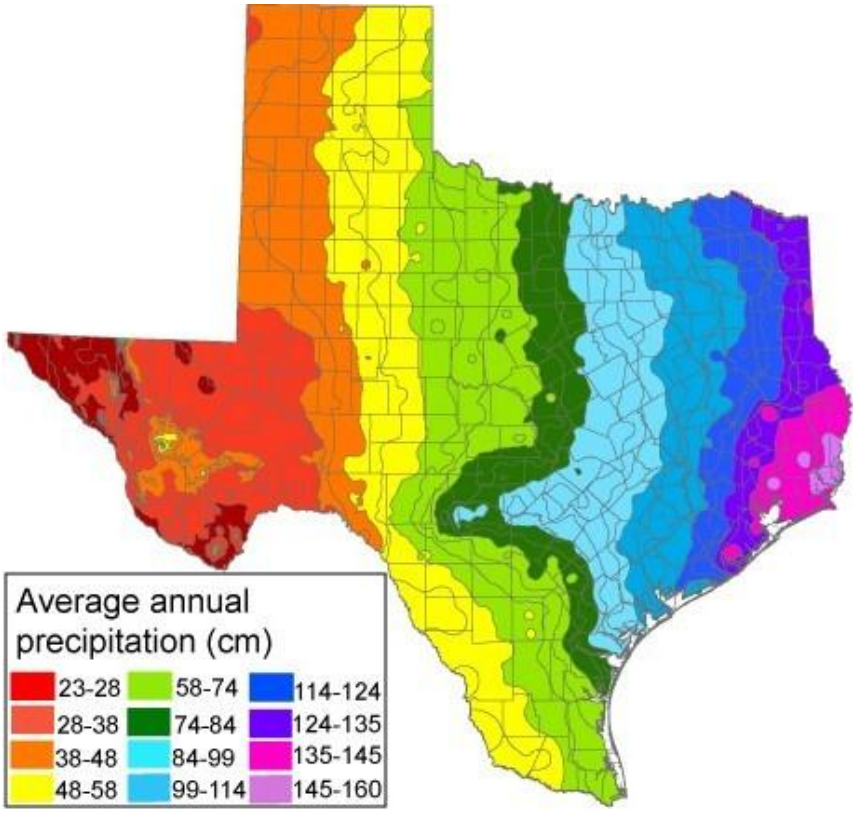

Figure 1. West to east rainfall gradient where there is less rainfall in the west and increasing precipitation to the east. The study area lies in a drought prone region of central Texas where average rainfall is 84-99 cm/yr (USDA NRCS, 2010).

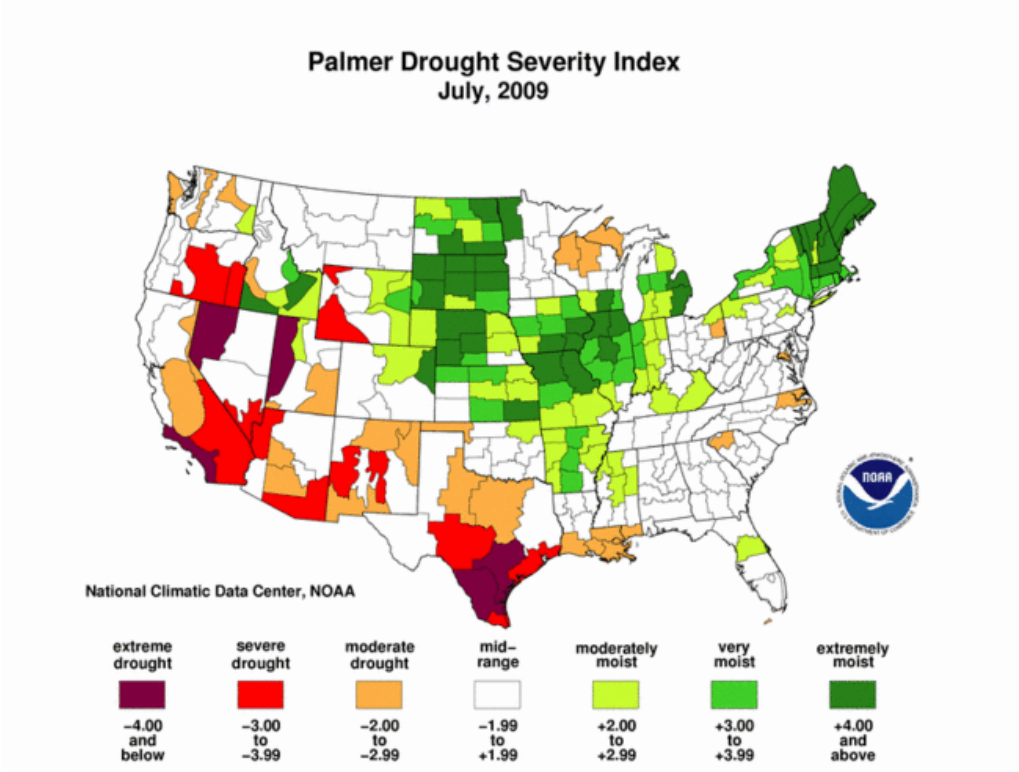

Figure 2. Palmer Drought Severity Index (PDSI) of July 2009 highlighting the drought of 2008-2009 in central Texas. The PDSI takes into account current and antecedent temperature, rainfall, and soil moisture conditions to construct a scale to measure drought/wetness conditions (NOAA, 2010).

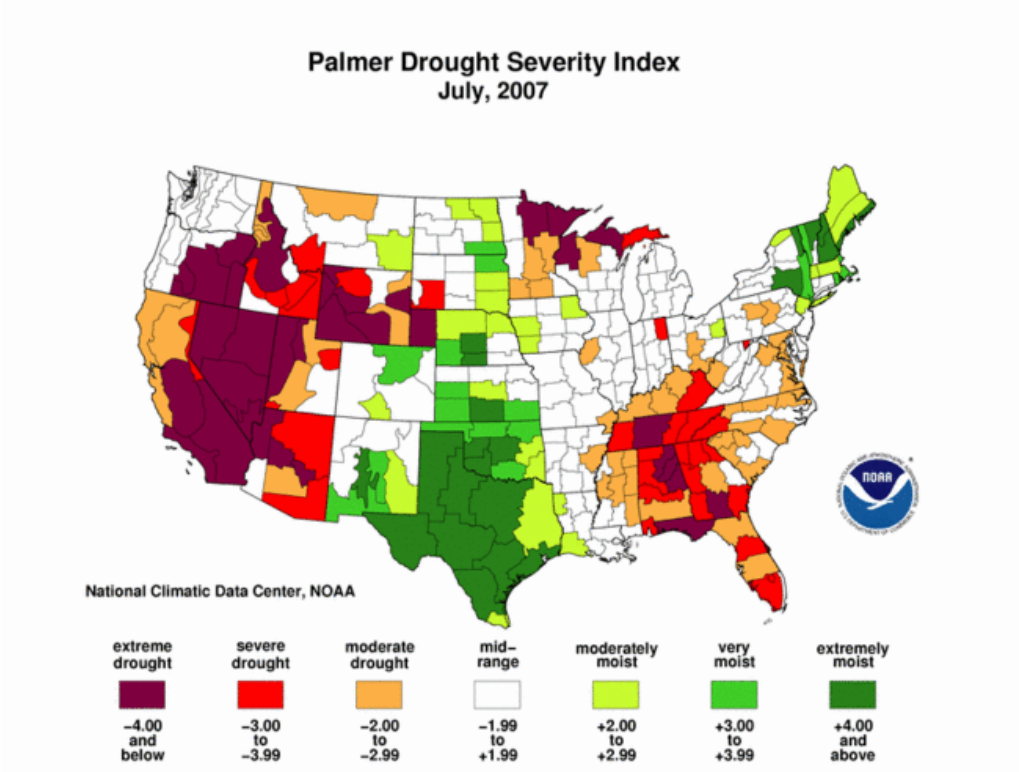

Figure 3. Palmer Drought Severity Index of July 2007 highlighting an abnormally wet period in central Texas. The PDSI takes into account current and antecedent temperature, rainfall, and soil moisture conditions to construct a scale to measure drought/wetness conditions (NOAA, 2010).

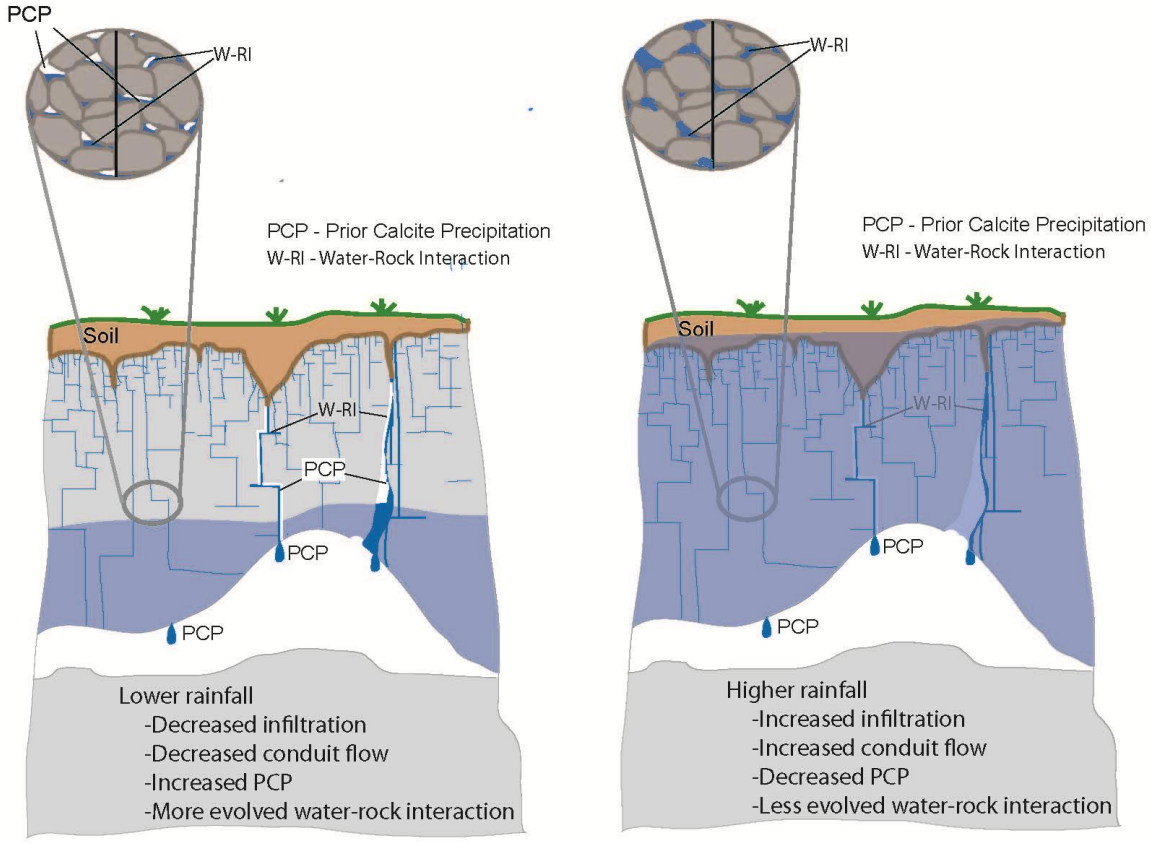

Figure 4. A schematic of the vadose zone above a cave during periods of (a) lower rainfall and (b) higher rainfall. During periods of lower rainfall less water infiltrates. This causes pore spaces to dry and increase prior calcite precipitation (PCP) and a higher proportion of more evolved water, with a longer residence time reaches the drip site. During periods of higher rainfall more water infiltrates. This causes pore spaces to be more fully saturated and decrease PCP. A higher proportion of less evolved water, with a shorter residence time will reach the drip site (modified from Wong et al., 2011).

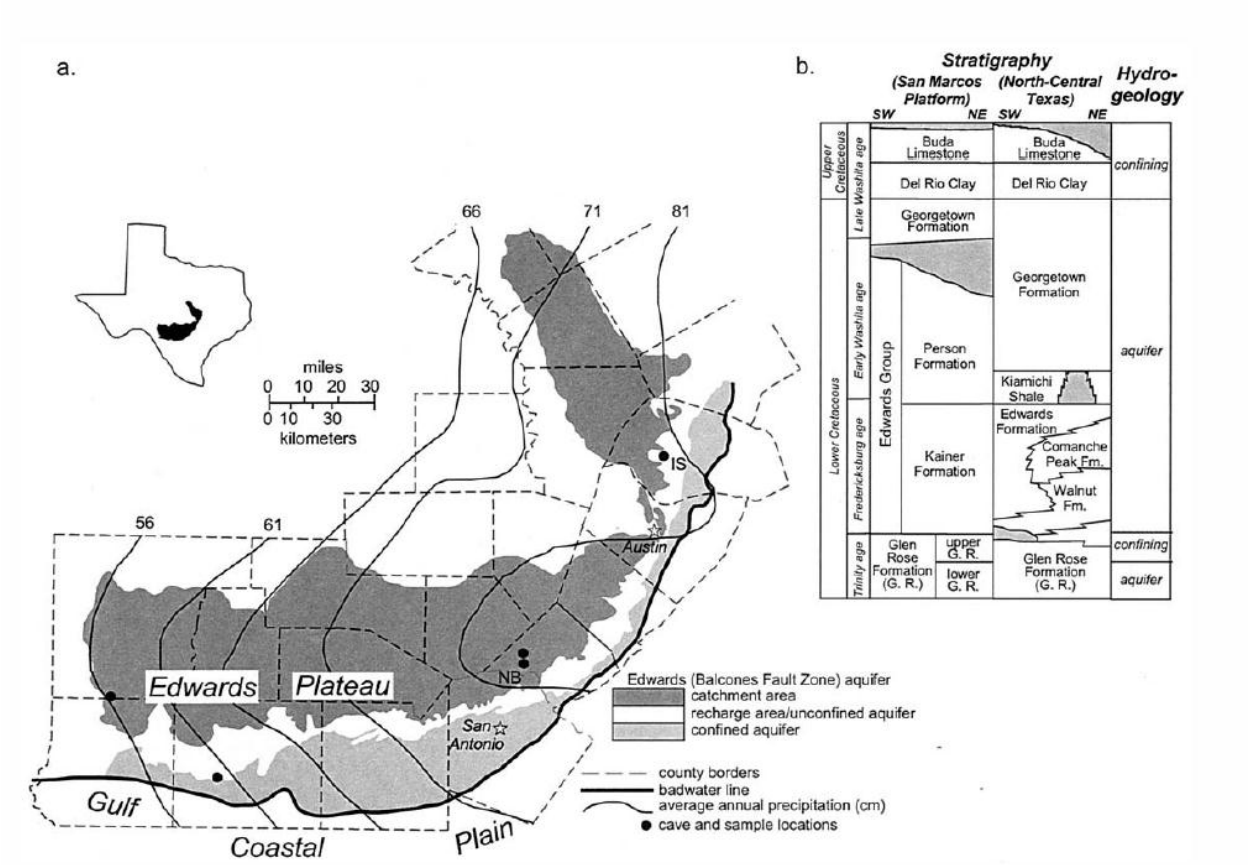

Figure 5. (a) Location of Inner Space Cavern in central TX and labeled IS on the map. NB represents Natural Bridge Caverns. Both caves are located on the eastern edge of the Edwards Plateau in the Edwards aquifer recharge zone. (b) Stratigraphic sequence in which cave IS is located (Musgrove and Banner, 2004).

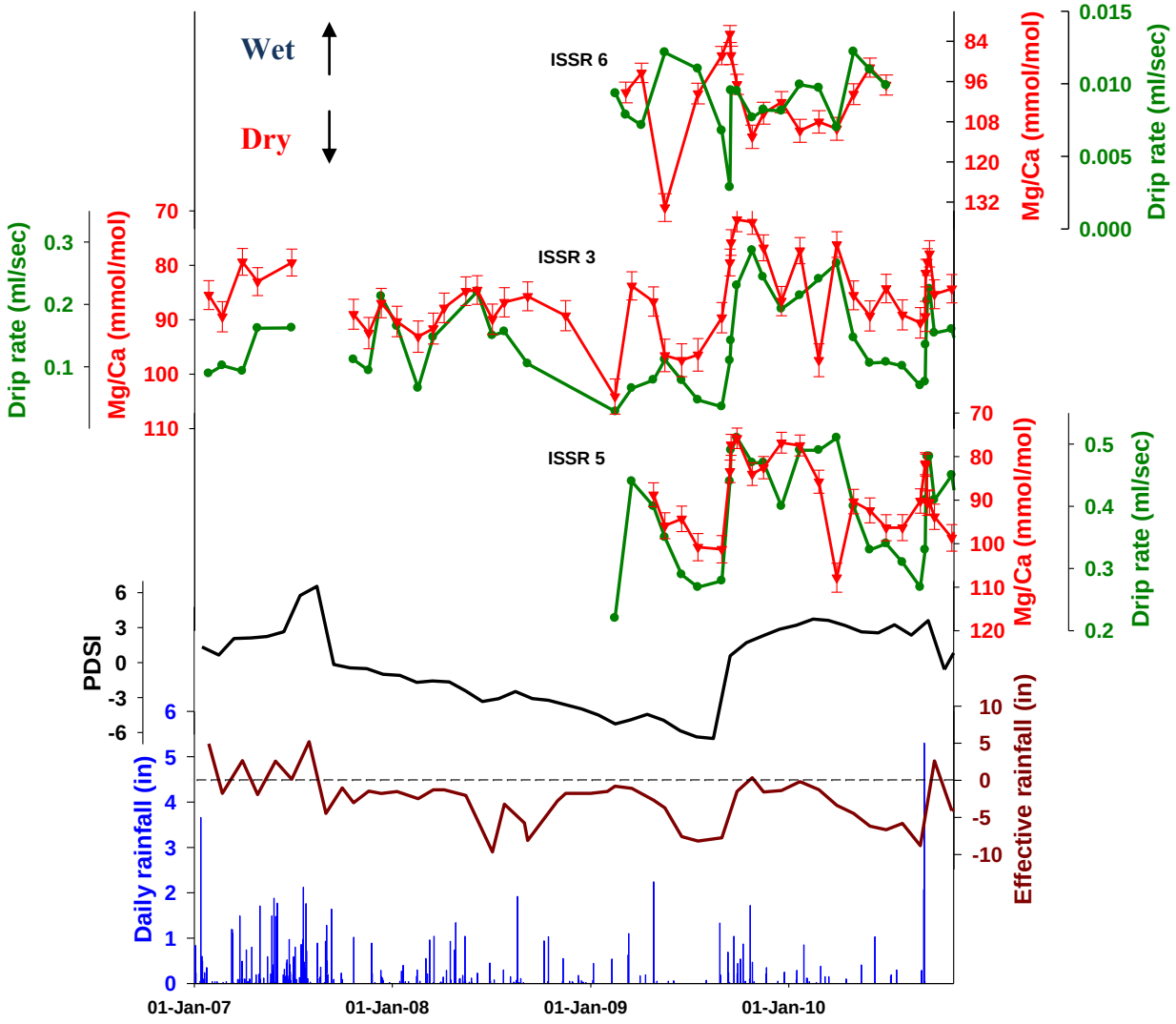

Figure 6. Time series of drip rates, Mg/Ca values, PDSI, and rainfall for Group 1 drip sites ISSR 3 and ISSR 5 and a representative Group 2 drip site, ISSR 6. At Group 1 sites, effective rainfall (effective rainfall = rainfall – potential evapotranspiration) is significantly related to drip rate; drip rate is significantly related to Mg/Ca values; effective rainfall is significantly related to Mg/Ca values; PDSI is significantly related to drip rate; and PDSI is significantly related to Mg/Ca values. At Group 2 sites relationships between water flux and Mg/Ca are not as consistent (e.g., ISSR 6). Mg/Ca values are plotted on a reversed axis.

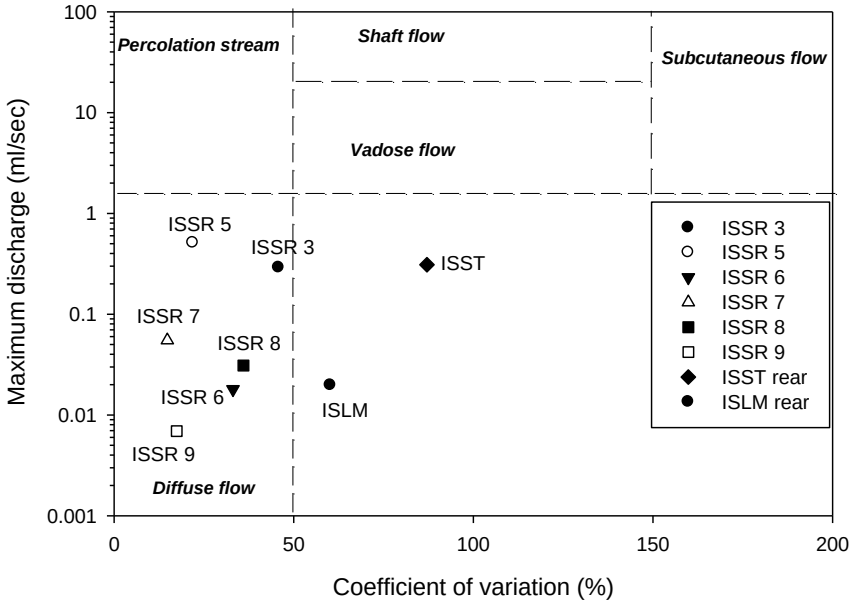

Figure 7. Maximum discharge (ml/sec) and coefficients of variation for the drip sites at Inner Space Cavern. The majority of drip sites can be classified as diffuse flow sites. It appears that the maximum discharge is a more important variable for locating intra-annual climate sensitive sites as Group 1 drip sites (ISSR 3 and ISSR 5) have the clearest intra-annual signal and the highest maximum discharge. (Classification scheme from Smart and Friederich, 1987).

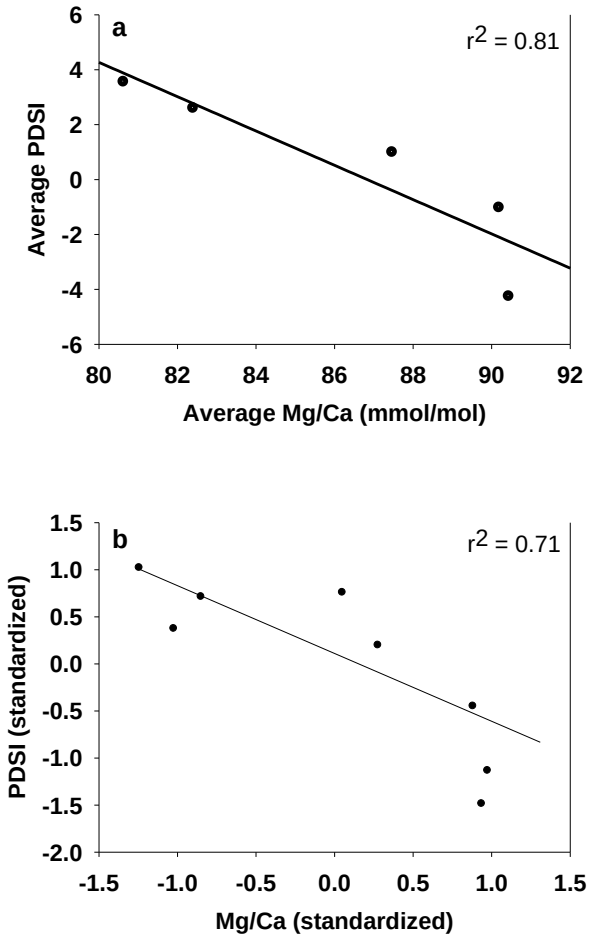

Figure 8. Average monthly PDSI and the corresponding average monthly drip water Mg/Ca values for the same time period at Group 1 drip site (a) ISSR 3; Mg/Ca and PDSI are significantly related ($r^2 = 0.81$; $p < 0.01$). Monthly PDSI was averaged during time periods when values were wetter than normal (PDSI greater than 2), near normal (PDSI between 0 and 2 as well as between 0 and -2), and when values were drier than normal (PDSI less than -2). Mg/Ca values for the same time periods as PDSI were averaged as well. This method equates the higher frequency variations of Mg/Ca to the lower frequency variations of PDSI. (b) Mg/Ca and PDSI values for Group 1 drip sites (n = 2). Mg/Ca and PDSI values have been averaged for time periods when values were wetter than normal (PDSI greater than 2), near normal (PDSI between 0 and 2 as well as between 0 and -2), and when values were drier than normal (PDSI less than -2). Mg/Ca and PDSI values were then standardized to each drip sites' mean and graphed for between site comparisons. Mg/Ca and PDSI are significantly related ($r^2 = 0.71$; $p < 0.01$).

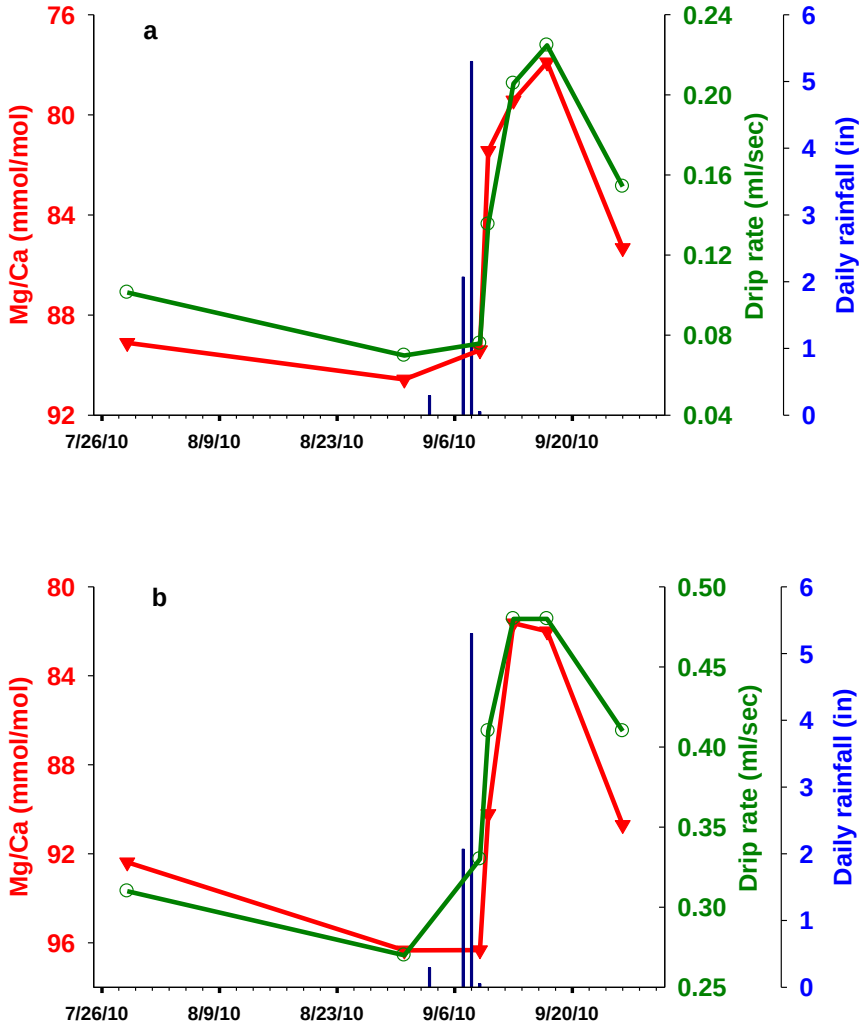

Figure 9. (a) Drip rate and Mg/Ca variations at drip site ISSR 3 for the time period prior to and after Tropical Storm Hermine. The large rain event is Tropical Storm Hermine, which originated in the Gulf of Mexico and passed through the region from 9/7/10 to 9/8/10. The axis for Mg/Ca values is reversed. Drip rate and Mg/Ca values are significantly correlated ($r^2 = 0.89$, $p < 0.005$). (b) Drip rate and Mg/Ca variations at drip site ISSR 5 for the time period prior to and after Tropical Storm Hermine. The large rain event is Tropical Storm Hermine, which passed through the region from 9/7/10 to 9/8/10. The axis for Mg/Ca values is reversed. Drip rate and Mg/Ca values are significantly correlated ($r^2 = 0.91$, $p < 0.005$).

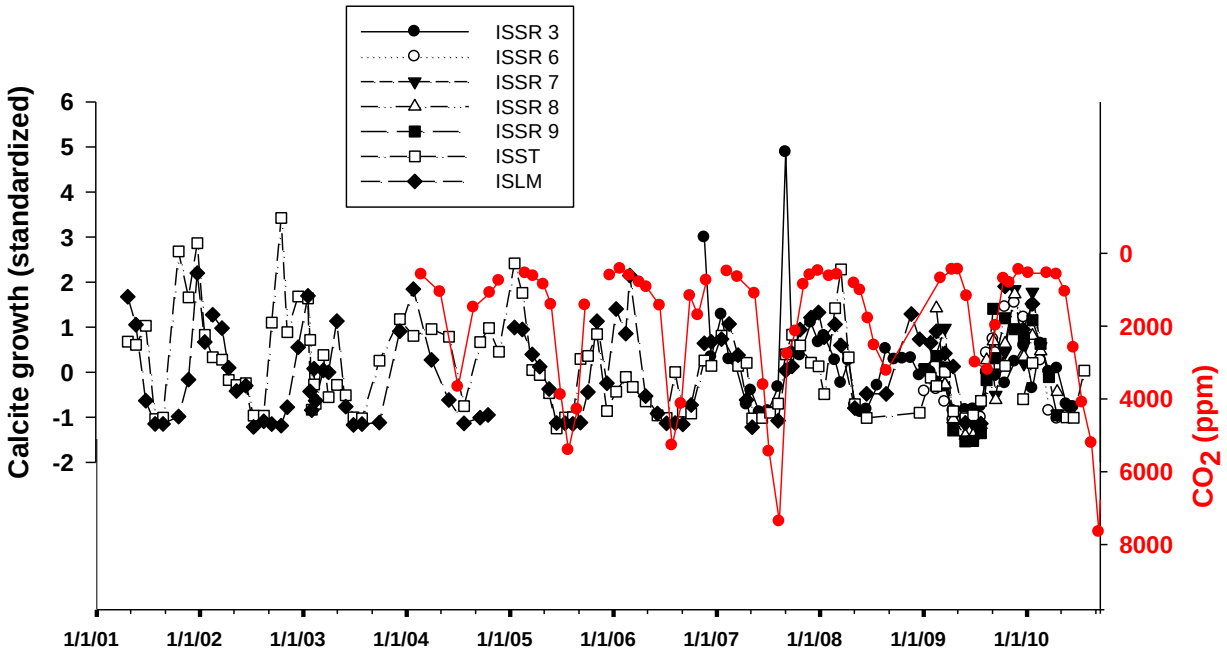

Figure 10. Calcite growth from glass substrates versus cave air CO_2 variations for drip sites in the study. Calcite growth rate was standardized to each drip site's mean to allow for comparison on a similar scale. CO_2 concentrations peak in the summer and reach a low point in the winter. Calcite growth peaks in the winter and reaches a low point in the summer.

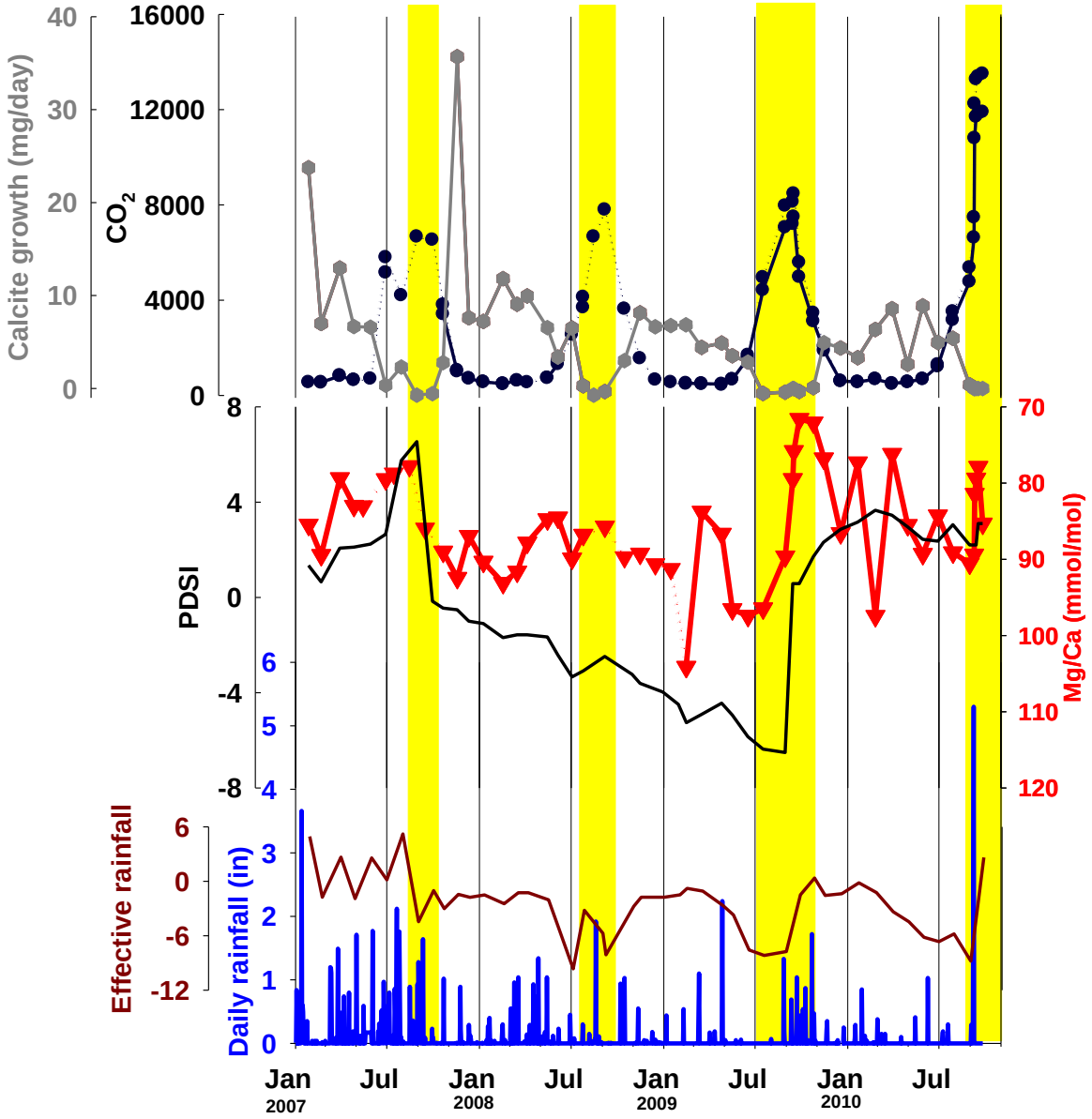

Figure 11. Time series of drip site ISSR 3 from January 2007 to September 2010. The yellow bars represent periods of high CO_2, which inhibit calcite deposition. Mg/Ca values are on a reversed axis. Even though calcite deposition is inhibited for ~4 months annually, there is a correlation between Mg/Ca and PDSI ($r^2 = 0.24$, $p < 0.05$; $\beta = -0.44$) when analyzing the data when CO_2 is less than 1000 ppm.

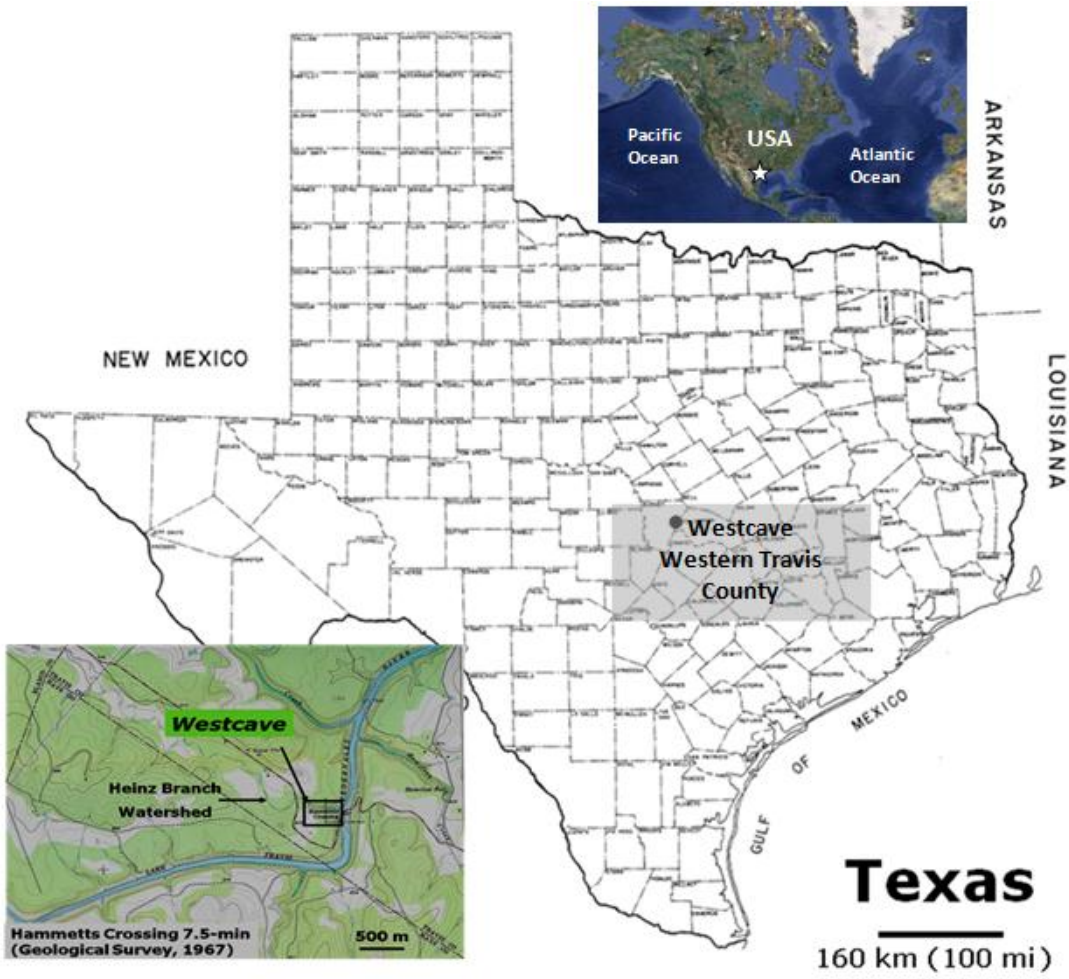

Figure 12. Regional setting of Westcave, located in the Heinz Branch Watershed in SW Travis County. The colored map of the USA is from Google Maps. (Modified from Caran, 2004b).

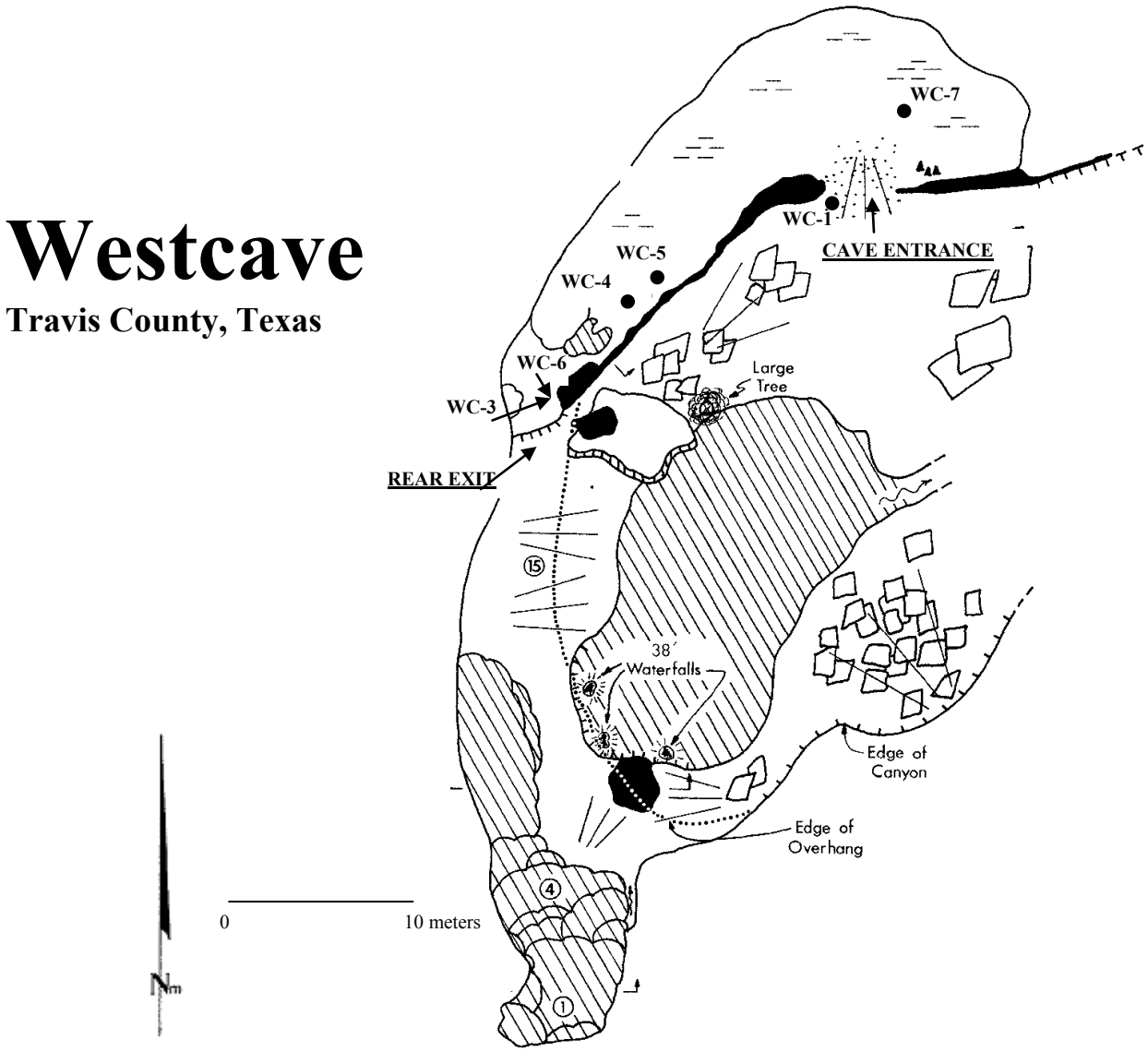

Figure 13. Site map of Westcave with drip sites WC-1, WC-3, WC-4, WC-5, WC-6, and WC-7 labeled. (Modified from Reddell and Smith, 1961; Fieseler et al., 1972)

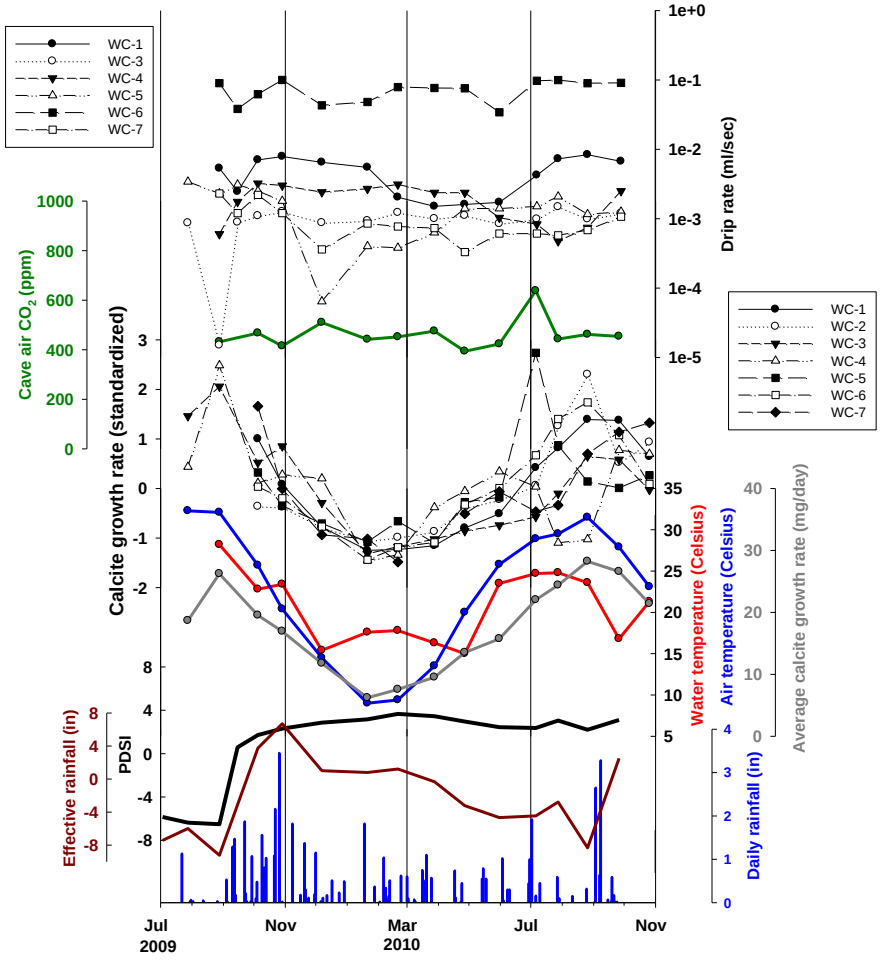

Figure 14. Time series of daily rainfall, effective rainfall, PDSI, drip water temperature, average monthly surface air temperature, average calcite growth for all drip sites combined, standardized calcite growth rate, cave air CO_2 concentration, and drip rate at Westcave during the study period. Air temperature is the average of the time period between sampling trips. Water temperature is directly measured in the cave. Average calcite growth rate is the mean rate (mg/day) for all drip sites. There is a significant positive correlation between average calcite growth and air temperature ($r^2 = 0.83$; $p < 0.001$) as well as average calcite growth and water temperature ($r^2 = 0.42$; $p < 0.01$). There is a positive correlation between calcite growth for each site and average air temperature. There is a positive correlation between calcite growth and water temperature for 5 of 7 drip sites. CO_2 concentration remains near atmospheric and does not significantly influence average calcite growth ($r^2 = 0.02$; $p = 0.33$). Daily rainfall, effective rainfall, and PDSI are not significantly related to calcite growth.

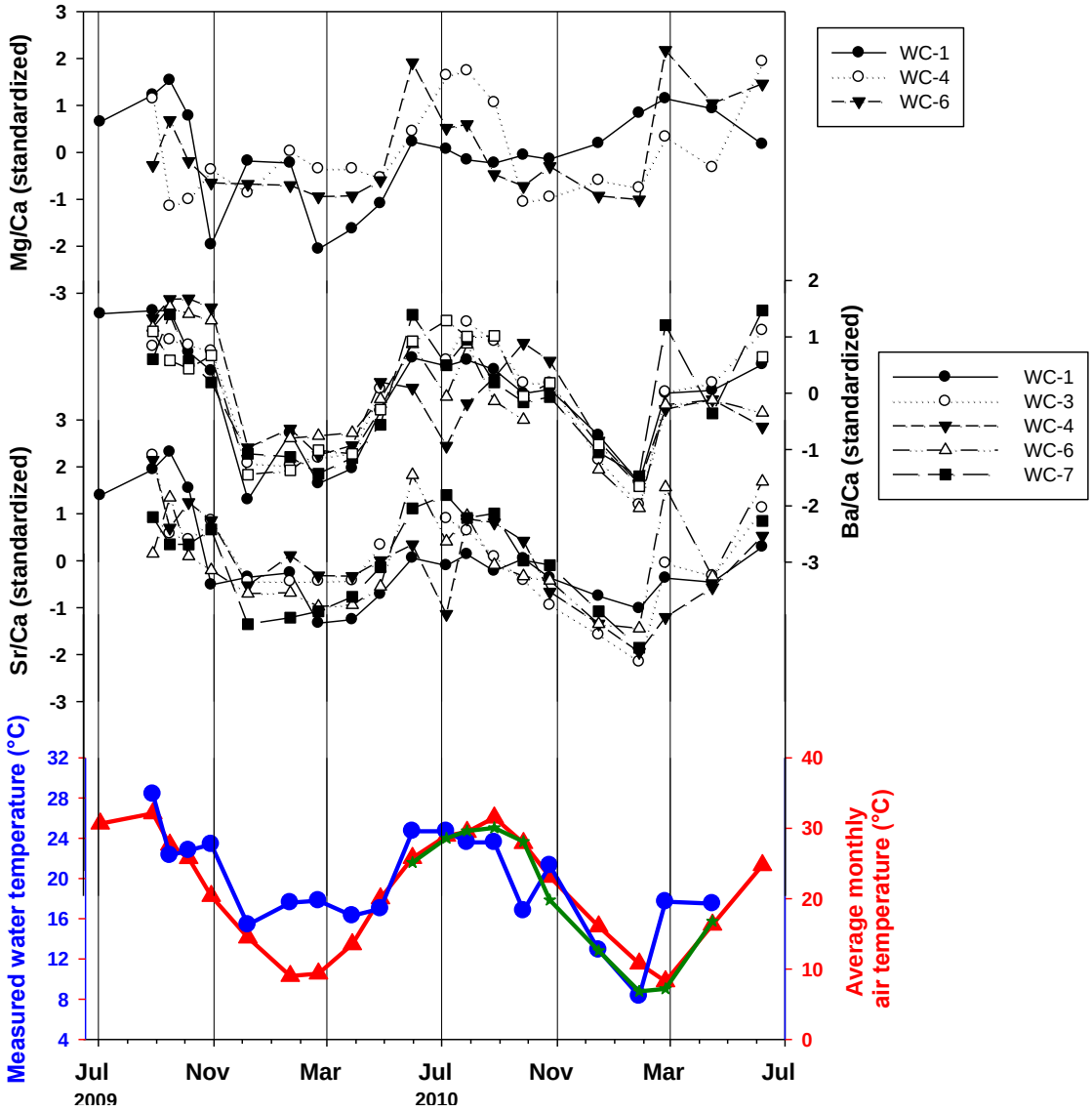

Figure 15. Time series of Mg/Ca, Ba/Ca, and Sr/Ca versus temperature for Westcave drip sites where temperature is significantly related to Mg/Ca, Ba/Ca, or Sr/Ca. Mg/Ca, Ba/Ca, and Sr/Ca values were standardized to each drip sites' mean to allow for between site comparisons. In the warmer months, at all sites depicted, Mg/Ca, Ba/Ca, and Sr/Ca values are highest and in the cooler months the values are the lowest.

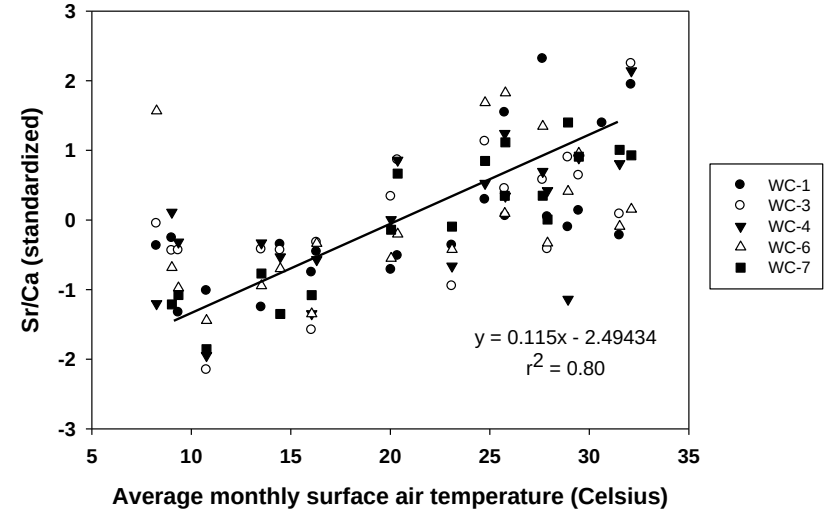

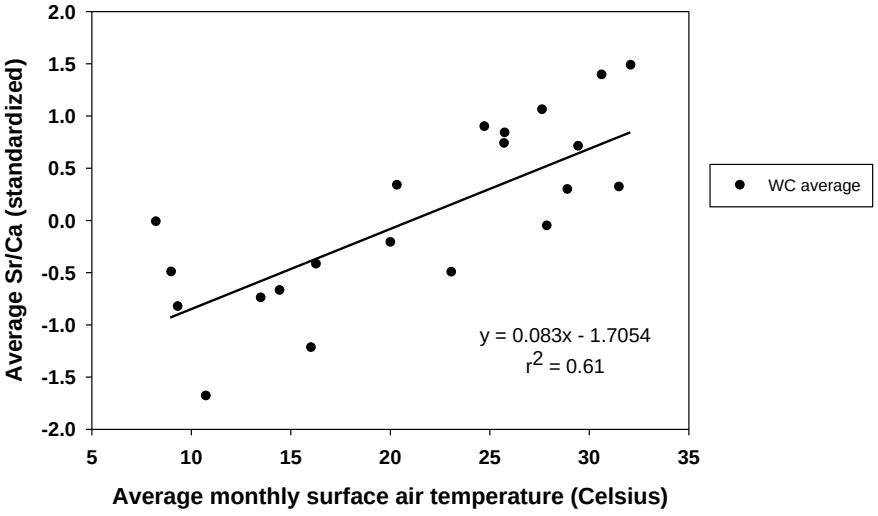

Figure 16. (a) Standardized Sr/Ca versus average monthly surface air temperature for all drip sites where Sr/Ca and average surface air temperature are significantly correlated. For five of six drip sites, Sr/Ca is significantly correlated to average surface air temperature; $r^2 = 0.80$. (b) Average standardized Sr/Ca of all drip sites where Sr/Ca is significantly correlated with average monthly surface air temperature. Average Sr/Ca is significantly correlated with average monthly surface air temperature; $r^2 = 0.61$.

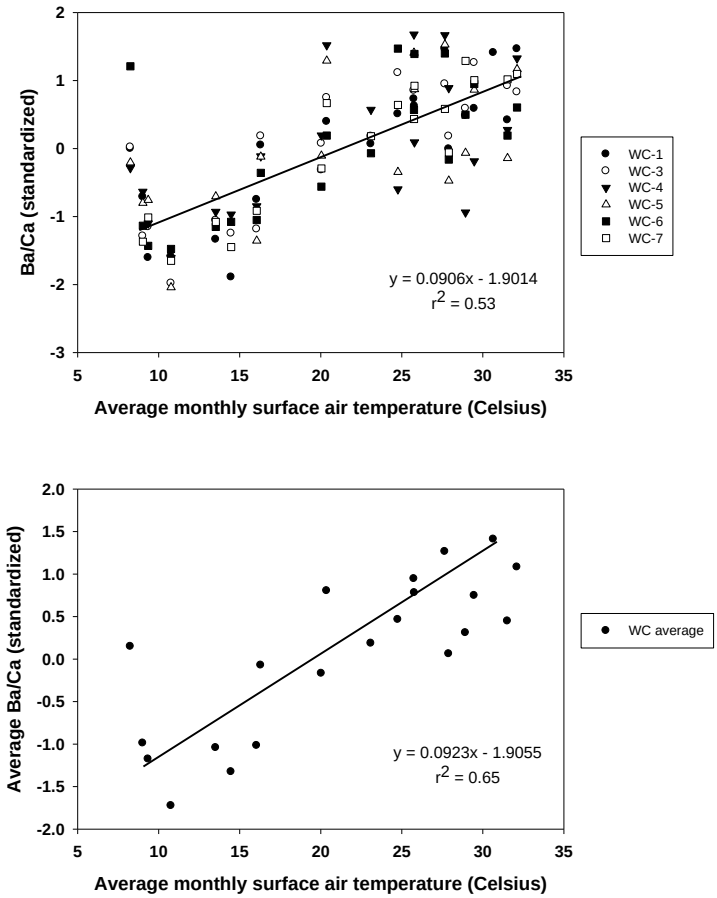

Figure 17. (a) Standardized Ba/Ca versus average monthly surface air temperature for all drip sites where Ba/Ca and average surface air temperature are significantly correlated. For six of six drip sites, Ba/Ca is significantly correlated to average surface air temperature; $r^2 = 0.53$. (b) Average standardized Ba/Ca of all drip sites where Ba/Ca is significantly correlated with average monthly surface air temperature. Average Ba/Ca is significantly correlated with average monthly surface air temperature; $r^2 = 0.65$.

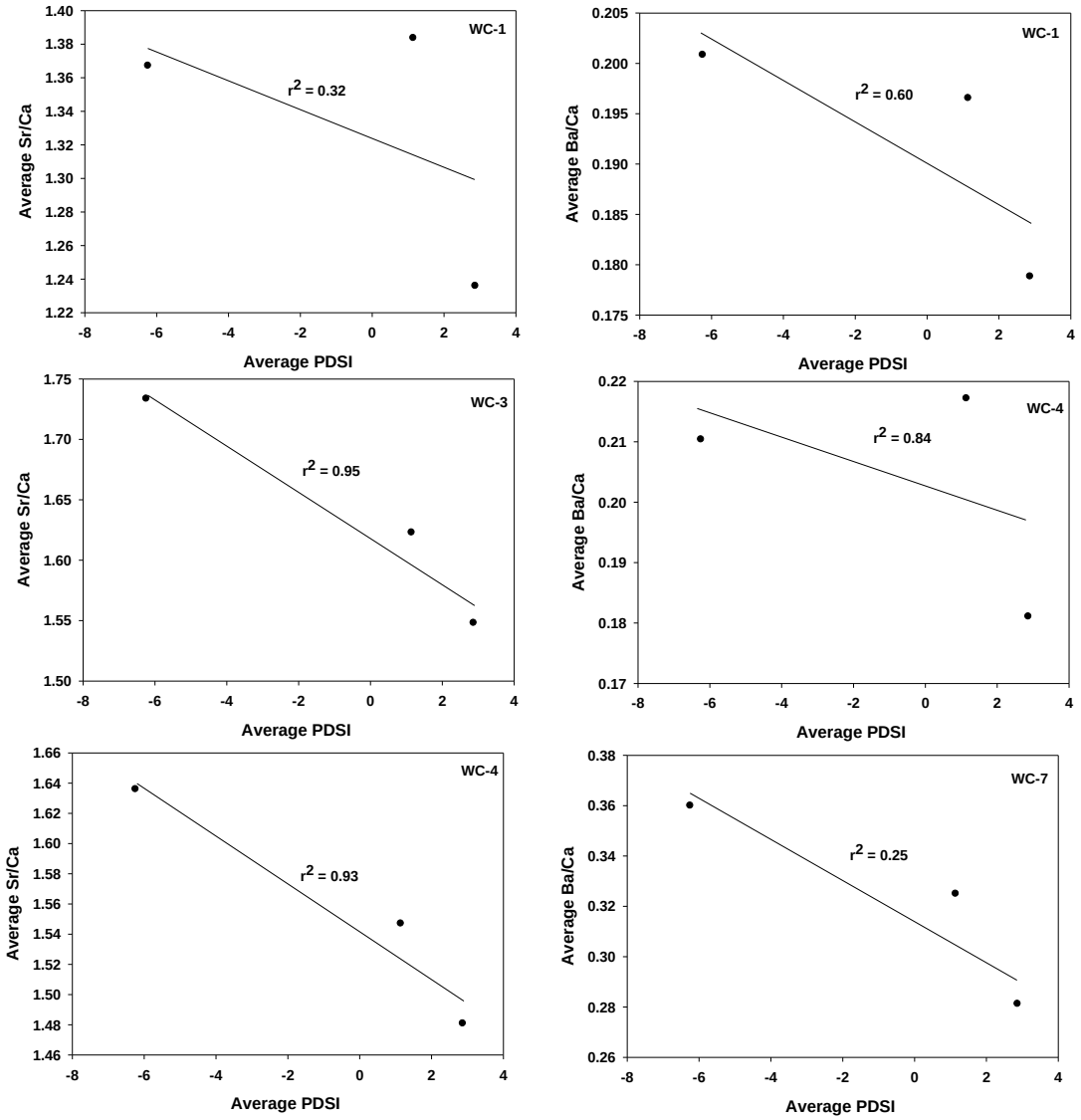

Figure 18. Significant correlations between average Sr/Ca values (mmol/mol) versus average PDSI values for when PDSI was wetter than normal (+2 and above), near normal (between -2 and 2), and drier than normal (-2 and below) at drip sites WC-1 ($r^2 = 0.80$) , WC-4 ($r^2 = 0.84$), and WC-7 ($r^2 = 0.26$). These are the only drip sites where there is a significant correlation between Sr/Ca and PDSI. Significant correlations between average Ba/Ca values (mmol/mol) versus average PDSI values for when PDSI was wetter than normal (+2 and above), near normal (between -2 and 2), and drier than normal (-2 and below) at drip sites WC-1 ($r^2 = 0.32$) , WC-3 ($r^2 = 0.95$), and WC-4 ($r^2 = 0.93$). These are the only drip sites where there is a significant correlation between Ba/Ca and PDSI.

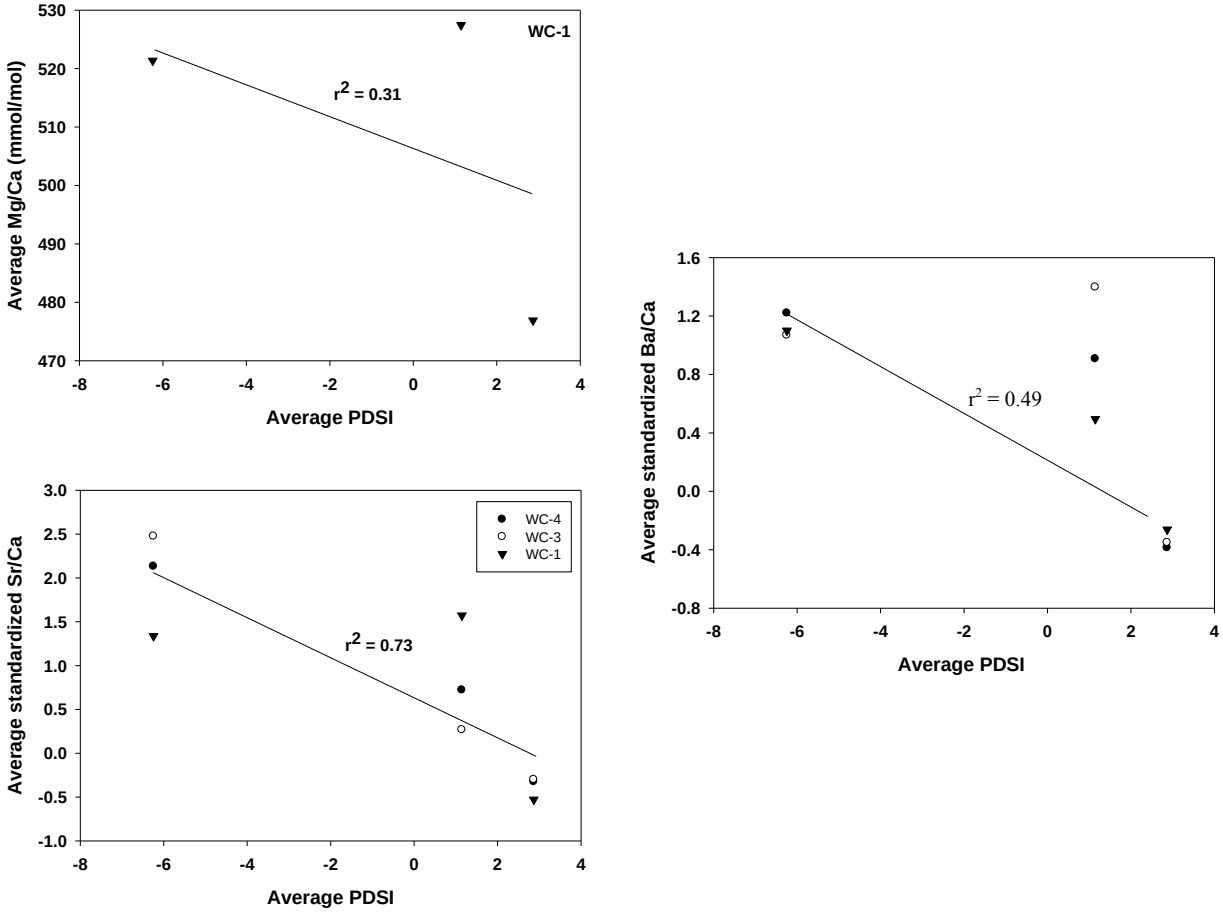

Figure 19. Average Mg/Ca, Sr/Ca, and Ba/Ca values (mmol/mol) versus average PDSI values for when PDSI was wetter than normal (+2 and above), near normal (between -2 and 2), and drier than normal (-2 and below) at drip site WC-1 where is a significant correlation between average Mg/Ca and average PDSI ($r^2 = 0.31$); at WC-4, WC-3, and WC-1 there is a significant correlation between average standardized Sr/Ca values and average PDSI ($r^2 = 0.73$); and at WC-1, WC-3, and WC-4 there is a significant correlation between average standardized Ba/Ca values and average PDSI ($r^2 = 0.49$).

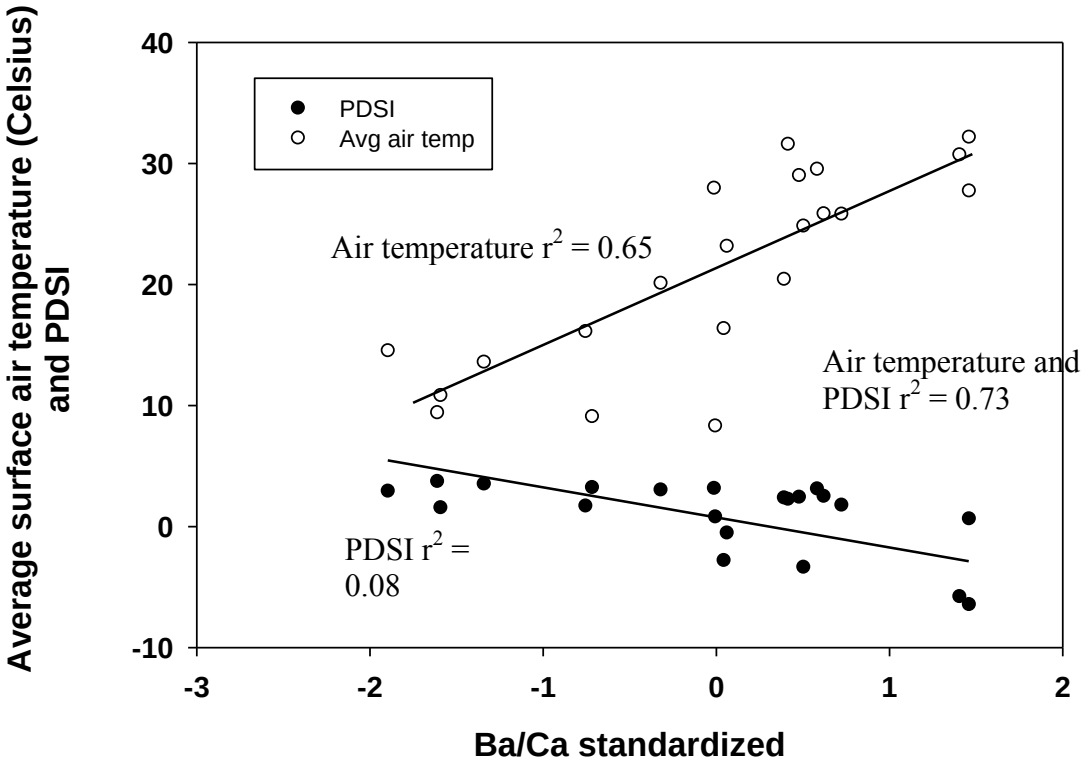

Figure 20. Graphical representation of the relationship between standardized Ba/Ca and average monthly surface air temperature and PDSI at WC-1 and is represented by the equation: Ba/Ca = (0.161 + 0.001)*(average monthly surface air temperature) – (0.001*(PDSI)). The total variance in Ba/Ca explained by both average surface air temperature and PDSI is 73%. Average surface air temperature accounts for 65% of the variance while PDSI accounts for 8% of the variance.

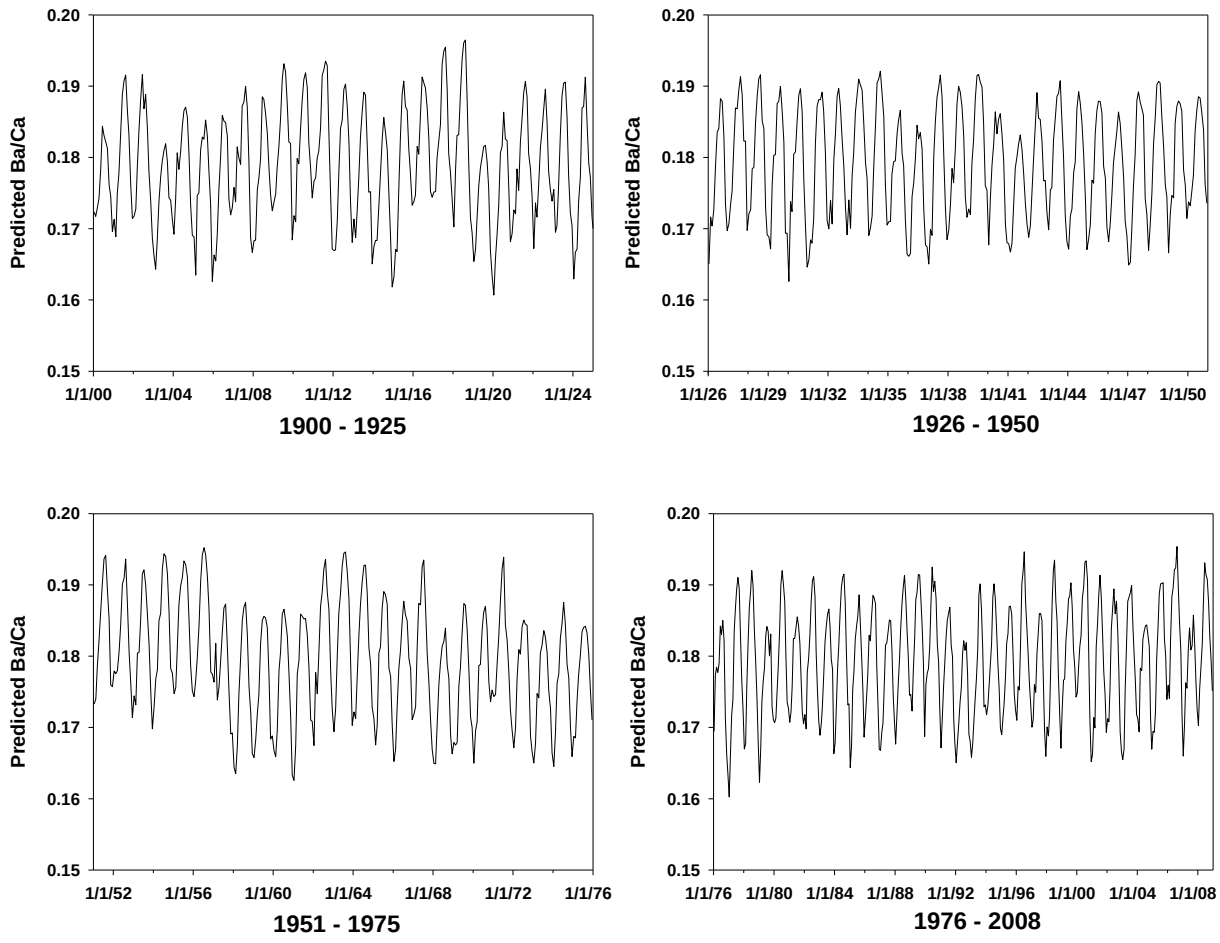

Figure 21. Predicted Ba/Ca values of cave drip waters for the time period of 1900 – 2008 at site WC-1 using the equation, Ba/Ca = 0.161 + 0.001*(average monthly surface air temperature) – (0.001*(PDSI)). Historic monthly surface air temperature and PDSI values were used as independent variables.

Appendix A2: Cave stratigraphic location, cave maps, and drip site descriptions at Inner Space Cavern

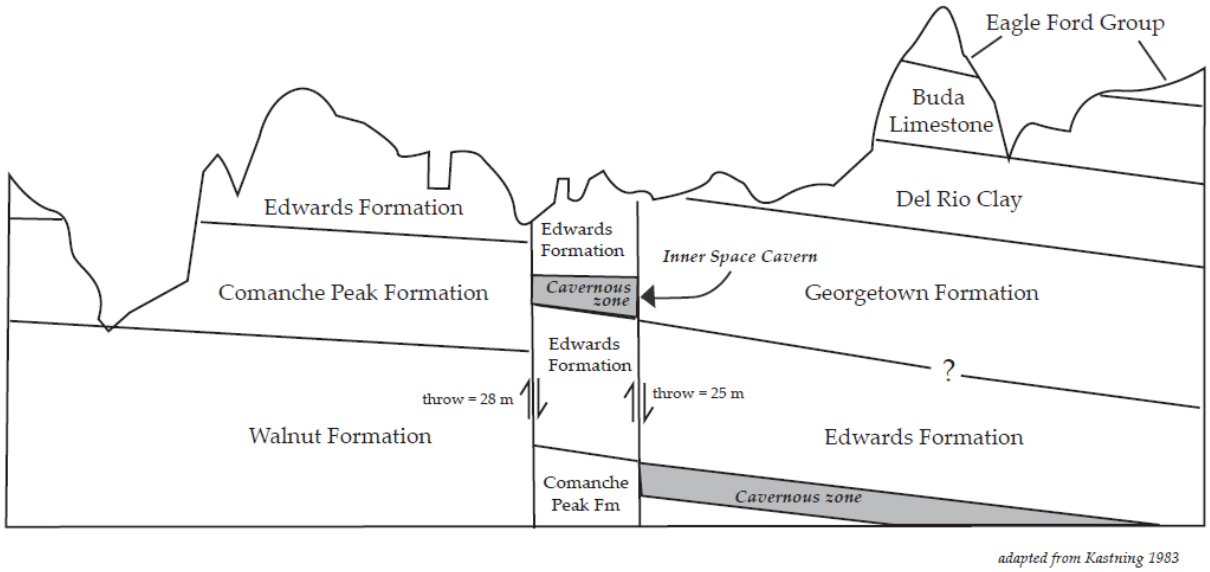

Figure A2.1. Stratigraphic cross section of the location of Inner Space Cavern in the Edwards Formation (From Kastning, 1983).

Figure A2.2. Google Earth image showing the locations of the drip sites on the surface. Directly above ISSR 3 and ISSR 5 is a concrete drainage ditch. The other sites in the picture have soil above them. The soils in the area are thin (5 to 90 cm) and consist of Crawford stony clay and Denton stony clay. The soils are calcareous, clayey, and loamy. (Godfrey, 1973; Musgrove, 2000).

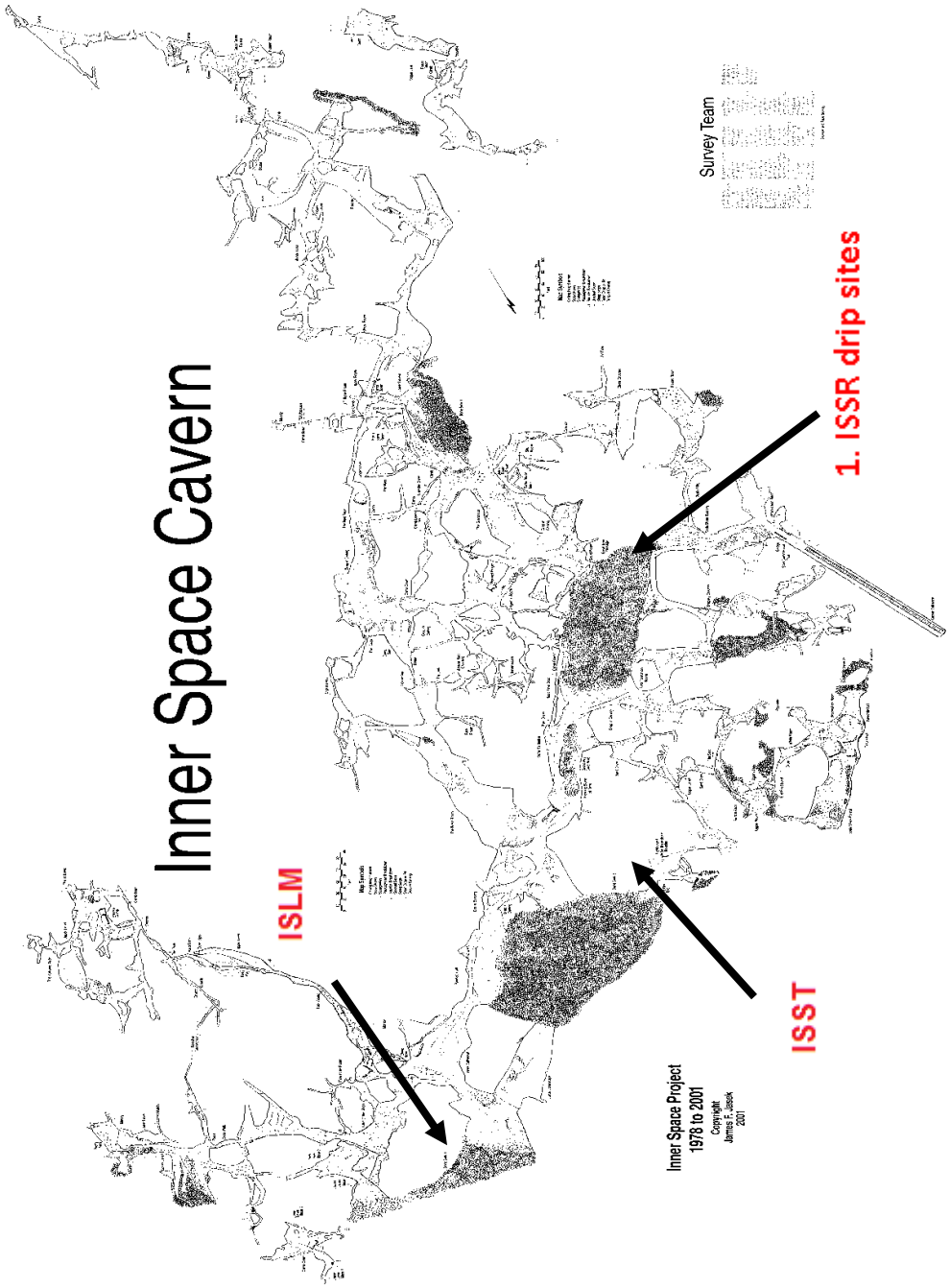

Figure A2.3. Map of Inner Space Cavern. Numbers refer to drip site locations (Jasek, 2001).

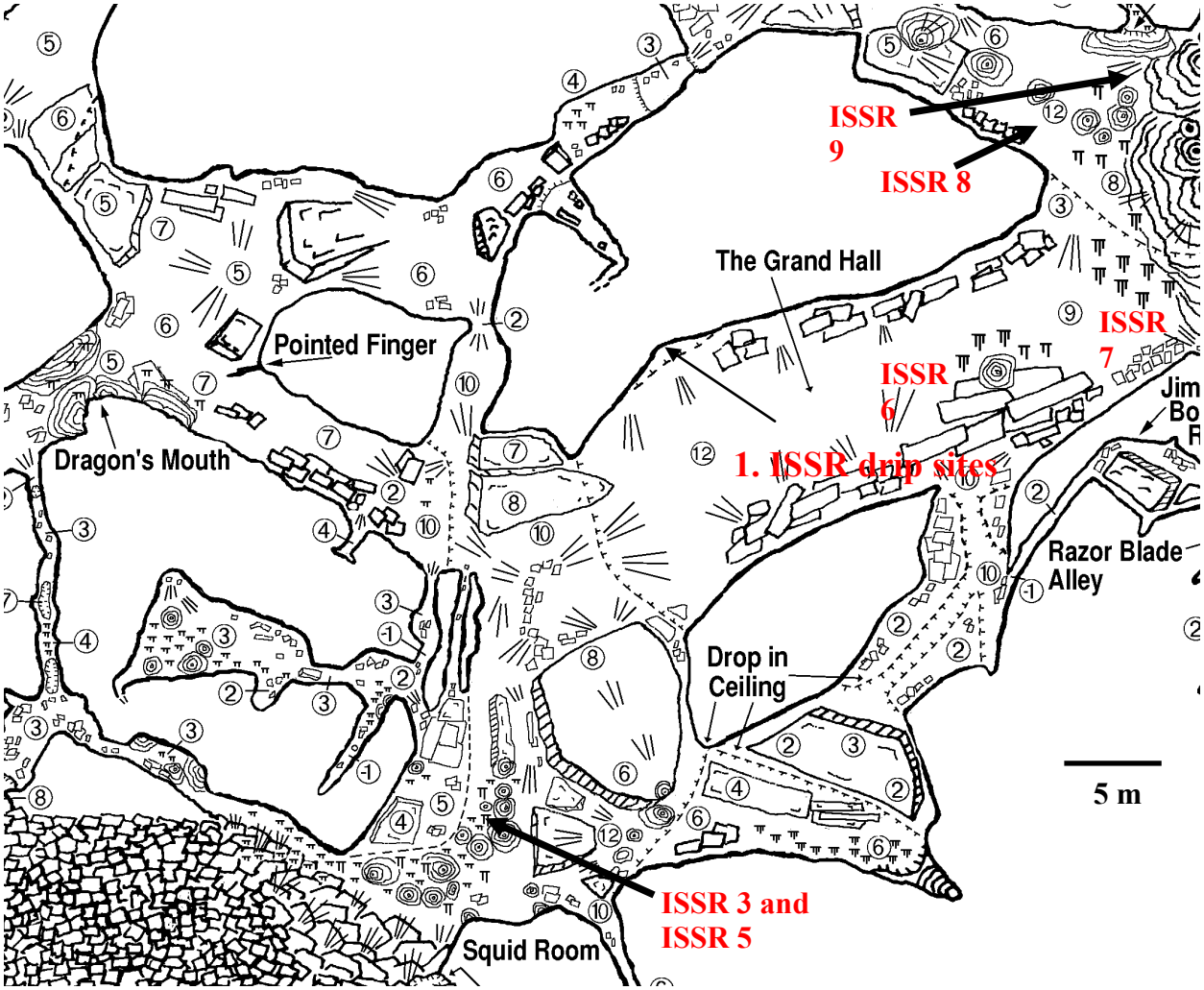

Figure A2.4. Locations of the drip sites ISSR 3, ISSR 5, ISSR 6, ISSR 7, ISSR 8, ISSR 9 at Inner Space Cavern (Jasek, 2001).

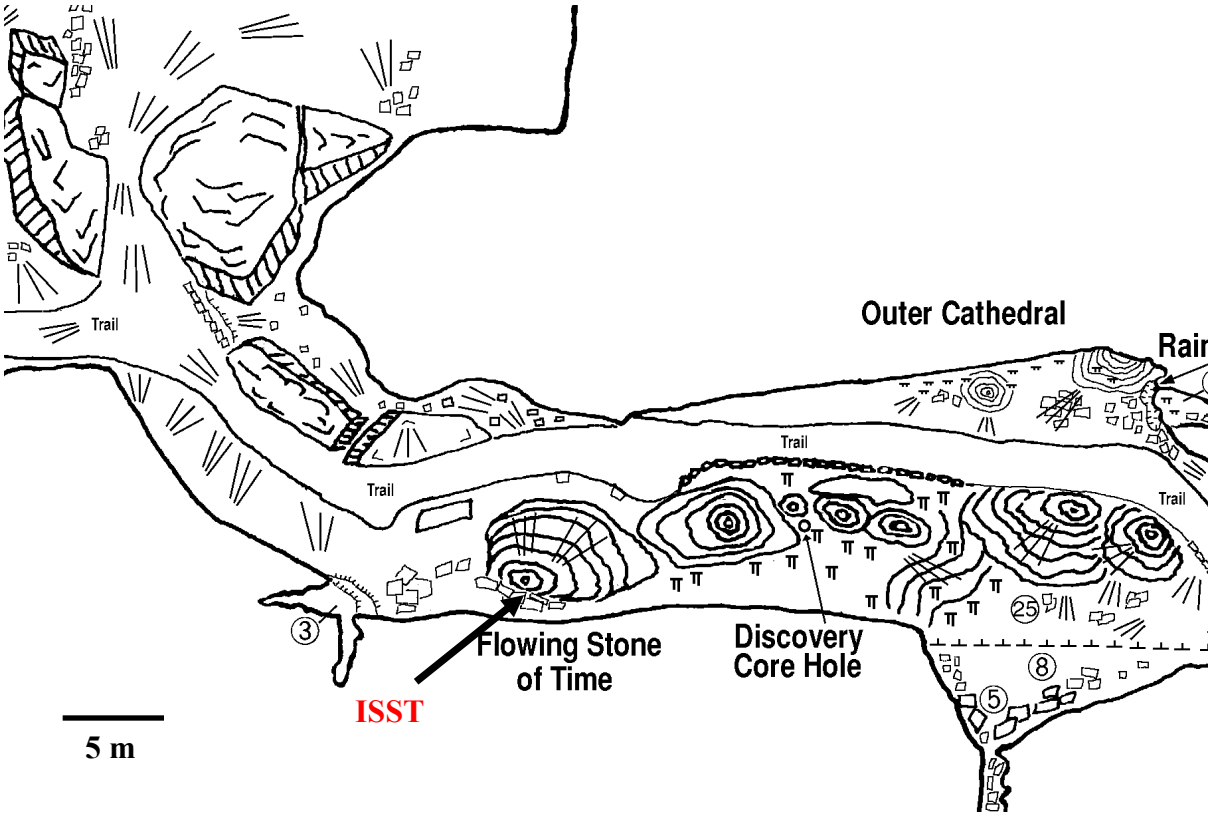

Figure A2.5. Location of drip site ISST at Inner Space Cavern (Jasek, 2001).

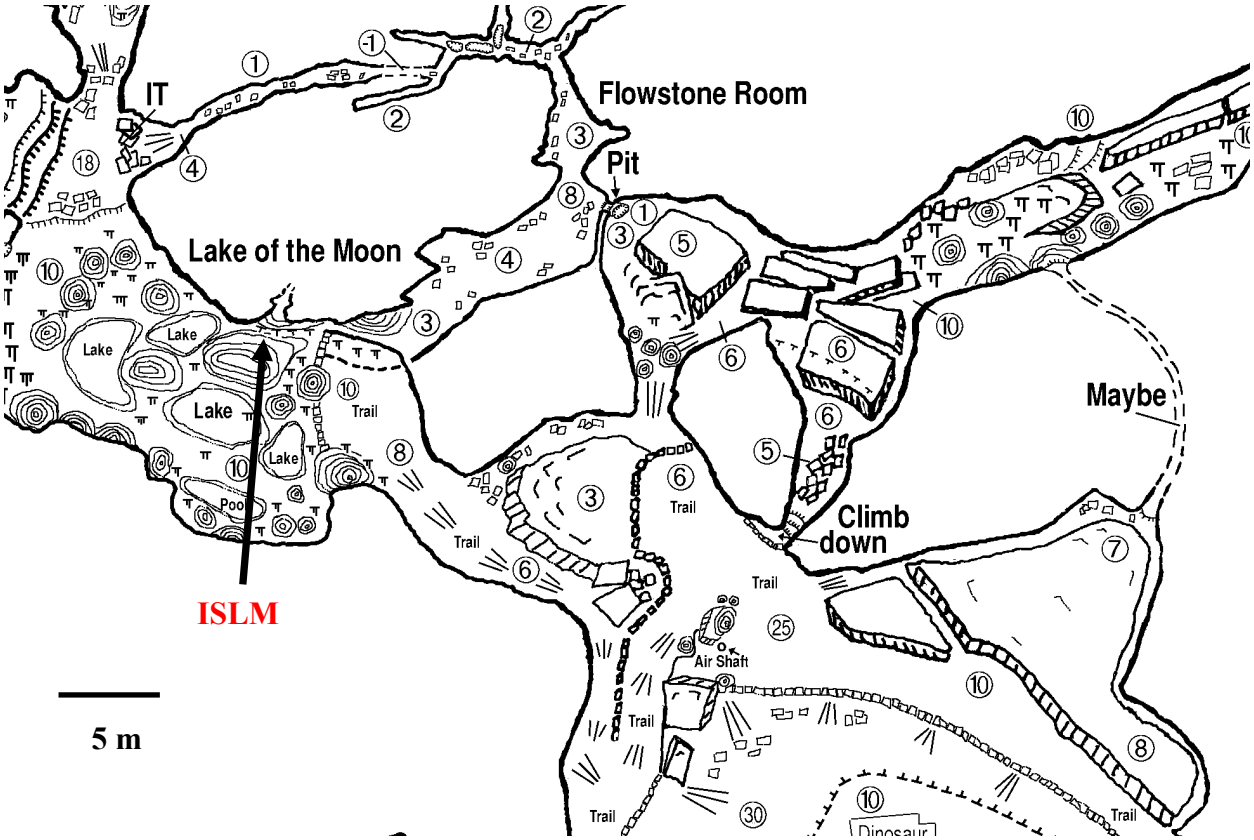

Figure A2.6. Location of drip site ISLM at Inner Space Cavern (Jasek, 2001).

Inner Space Cavern site descriptions

Figure A2.7. Drip site ISSR 3 located in the Squid Room. The drip falls from ~7 meters above the ~2 meter high stalagmite. Prior to drip the water flows down a ~30 cm soda straw. Drip site location is depicted in Figures A2-A3.

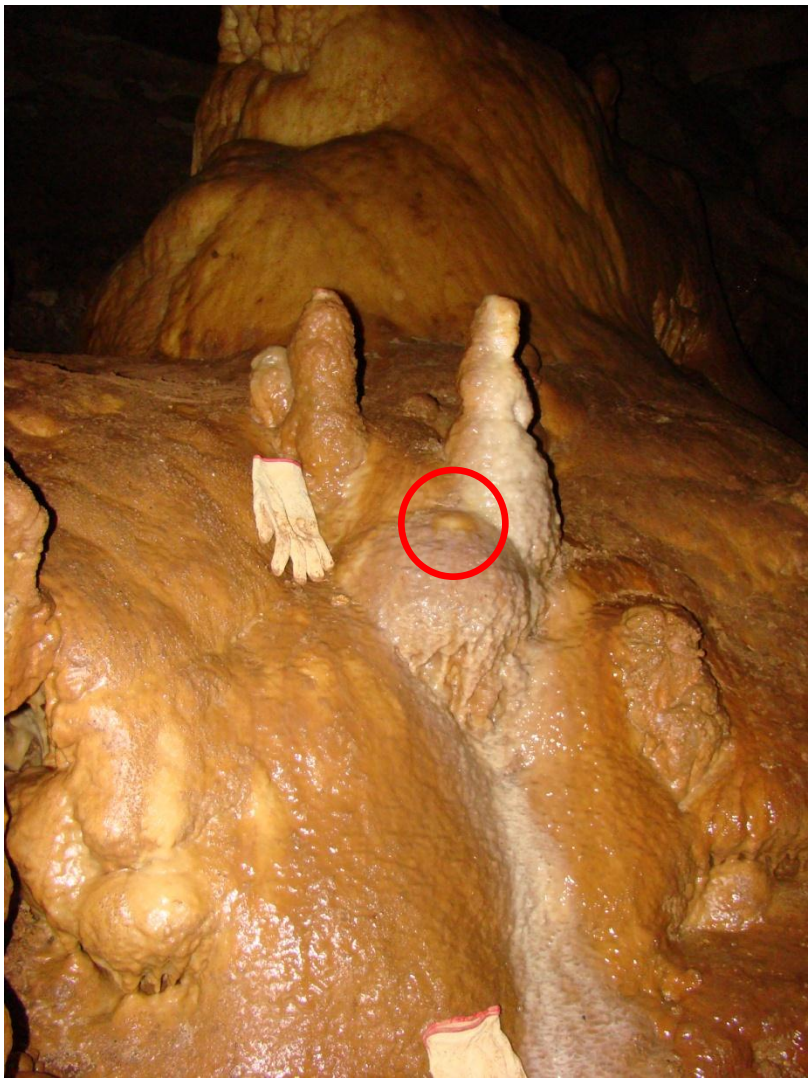

Figure A2.8. Drip site ISSR 5 located in the Squid Room approximately 2 meters to the left of ISSR 3. The drip falls from ~7 meters above the area depicted inside the red circle. Prior to drip the water flows down a ~48 cm soda straw. Drip site location is depicted in Figures A2-A3.

Figure A2.9. Drip site ISSR 6. The drip falls approximately 8 meters from a ~15 cm stalactite. Drip site location is depicted in Figures A2-A3.

Figure A2.10. The stalagmite the drip from ISSR 6 falls onto. The stalagmite is ~120 cm high. Drip site location is depicted in Figures A2-A3.

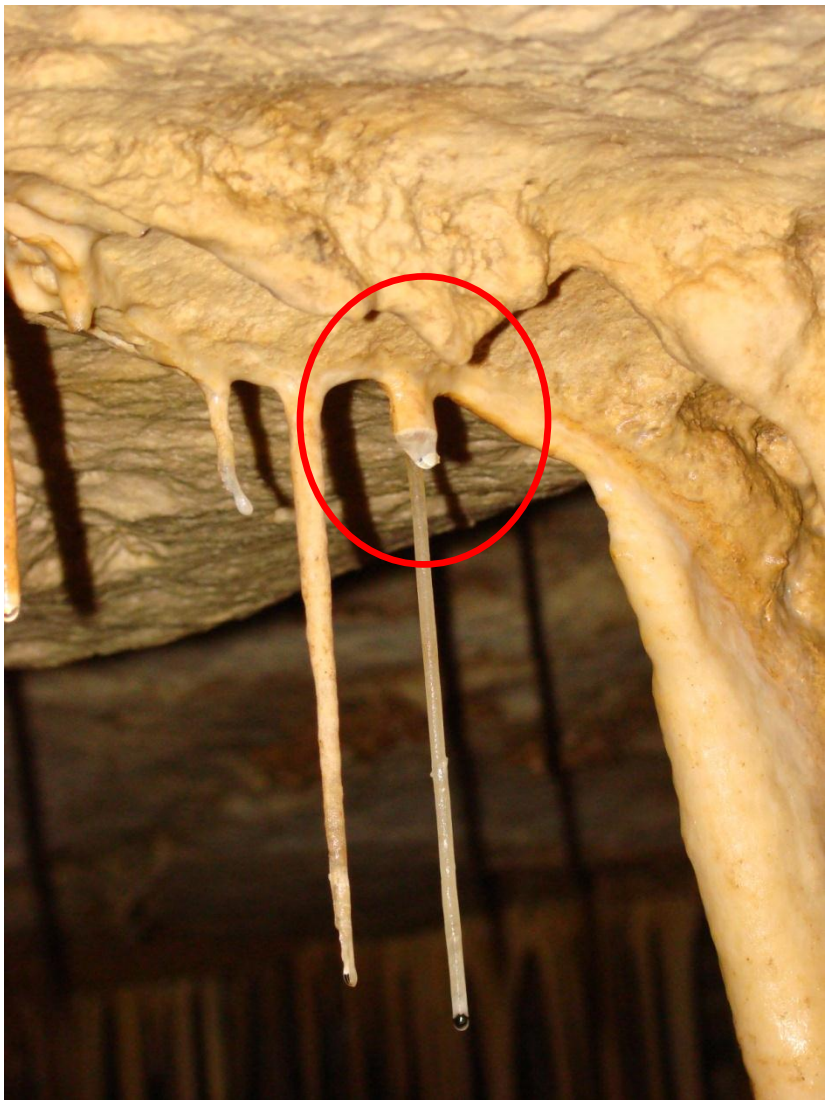

Figure A2.11. The soda straw from which ISSR 7 drips. The soda straw is ~2.5 cm in length. Drip site location is depicted in Figures A2-A3.

Figure A2.12. The stalagmite the drip from ISSR 7 falls onto. The stalagmite is ~12 cm high. Drip site location is depicted in Figures A2-A3.

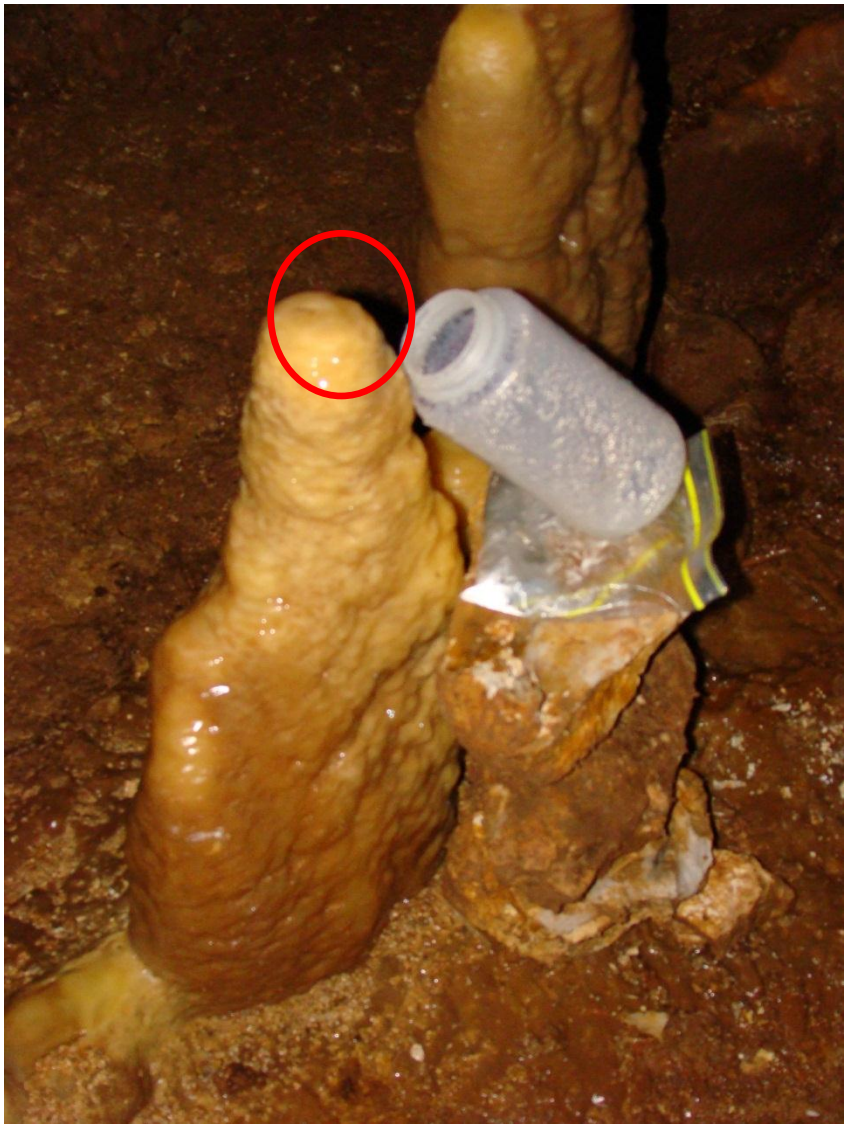

Figure A2.13. The stalagmite the drip from ISSR 8 falls onto. The area circled in red is where the drip lands. The stalagmite is ~12 cm high. Drip site location is depicted in Figures A2-A3.

Figure A2.14. The flow stone where ISST is located. The drip flows down the back of the flowstone (not pictured). Drip site location is depicted in Figures A2 and A4.

Figure A2.15. The location from which ISST emanates, circled in red. The distance between the drip and where it lands on the ground is ~45 cm. Drip site location is depicted in Figures A2 and A4.

Figure A2.16. ISLM. The drip emanates from a small soda straw. Drip site location is depicted in Figures A2 and A4.

Appendix A3: Geologic setting, cave description and drip site descriptions at Westcave

Geologic setting:

Westcave is located within the Westcave Preserve in western Travis County. The cave is ~ 7 meters off a valley floor within a side wall of a 30 meter deep canyon, created by Westcave Creek, a tributary of the Perdanales River (Caran, 2004). Westcave is in the Cow Creek Formation, which is Lower Cretaceous limestone (120 ma) that is porous and resistant to erosion. The limestone is ~14 meters thick and also forms the canyon rim. The Cow Creek Formation is a regional aquifer and is important due to its high permeability. Beneath the Cow Creek Formation is the Hammett Formation (19 meters thick), which is more easily erodible and is comprised of siltstone, sandstone, and shale. The Hammett Formation is less permeable than the Cow Creek, but it does transmit ground water (Caran, 2004).

Cave description:

The cave resides in a valley approximately 7 meters above the valley floor. It is composed of travertine deposits and is thought to be relatively young in age. The entrance to Westcave is approximately 8 meters high and 4 meters wide (Figures A2-A3). The cave has an overburden that is approximately 10 meters above the cave entrance. Drip site WC-1 is located at the cave entrance approximately 2 meters to the left (Figure A4). Once inside the cave, the back wall is approximately 10 meters from the entrance with 2.5 meter tall ceilings; drip site WC-7 is located approximately 6.5 meters into the cave and to the right by 1.5 meters (Figure A5). Further to the right the cave extends approximately 18 meters until the ceiling and the floor meet. To the left the cave extends 20 meters and has several openings, the largest being 2 meters by 1.5 meters (Figures A6-A7). The ceilings lower to ~1.5 meters and then rise to 2.5 meters towards the back of the cave. Drip sites WC-5, WC-4, WC-3, and WC-6 are located at the back of the cave (Figures A8-A9). Drip site pictures and descriptions are listed below:

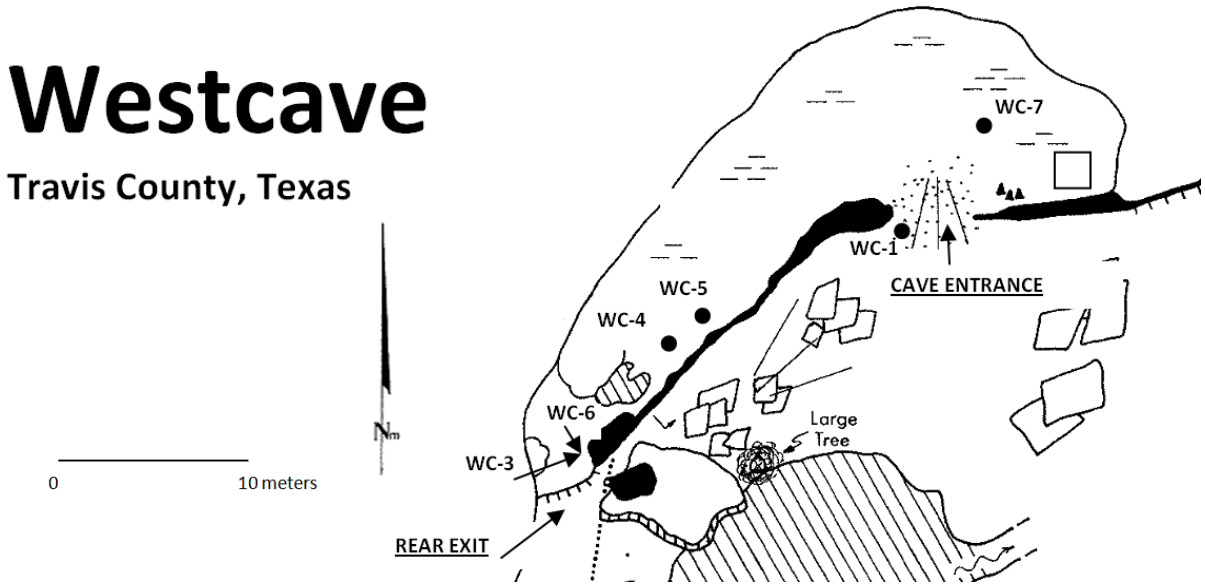

Figure A3.1. A map of Westcave with drip site locations. From southwest to northeast the cave is approximately 30 meters long (Modified from Reddell and Smith, 1961; Fieseler et al., 1972).

Figure A3.2. The entrance to Westcave looking from the valley floor towards the cave entrance.

Figure A3.3. The entrance to Westcave looking from the inside of the cave to the valley outside.

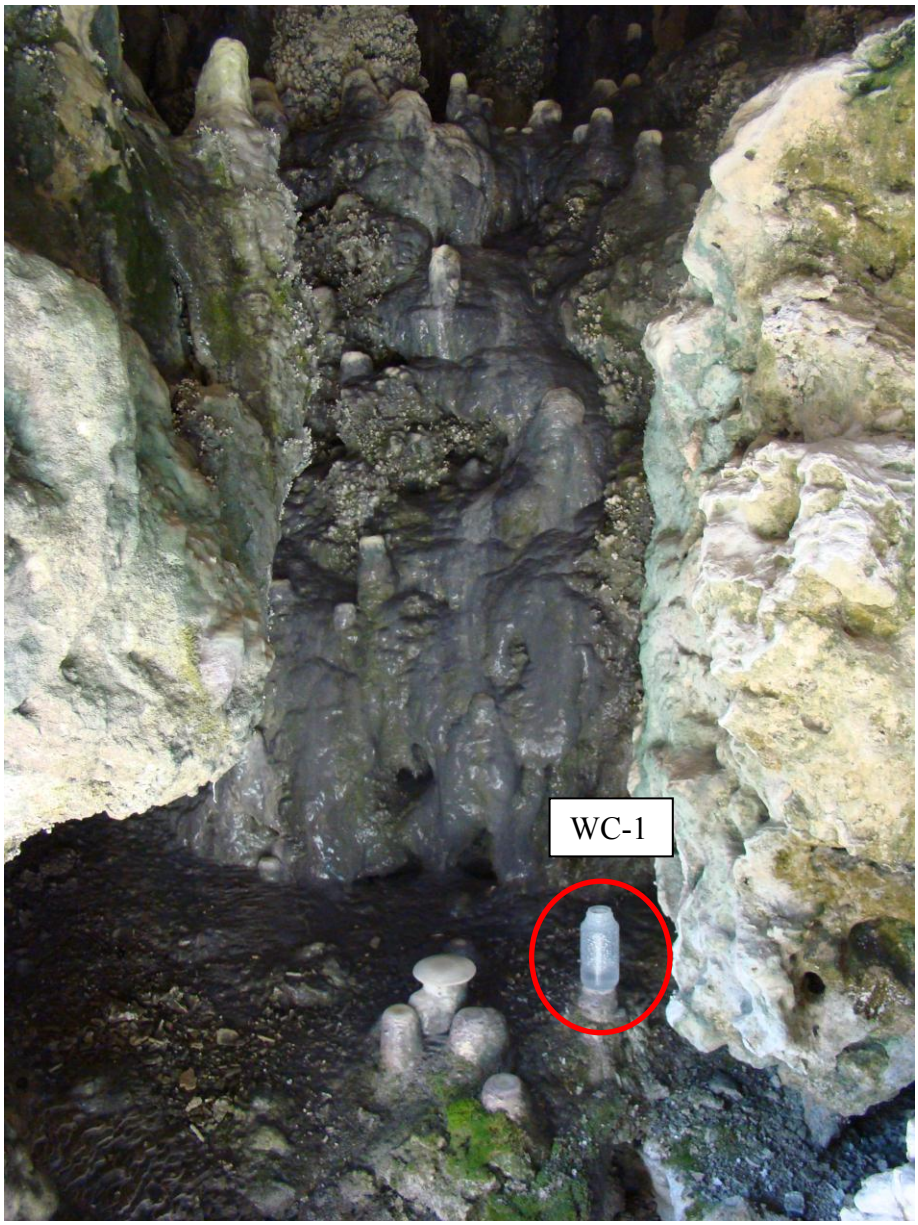

Figure A3.4. Drip site WC-1, located directly to the left at the cave entrance. The drip originates from a 7 cm long soda straw and falls 6 meters onto a stalagmite.

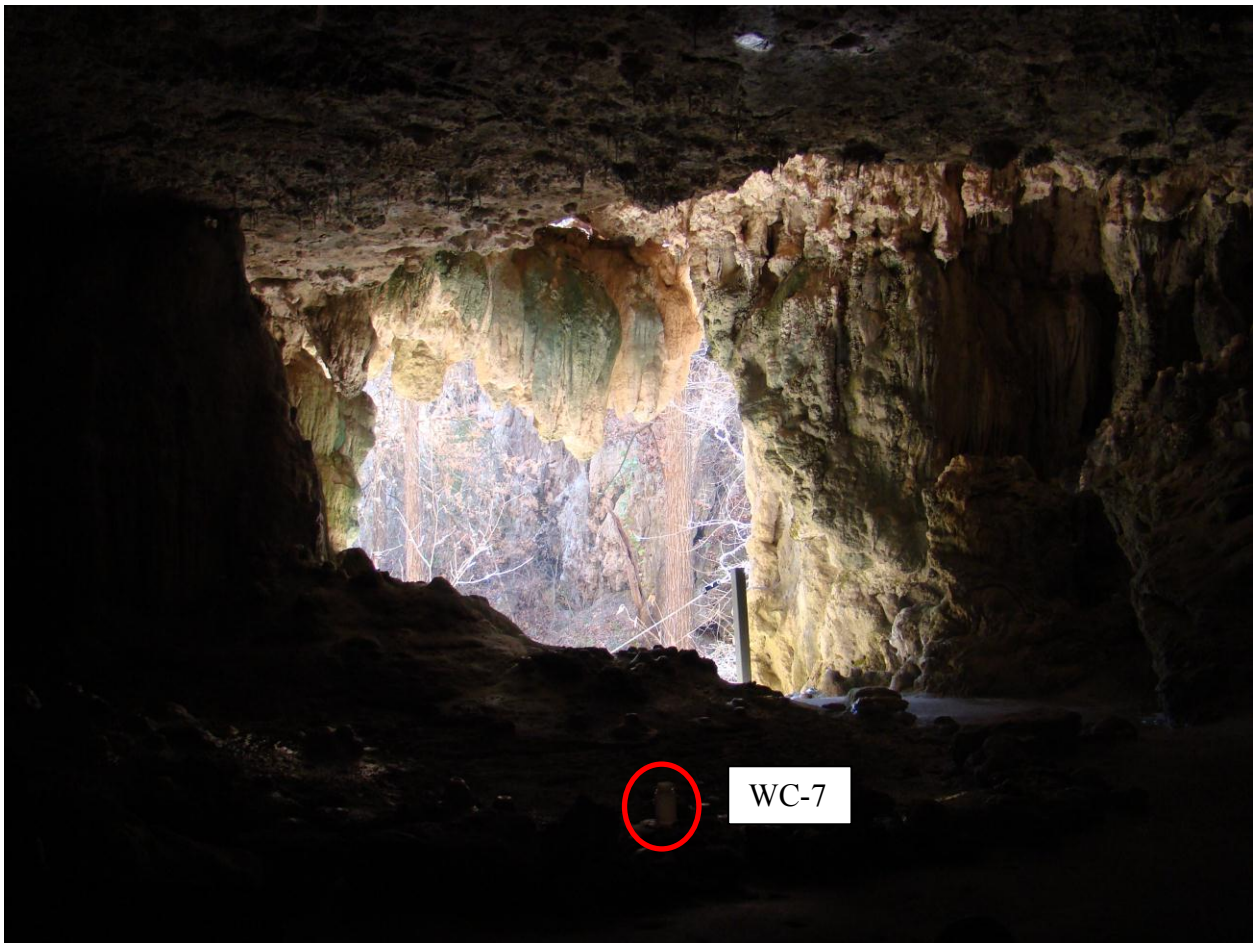

Figure A3.5. Drip site WC-7; this site is ~7meters from the cave entrance on the right. The drip originates from the front soda straw of the two and falls 3 meters onto a stalagmite. The soda straw is 2.5 cm long.

Figure A3.6. Looking to the left of the entrance towards drip sites WC-4, WC-5, WC-6, WC-3, and the rear exit of Westcave.

Figure A3.7. The rear exit to Westcave, near drip sites WC-6 and WC-3.

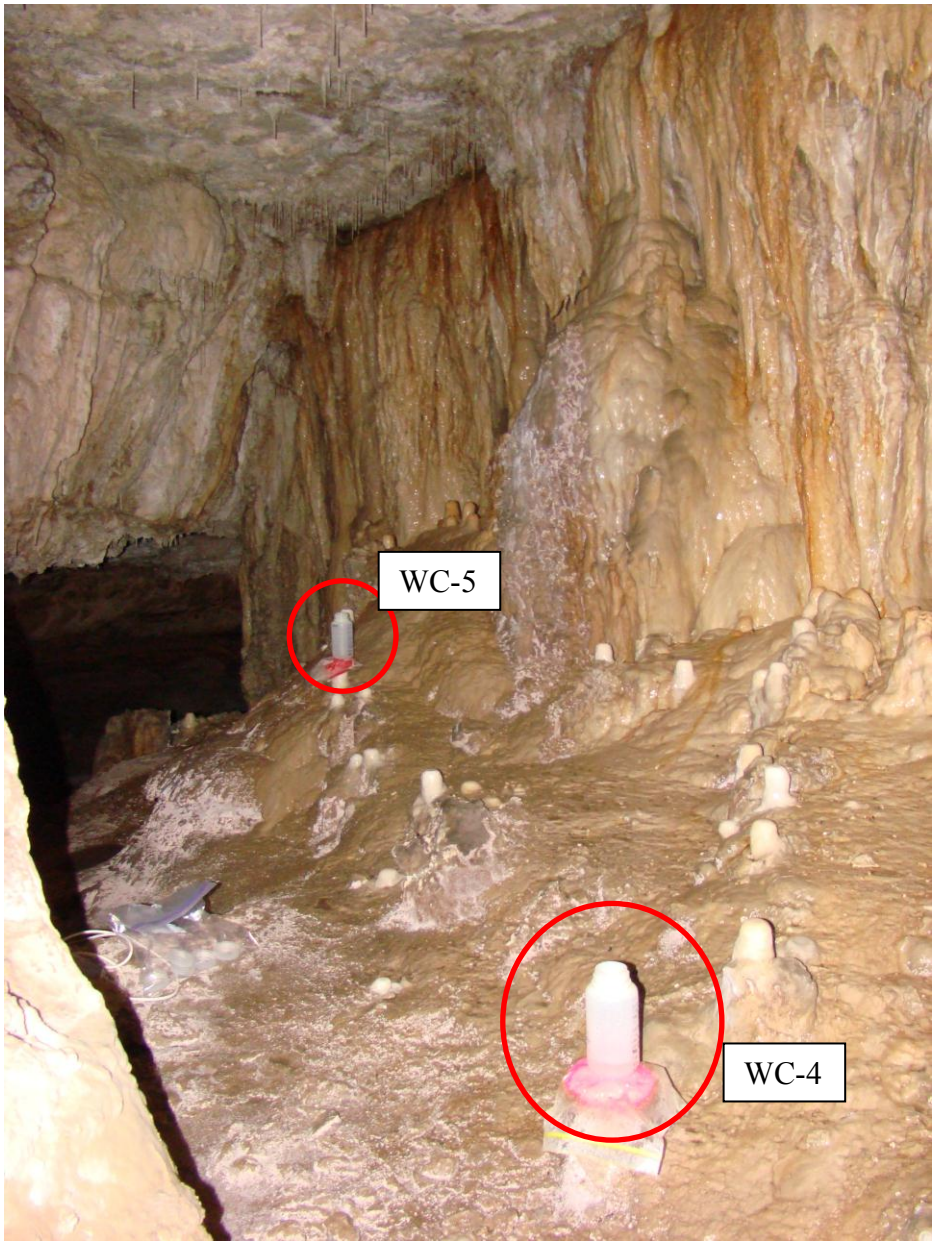

Figure A3.8. Drip site WC-4; this drip site is the second site on the left going towards the back of the cave. The drip originates from a 15 cm long soda straw and falls 2.5 meters onto a stalagmite. Drip sites WC-5; this site is the first site on the left going towards the back of the cave. Of the three soda straws it is the back left one. The drip originates from a 20 cm long soda straw and falls 2.5 meters onto a stalagmite.

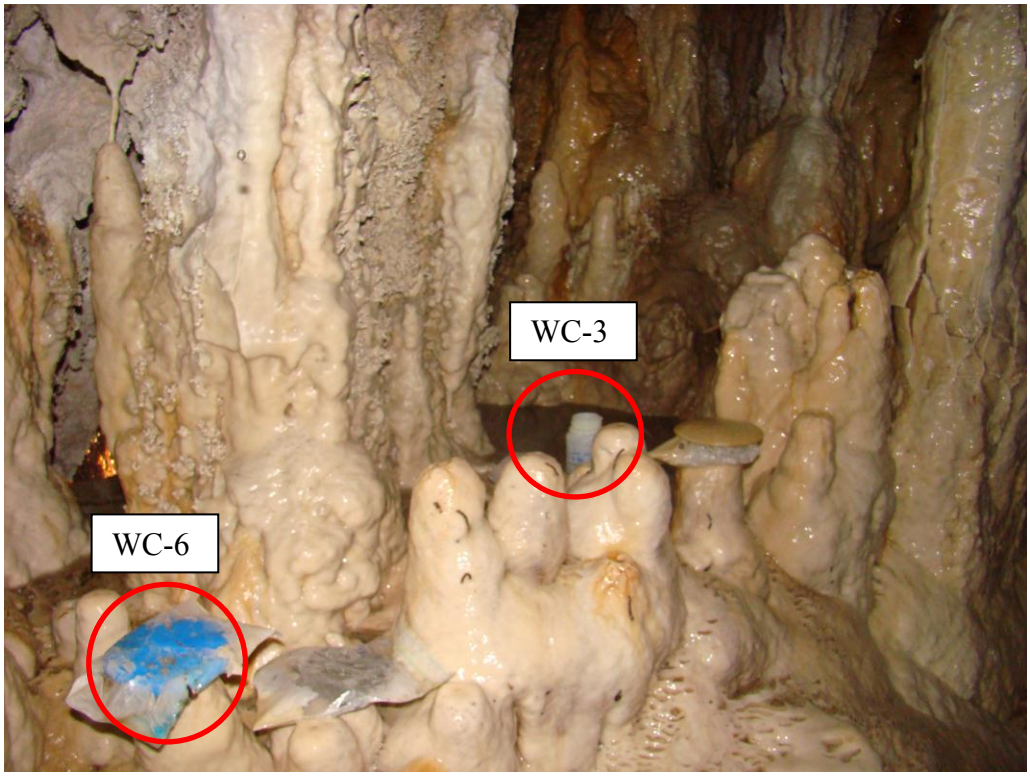

Figure A3.9. Drip site WC-3; this drip site is located at the back of the cave on the left. The drip originates from the 5 cm soda straw to the right of the drapery and falls 0.3 meters onto a stalagmite. Drip site WC-6; the left most drip site near WC-3. The drip originates from a 30 cm long drapery and falls 0.3 meters onto a stalagmite.

Appendix B2: Physical and geochemical parameters of cave air, cave drip water, and calcite at Inner Space Cavern

Table B2.1. Drip rate, calcite growth rate, Ca concentration, Mg concentration and Mg/Ca for drip sites.

Site	Date	drip rate (ml/sec)	calcite growth (mg/day)	Ca (ppm)	Mg (ppm)	Sr (ppm)	Mg/Ca (mmol/mol)
ISSR 3	1/27/2007	0.089	23.7	93.8	4.9	0.121	85.4
ISSR 3	2/21/2007	0.102	7.0	93.9	5.1	0.108	89.4
ISSR 3	3/30/2007	0.093	12.9	94.1	4.5	0.108	79.3
ISSR 3	4/27/2007	0.162	n/a	93.1	4.7	0.106	82.9
ISSR 3	6/29/2007	0.162	n/a	93.5	4.5	0.109	79.5
ISSR 3	10/21/2007	0.111	n/a	95.9	5.2	0.109	89.0
ISSR 3	11/18/2007	0.094	35.7	94.7	5.3	0.108	92.4
ISSR 3	12/11/2007	0.213	7.6	91.7	4.8	0.104	86.9
ISSR 3	1/9/2008	0.165	7.2	92.0	5.0	0.104	90.3
ISSR 3	2/17/2008	0.065	11.8	89.1	5.0	0.102	93.1
ISSR 3	3/16/2008	0.147	9.0	85.9	4.8	0.100	91.6
ISSR 3	4/5/2008	n/a	9.9	88.0	4.7	0.101	87.8
ISSR 3	5/15/2008	n/a	n/a	88.3	4.5	0.100	84.7
ISSR 3	6/5/2008	0.220	3.3	89.2	4.6	0.102	84.5
ISSR 3	7/3/2008	0.150	6.	89.8	4.9	0.102	89.9
ISSR 3	7/25/2008	0.156	0.3	92.5	4.9	0.104	86.7
ISSR 3	9/6/2008	0.104	-0.3	89.5	4.7	0.101	85.7
ISSR 3	11/15/2008	0.028	8.1	87.7	4.7	0.099	89.2
ISSR 3	2/14/2009	0.065	n/a	79.2	5.0	0.093	104.1
ISSR 3	3/17/2009	0.078	4.4	79.5	4.0	0.091	83.7
ISSR 3	4/26/2009	0.111	4.8	79.1	4.2	0.092	86.6
ISSR 3	5/17/2009	0.078	3.5	74.5	4.4	0.089	96.5
ISSR 3	6/17/2009	0.046	2.8	77.5	4.6	0.090	97.4
ISSR 3	7/17/2009	0.036	-0.5	81.2	4.7	0.095	96.4
ISSR 3	8/30/2009	0.109	-0.4	84.1	4.6	0.133	89.6
ISSR 3	9/14/2009	0.142	n/a	90.1	4.3	0.136	79.4
ISSR 3	9/16/2009	0.230	n/a	88.9	4.1	0.134	75.8
ISSR 3	9/27/2009	0.286	-0.3	90.3	3.9	0.137	71.6
ISSR 3	10/25/2009	0.244	0.1	92.1	4.0	0.139	72.0
ISSR 3	11/15/2009	0.192	n/a	90.2	4.2	0.136	76.7
ISSR 3	12/18/2009	0.214	4.3	85.9	4.5	0.103	86.5
ISSR 3	1/21/2010	0.240	3.3	88.0	4.1	0.105	77.3
ISSR 3	2/25/2010	0.265	6.3	86.0	5.1	0.104	97.4
ISSR 3	3/30/2010	0.146	8.5	88.1	4.1	0.106	76.1

ISSR 3	4/30/2010	0.105	2.6	87.4	4.5	0.104	85.5
ISSR 3	5/30/2010	0.107	8.8	84.9	4.6	0.103	89.3
ISSR 3	6/29/2010	0.101	4.9	87.7	4.5	0.104	84.2
ISSR 3	7/29/2010	0.069	5.4	82.4	4.5	0.100	89.1
ISSR 3	8/31/2010	0.075	0.4	84.0	4.6	0.104	90.5
ISSR 3	9/9/2010	0.135	n/a	83.5	4.5	0.101	89.3
ISSR 3	9/10/2010	0.205	n/a	86.0	4.2	0.103	81.4
ISSR 3	9/13/2010	0.224	n/a	88.3	4.3	0.105	79.4
ISSR 3	9/17/2010	0.154	n/a	87.8	4.1	0.105	77.8
ISSR 3	9/26/2010	0.089	n/a	84.3	4.4	0.104	85.3
ISSR 5	2/15/2009	0.220	n/a	n/a	n/a	0.119	n/a
ISSR 5	3/17/2009	0.437	n/a	n/a	n/a	0.092	n/a
ISSR 5	4/26/2009	0.396	n/a	74.9	4.0	0.120	88.7
ISSR 5	5/17/2009	0.352	n/a	73.5	4.3	0.090	95.8
ISSR 5	6/17/2009	0.290	n/a	75.7	4.3	0.123	94.3
ISSR 5	7/17/2009	0.273	n/a	71.3	4.4	0.137	100.8
ISSR 5	8/30/2009	0.283	n/a	75.9	4.7	0.106	101.2
ISSR 5	9/16/2009	0.443	n/a	87.3	4.4	0.143	83.4
ISSR 5	9/27/2009	0.492	n/a	88.6	4.2	0.135	77.
ISSR 5	10/25/2009	0.511	n/a	93.6	4.3	0.103	75.8
ISSR 5	11/15/2009	0.469	n/a	88.3	4.5	0.106	84.0
ISSR 5	12/9/2009	0.468	n/a	n/a	n/a	0.108	82.5
ISSR 5	12/18/2009	0.398	n/a	86.7	4.3	0.103	76.8
ISSR 5	1/23/2010	0.485	n/a	89.6	4.2	0.100	77.4
ISSR 5	2/25/2010	0.486	n/a	n/a	n/a	0.100	n/a
ISSR 5	3/30/2010	0.506	n/a	91.1	4.3	0.098	85.7
ISSR 5	4/30/2010	0.396	n/a	86.6	4.5	0.094	107.8
ISSR 5	5/30/2010	0.325	n/a	81.3	5.3	0.094	90.3
ISSR 5	6/29/2010	0.339	n/a	82.7	4.5	0.098	92.3
ISSR 5	7/29/2010	0.310	n/a	79.3	4.4	0.106	96.3
ISSR 5	8/31/2010	0.271	n/a	76.4	4.5	0.104	96.3
ISSR 5	9/9/2010	0.325	n/a	74.8	4.4	0.102	90.2
ISSR 5	9/10/2010	0.411	n/a	79.4	4.3	0.119	81.6
ISSR 5	9/13/2010	0.484	n/a	88.1	4.4	0.092	81.9
ISSR 5	9/17/2010	0.476	n/a	87.0	4.3	0.120	90.7
ISSR 5	9/26/2010	0.407	n/a	84.7	4.7	0.090	90.7
ISSR 6	2/15/2009	9.33e-3	n/a	n/a	n/a	0.0832	n/a
ISSR 6	3/6/2009	7.85e-3	n/a	72.1	4.3	0.0780	99.2
ISSR 6	4/4/2009	7.14e-3	1.26	66.7	3.8	0.0828	93.4
ISSR 6	5/17/2009	0.0122	1.39	71.1	5.8	0.0957	133.6

ISSR 6	6/17/2009	0.0110	.63	n/a	n/a	0.1354	n/a
ISSR 6	7/17/2009	6.77e-3	-.45	91.5	5.5	0.1066	99.5
ISSR 6	8/30/2009	2.86e-3	-.31	100.0	5.4	0.1142	88.2
ISSR 6	9/14/2009	9.53e-3	n/a	81.1	4.0	0.1227	81.8
ISSR 6	9/16/2009	9.49e-3	n/a	85.7	4.6	0.1412	88.1
ISSR 6	9/27/2009	7.66e-3	-.51	90.5	5.3	0.1262	96.
ISSR 6	10/25/2009	8.20e-3	-.31	101.3	6.9	0.0906	112.4
ISSR 6	11/15/2009	8.13e-3	3.54	89.8	5.7	0.1005	105.4
ISSR 6	12/9/2009	9.93e-3	4.38	n/a	n/a	0.0885	n/a
ISSR 6	12/18/2009	9.70e-3	3.56	82.3	5.1	0.0957	102.1
ISSR 6	1/21/2010	6.99e-3	6.30	90.4	6.1	0.0899	110.7
ISSR 6	2/25/2010	0.0122	6.55	79.8	5.2	0.0945	108.0
ISSR 6	3/30/2010	0.0110	5.68	84.9	5.7	0.0986	110.1
ISSR 6	4/30/2010	9.89e-3	6.42	79.3	4.8	0.0832	99.7
ISSR 6	5/30/2010	0.0129	3.11	82.2	4.6	0.0780	91.8
ISSR 6	6/29/2010	0.0160	.10	87.7	5.2	0.0828	97.0
ISSR 7	2/15/2009	0.0454	n/a	n/a	n/a	0.0891	n/a
ISSR 7	3/6/2009	0.0537	n/a	64.7	9.2	0.0861	233.9
ISSR 7	4/4/2009	0.0544	1.52	64.9	5.6	0.0858	141.3
ISSR 7	5/17/2009	0.0437	2.01	67.1	6.1	0.0908	150.7
ISSR 7	6/17/2009	0.0413	2.89	65.3	7.7	0.0881	194.
ISSR 7	7/17/2009	0.0393	-.42	72.5	9.0	0.1346	205.5
ISSR 7	8/30/2009	0.0404	-.38	89.7	7.8	0.1216	143.3
ISSR 7	9/14/2009	0.0440	n/a	95.9	5.7	0.1228	98.1
ISSR 7	9/16/2009	0.0250	n/a	83.1	5.6	0.1276	110.5
ISSR 7	9/27/2009	0.0392	-.37	85.1	5.4	0.1424	104.3
ISSR 7	10/25/2009	0.0427	-.45	91.8	5.6	0.1310	100.9
ISSR 7	11/15/2009	0.0447	1.27	82.8	5.4	0.0975	107.5
ISSR 7	12/9/2009	0.0450	1.39	n/a	n/a	0.0931	n/a
ISSR 7	12/18/2009	0.0424	.63	78.8	5.4	0.0991	113.8
ISSR 7	1/21/2010	0.0468	2.08	n/a	n/a	0.0982	n/a
ISSR 7	2/25/2010	0.0473	4.20	76.0	4.8	0.0963	104.8
ISSR 7	3/30/2010	0.0376	1.69	80.7	4.9	0.0978	101.0
ISSR 7	4/30/2010	0.0513	4.11	80.7	5.1	0.0891	104.3
ISSR 7	5/30/2010	0.0536	2.28	76.0	7.3	0.0861	157.9
ISSR 7	6/29/2010	0.0513	n/a	74.8	7.0	0.0858	153.5
ISSR 8	3/6/2009	0.0202	18.06	80.4	7.5	0.092	153.9
ISSR 8	4/4/2009	0.0193	7.00	77.1	8.9	0.098	189.4
ISSR 8	5/17/2009	0.0220	1.99	87.9	8.2	0.101	154.2
ISSR 8	6/17/2009	0.0240	-.39	84.0	8.4	0.106	165.

ISSR 8	7/17/2009	0.0265	n/a	92.9	8.5	0.104	151.1
ISSR 8	8/30/2009	0.0246	n/a	93.0	7.6	0.138	134.4
ISSR 8	9/14/2009	0.0310	-.37	88.9	6.9	0.130	128.7
ISSR 8	9/16/2009	0.0324	1.14	100.9	8.4	0.150	137.3
ISSR 8	9/27/2009	0.0313	10.55	110.3	9.6	0.163	143.6
ISSR 8	10/25/2009	0.0303	13.28	104.5	9.5	0.156	149.3
ISSR 8	11/15/2009	0.0249	4.77	94.5	8.4	0.110	146.5
ISSR 8	12/9/2009	0.0234	12.93	95.3	8.3	0.112	143.9
ISSR 8	12/18/2009	0.0229	20.08	100.9	9.4	0.117	154.2
ISSR 8	1/21/2010	0.0229	11.04	98.9	8.9	0.115	147.
ISSR 8	2/25/2010	0.0259	14.08	91.3	8.1	0.106	146.7
ISSR 8	3/30/2010	0.0288	11.84	93.2	8.3	0.109	147.4
ISSR 8	4/30/2010	0.0279	10.48	91.8	7.7	0.106	138.5
ISSR 8	5/30/2010	0.0259	18.06	80.4	7.5	0.092	99.7
ISSR 8	6/29/2010	0.0222	7.00	77.1	8.9	0.098	105.4
ISSR 9	3/6/2009	6.90e-3	n/a	84.4	7.3	0.096	143.2
ISSR 9	4/4/2009	6.25e-3	6.86	80.3	7.4	0.100	151.0
ISSR 9	5/17/2009	6.17e-3	8.17	89.8	7.5	0.110	137.8
ISSR 9	6/17/2009	6.89e-3	7.02	83.0	7.1	0.093	140.2
ISSR 9	7/17/2009	5.41e-3	.71	82.8	7.1	0.094	141.4
ISSR 9	8/30/2009	6.92e-3	-.37	85.2	6.8	0.128	131.3
ISSR 9	9/14/2009	6.29e-3	n/a	86.1	6.9	0.129	131.8
ISSR 9	9/16/2009	5.72e-3	n/a	86.4	6.9	0.129	131.4
ISSR 9	9/27/2009	5.73e-3	-.34	87.0	7.1	0.134	135.1
ISSR 9	10/25/2009	6.26e-3	.45	98.7	8.0	0.147	133.0
ISSR 9	11/15/2009	6.28e-3	5.76	106.3	8.6	0.160	134.1
ISSR 9	12/9/2009	5.14e-3	12.90	n/a	n/a	0.120	n/a
ISSR 9	12/18/2009	6.14e-3	7.96	101.4	8.3	0.115	135.0
ISSR 9	1/21/2010	5.64e-3	11.95	97.7	7.9	0.115	133.9
ISSR 9	2/25/2010	5.48e-3	10.86	96.5	8.1	0.110	137.9
ISSR 9	3/30/2010	5.25e-3	9.97	93.4	7.9	0.113	138.7
ISSR 9	4/30/2010	5.11e-3	11.76	94.1	7.7	0.105	135.6
ISSR 9	5/30/2010	4.16e-3	9.39	n/a	n/a	0.096	n/a
ISSR 9	6/29/2010	4.75e-3	6.06	89.3	7.3	0.100	134.7
ISST rear drip	6/17/2009	.0940	xx	65.7	12.1	0.096	304.9
ISST rear drip	7/17/2009	.0380	xx	71.6	13.6	0.100	312.7
ISST rear drip	8/30/2009	.0180	xx	75.3	14.1	0.108	309.8

ISST rear drip	9/16/2009	.0231	xx	79.7	13.8	0.107	286.1
ISST rear drip	9/27/2009	.0320	xx	68.0	12.4	0.101	301.0
ISST rear drip	10/25/2009	.0188	xx	69.7	11.7	0.097	276.2
ISST rear drip	11/15/2009	.134	xx	69.8	10.9	0.097	256.9
ISST rear drip	12/18/2009	.199	xx	64.3	10.2	0.092	261.3
ISST rear drip	1/23/2010	n/a	xx	58.9	9.5	0.085	266.2
ISST rear drip	2/26/2010	.114	xx	54.7	8.0	0.076	241.2
ISST rear drip	3/27/2010	.0210	xx	60.7	9.5	0.086	257.0
ISST rear drip	4/30/2010	.0543	xx	58.8	10.6	0.090	296.7
			xx				
ISLM rear drip	6/17/2009	.003630	xx	84.2	5.7	0.107	112.1
ISLM rear drip	7/17/2009	.003630	xx	83.6	5.7	0.107	113.1
ISLM rear drip	8/30/2009	.002350	xx	83.1	5.8	0.107	114.6
ISLM rear drip	9/16/2009	.003750	xx	82.8	5.8	0.106	116.2
ISLM rear drip	9/27/2009	.002540	xx	82.8	5.8	0.106	116.1
ISLM rear drip	10/25/2009	.003750	xx	83.8	5.9	0.106	116.2
ISLM rear drip	11/15/2009	.002410	xx	84.4	5.9	0.107	115.3
ISLM rear drip	12/18/2009	.005880	xx	86.7	6.2	0.112	118.4
ISLM rear drip	2/26/2010	n/a	xx	88.7	6.3	0.112	116.3
ISLM rear drip	3/27/2010	.007250	xx	79.7	6.1	0.109	127.2
ISLM rear drip	4/30/2010	.003960	xx	86.1	5.9	0.108	112.9

Table B2.2. Calcite growth rate and cave air CO_2 for ISLM and ISST drip sites.

Site	Date	Calcite growth (mg/day)	Cave air CO_2 (ppm)
ISST	5/8/2001	13.6	xx
ISST	6/7/2001	13.0	xx
ISST	7/12/2001	16.5	xx
ISST	8/15/2001	-0.6	xx
ISST	9/13/2001	-0.3	xx
ISST	11/8/2001	30.1	xx
ISST	12/14/2001	21.7	xx
ISST	1/15/2002	31.6	xx
ISST	2/11/2002	14.9	xx
ISST	3/12/2002	10.7	xx
ISST	4/15/2002	10.3	xx
ISST	5/9/2002	6.6	xx
ISST	6/6/2002	5.7	xx
ISST	7/10/2002	6.0	xx
ISST	8/7/2002	0.1	xx
ISST	9/13/2002	4.5e-2	xx
ISST	10/12/2002	17.1	xx
ISST	11/15/2002	36.2	xx
ISST	12/7/2002	15.3	xx
ISST	1/16/2003	21.9	xx
ISST	2/20/2003	21.5	xx
ISST	2/28/2003	13.9	xx
ISST	3/6/2003	1.1	xx
ISST	3/14/2003	5.8	xx
ISST	3/20/2003	2.2	xx
ISST	4/17/2003	11.1	xx
ISST	5/6/2003	3.4	xx
ISST	6/5/2003	5.7	xx
ISST	7/7/2003	3.8	xx
ISST	8/4/2003	-0.2	xx
ISST	9/4/2003	-0.4	xx
ISST	11/6/2003	10.1	xx
ISST	1/19/2004	17.7	xx
ISST	3/8/2004	14.7	589
ISST	5/13/2004	15.9	1067
ISST	7/15/2004	14.5	3674
ISST	9/8/2004	1.8	1492
ISST	11/5/2004	13.5	1089
ISST	12/7/2004	16.1	757

ISST	3/10/2005	11.8	552
ISST	3/10/2005	22.5	632
ISST	4/7/2005	8.4	861
ISST	5/13/2005	7.5	1416
ISST	6/9/2005	4.2	3894
ISST	7/13/2005	-2.3	5413
ISST	8/9/2005	-0.3	4294
ISST	9/9/2005	-0.2	1433
ISST	10/7/2005	10.4	xx
ISST	11/4/2005	11.0	xx
ISST	12/1/2005	15.0	610
ISST	1/3/2006	0.9	430
ISST	2/8/2006	4.5	617
ISST	3/13/2006	7.1	798
ISST	4/17/2006	5.3	931
ISST	5/12/2006	2.7	1441
ISST	6/28/2006	0.1	5282
ISST	8/10/2006	-0.4	4141
ISST	9/12/2006	8.0	1174
ISST	10/13/2006	0.8	1705
ISST	11/10/2006	0.5	750
ISST	12/10/2006	10.1	xx
ISST	1/27/2007	9.2	501
ISST	2/21/2007	14.7	655
ISST	3/30/2007	9.2	1109
ISST	5/29/2007	9.7	3623
ISST	6/29/2007	-0.5	5452
ISST	7/19/2007	-0.3	7369
ISST	8/24/2007	0.6	2772
ISST	9/22/2007	2.3	2150
ISST	10/21/2007	11.3	866
ISST	11/18/2007	14.9	602
ISST	12/11/2007	12.9	488
ISST	1/9/2008	9.7	631
ISST	2/17/2008	9.1	593
ISST	3/16/2008	4.0	xx
ISST	4/5/2008	19.7	829
ISST	5/15/2008	26.8	1021
ISST	6/5/2008	10.7	1793
ISST	7/3/2008	2.2	2532
ISST	7/25/2008	-0.4	3235
ISST	9/6/2008	0.6	691

ISST	3/17/2009	7.0	452
ISST	4/26/2009	5.5	450
ISST	5/17/2009	8.1	1178
ISST	6/17/2009	0.9	3004
ISST	7/17/2009	-0.4	3204
ISST	8/30/2009	0.1	1988
ISST	9/27/2009	2.8	700
ISST	10/25/2009	14.1	814
ISST	11/15/2009	8.4	458
ISST	12/18/2009	9.2	550
ISST	1/21/2010	3.1	550
ISST	3/27/2010	9.7	583
ISST	4/30/2010	2.8	1058
ISST	5/30/2010	4.6	2594
ISST	6/29/2010	-0.1	4100
ISST	7/29/2010	-0.2	5215
ISST	8/31/2010	-0.3	7655
ISST	9/26/2010	8.3	688
ISLM	5/8/2001	7.90	xx
ISLM	6/7/2001	6.11	xx
ISLM	7/12/2001	1.26	xx
ISLM	8/15/2001	-0.22	xx
ISLM	9/13/2001	-0.22	xx
ISLM	11/8/2001	0.25	xx
ISLM	12/14/2001	2.61	xx
ISLM	1/15/2002	9.41	xx
ISLM	2/11/2002	5.01	xx
ISLM	3/12/2002	6.75	xx
ISLM	4/15/2002	5.90	xx
ISLM	5/9/2002	3.36	xx
ISLM	6/6/2002	1.88	xx
ISLM	7/10/2002	2.22	xx
ISLM	8/7/2002	-0.41	xx
ISLM	9/13/2002	-0.06	xx
ISLM	10/12/2002	-0.23	xx
ISLM	11/15/2002	-0.32	xx
ISLM	12/7/2002	0.85	xx
ISLM	1/16/2003	4.67	xx
ISLM	2/20/2003	7.95	xx
ISLM	2/28/2003	1.86	xx
ISLM	3/6/2003	0.66	xx

ISLM	3/14/2003	3.31	xx
ISLM	3/20/2003	1.27	xx
ISLM	4/17/2003	3.20	xx
ISLM	5/6/2003	3.08	xx
ISLM	6/5/2003	6.34	xx
ISLM	7/7/2003	0.89	xx
ISLM	8/4/2003	-0.28	xx
ISLM	9/4/2003	-0.23	xx
ISLM	11/6/2003	-0.13	xx
ISLM	1/19/2004	5.70	xx
ISLM	3/8/2004	8.38	643
ISLM	5/13/2004	3.87	1763
ISLM	7/15/2004	1.31	4654
ISLM	9/8/2004	-0.18	5173
ISLM	11/5/2004	0.18	4578
ISLM	12/4/2004	0.35	2270
ISLM	3/10/2005	5.94	783
ISLM	4/7/2005	5.81	560
ISLM	5/13/2005	4.22	624
ISLM	6/9/2005	3.44	843
ISLM	7/13/2005	2.01	2012
ISLM	8/9/2005	-0.16	4120
ISLM	9/9/2005	-0.17	6205
ISLM	10/7/2005	-0.22	7217
ISLM	11/4/2005	-0.13	8485
ISLM	12/1/2005	1.81	xx
ISLM	1/3/2006	6.34	xx
ISLM	2/8/2006	2.37	840
ISLM	3/13/2006	7.12	xx
ISLM	4/17/2006	5.54	xx
ISLM	5/2/2006	9.25	xx
ISLM	6/28/2006	1.56	1152
ISLM	8/10/2006	0.44	3312
ISLM	9/12/2006	-0.18	5300
ISLM	10/13/2006	-0.16	6417
ISLM	11/10/2006	-0.24	7584
ISLM	12/10/2006	0.98	3778
ISLM	1/27/2007	4.93	907
ISLM	2/21/2007	5.02	945
ISLM	3/30/2007	5.19	572
ISLM	4/27/2007	6.16	xx
ISLM	5/29/2007	4.18	684

ISLM	6/29/2007	1.31	2287
ISLM	7/19/2007	-0.43	4507
ISLM	10/21/2007	-0.02	5793
ISLM	11/18/2007	3.20	5200
ISLM	12/11/2007	3.45	4188
ISLM	1/9/2008	5.80	2644
ISLM	2/17/2008	6.57	1398
ISLM	3/16/2008	6.89	401
ISLM	4/5/2008	5.32	631
ISLM	5/15/2008	6.13	5905
ISLM	6/5/2008	4.80	883
ISLM	7/25/2008	0.80	762
ISLM	9/6/2008	1.70	1961
ISLM	11/16/2008	2.68e-3	3385
ISLM	2/15/2009	6.79	5287
ISLM	3/17/2009	5.18	7336
ISLM	4/26/2009	4.96	5851
ISLM	5/17/2009	5.69	5916
ISLM	6/17/2009	4.29	488
ISLM	7/17/2009	3.45	525
ISLM	8/30/2009	-0.16	639
ISLM	9/27/2009	-0.16	648
ISLM	10/25/2009	-0.20	775
ISLM	11/15/2009	0.27	1704
ISLM	12/18/2009	3.28	3726
ISLM	1/21/2010	8.56	6238
ISLM	3/27/2010	5.81	6536
ISLM	4/30/2010	7.44	9520
ISLM	5/30/2010	5.12	xx
ISLM	6/29/2010	2.92	643
ISLM	7/29/2010	-0.19	1763
ISLM	8/31/2010	0.00	4654
ISLM	9/26/2010	-0.43	5173

Table B2.3. Conductivity, pH, water temperature, alkalinity, and cave air CO_2 concentration for drip sites ISSR 3, ISSR 5, ISSR 6, ISSR 7, ISSR 8, and ISSR 9.

Site	Date	Conductivity (µS)	pH	Water temperature (Celsius)	Alkalinity (ppm)	Cave air CO_2 (ppm)
ISSR 3	1/27/2007	xx	7.98	xx	246.93	xx
ISSR 3	2/21/2007	463.6	8.23	20.8	251.56	554
ISSR 3	3/30/2007	451	8.1	20.1	257.2	817
ISSR 3	4/27/2007	459.5	8.06	21.9	253.52	650
ISSR 3	6/29/2007	444.2	7.83	22.5	267	5159
ISSR 3	10/21/2007	479.3	7.67	xx	258.9	3413
ISSR 3	11/18/2007	477.3	7.63	21.7	246.93	1009
ISSR 3	12/11/2007	449.5	8.11	21.9	xx	711
ISSR 3	1/9/2008	439.8	7.69	20.5	240.34	573
ISSR 3	2/17/2008	426.1	7.85	22	235.7	497
ISSR 3	3/16/2008	430.5	7.57	21.5	238.39	629
ISSR 3	4/5/2008	xx	xx	xx	246.44	xx
ISSR 3	5/15/2008	426.2	7.64	22.1	xx	731
ISSR 3	6/5/2008	441.8	7.57	23.5	150.55	1317
ISSR 3	7/3/2008	443.3	7.33	21.8	247.66	xx
ISSR 3	7/25/2008	446.7	7.35	22	257.4	3697
ISSR 3	9/6/2008	xx	xx	xx	252.3	xx
ISSR 3	11/15/2008	xx	xx	xx	xx	xx
ISSR 3	2/14/2009	401.9	8.21	22.7	215.94	512
ISSR 3	3/17/2009	419.6	7.83	21.3	203.74	500
ISSR 3	4/26/2009	395.5	7.18	21.3	224.97	475
ISSR 3	5/17/2009	402.3	8.22	20.8	217.65	673
ISSR 3	6/17/2009	405.7	7.99	21.8	251.08	1567
ISSR 3	7/17/2009	433.5	7.38	20.7	217.65	4422
ISSR 3	8/30/2009	459.5	7.02	24.7	246.2	7054
ISSR 3	9/14/2009	xx	xx	xx	260.836	7198
ISSR 3	9/16/2009	461.3	7.69	23.7	242.048	7498
ISSR 3	9/27/2009	458.7	7.8	20.8	245.95	4975
ISSR 3	10/25/2009	453	7.82	21.7	264.008	3115
ISSR 3	11/15/2009	xx	8.02	22.3	227.16	1885
ISSR 3	12/18/2009	436.1	8.15	20.2	28.97	608
ISSR 3	1/21/2010	436.1	8.25	21.2	250.832	569
ISSR 3	2/25/2010	448.1	8.15	xx	xx	685
ISSR 3	3/30/2010	434.2	8.06	21.3	xx	505
ISSR 3	4/30/2010	442.3	8.11	21.4	xx	571
ISSR 3	5/30/2010	430	8.32	23	xx	687
ISSR 3	6/29/2010	438.4	8.18	21.4	256.2	1216

ISSR 3	7/29/2010	434.5	8.04	21.5	250.59	3167
ISSR 3	8/31/2010	440.6	7.98	xx	245.2	4780
ISSR 3	9/9/2010	xx	7.7	21.4	xx	6624
ISSR 3	9/10/2010	447.7	xx	21.9	xx	10800
ISSR 3	9/13/2010	446.9	7.71	21.5	xx	11700
ISSR 3	9/17/2010	462.9	7.4	xx	xx	11800
ISSR 3	9/26/2010	463.2	7.27	xx	243.3	11900
ISSR 5	2/15/2009	398.5	8.11	22.5	170.5	512
ISSR 5	3/17/2009	406.4	7.65	21.8	200.0	500
ISSR 5	4/26/2009	402.2	7.94	21.4	212.2	475
ISSR 5	5/17/2009	397.1	8.03	20.9	251.5	673
ISSR 5	6/17/2009	399.4	7.74	21.5	216.6	1567
ISSR 5	7/17/2009	392.7	7.53	21	172.7	4422
ISSR 5	8/30/2009	403.3	6.28	24.1	222.5	7054
ISSR 5	9/16/2009	453.9	7.71	23.4	215.9	7198
ISSR 5	9/27/2009	461.2	7.83	20.6	242.5	7498
ISSR 5	10/25/2009	462.9	7.95	22.9	253.5	4975
ISSR 5	11/15/2009	471	7.98	22.4	269.8	3115
ISSR 5	12/9/2009	439.9	8.3	18.8	xx	1885
ISSR 5	12/18/2009	440.3	8.18	20.3	246.1	608
ISSR 5	1/23/2010	452.6	7.95	21.1	xx	569
ISSR 5	2/25/2010	452.6	xx	xx	xx	685
ISSR 5	3/30/2010	xx	8.14	21.4	xx	505
ISSR 5	4/30/2010	429.1	8.15	21.6	xx	571
ISSR 5	5/30/2010	423.7	7.87	22.7	xx	687
ISSR 5	6/29/2010	412.7	7.76	22.0,22.1	234.2	1216
ISSR 5	7/29/2010	436.1	7.8	21.9	242.0	3167
ISSR 5	8/31/2010	409.9	7.35	21.5	222.0	4780
ISSR 5	9/9/2010	xx	7.26	21.7	xx	6624
ISSR 5	9/10/2010	436.1	xx	xx	xx	10800
ISSR 5	9/13/2010	xx	xx	xx	xx	11700
ISSR 5	9/17/2010	416.4	xx	xx	xx	11800
ISSR 5	9/26/2010	461	7.4	21.8	242.8	11900
ISSR 6	2/15/2009	xx	xx	xx	xx	xx
ISSR 6	3/6/2009	xx	xx	xx	xx	xx
ISSR 6	4/4/2009	xx	xx	xx	xx	485
ISSR 6	5/17/2009	409.3	8.09	xx	xx	673
ISSR 6	6/17/2009	403.6	7.62	21.7	xx	1567
ISSR 6	7/17/2009	478	7.62	20.6	xx	4422
ISSR 6	8/30/2009	511.7	xx	24.7	xx	7056

ISSR 6	9/14/2009	xx	xx	xx	xx	571
ISSR 6	9/16/2009	449.1	7.95	24	xx	7500
ISSR 6	9/27/2009	470.4	7.88	20.5	xx	4877
ISSR 6	10/25/2009	519.4	7.95	23.1	xx	3117
ISSR 6	11/15/2009	484.5	8.15	22.2	xx	1887
ISSR 6	12/9/2009	407.5	8.42	18	xx	610
ISSR 6	12/18/2009	425.3	8.32	20.2	xx	571
ISSR 6	1/21/2010	470	8.3	21.1	xx	687
ISSR 6	2/25/2010	407.6	8.34	19.7	xx	507
ISSR 6	3/30/2010	449.2	8.16	22.1	xx	519
ISSR 6	4/30/2010	397.1	8.29	21.5	xx	
ISSR 6	5/30/2010	414.1	8.12	24	xx	1111
ISSR 6	6/29/2010	437.1	7.81	21.1	253.7	3088
ISSR 7	2/15/2009	xx	xx	xx	xx	xx
ISSR 7	3/6/2009	xx	xx	xx	xx	xx
ISSR 7	4/4/2009	xx	xx	xx	xx	475
ISSR 7	5/17/2009	390.1	8.11	xx	209.8	673
ISSR 7	6/17/2009	397.8	7.75	21.5	204.7	1567
ISSR 7	7/17/2009	433.5	7.45	20.8	232.5	4422
ISSR 7	8/30/2009	479.3	7.25	24.6	271.3	7056
ISSR 7	9/14/2009	xx	xx	xx	231.0	xx
ISSR 7	9/16/2009	xx	xx	xx	xx	7500
ISSR 7	9/27/2009	450.6	7.72	20.5	240.3	4977
ISSR 7	10/25/2009	467.4	7.8	22.5	269.1	3117
ISSR 7	11/15/2009	452.1	7.89	21.8	244.2	1887
ISSR 7	12/9/2009	401.4	8.22	19.5	xx	610
ISSR 7	12/18/2009	413.1	8.24	19.9	xx	571
ISSR 7	1/21/2010	420.6	8.15	21.1	218.6	687
ISSR 7	2/25/2010	391.6	8.26	19.7	xx	507
ISSR 7	3/30/2010	421.1	8	22	xx	519
ISSR 7	4/30/2010	393.9	8.22	21.6	xx	571
ISSR 7	5/30/2010	419.1	8.09	23.2	xx	1111
ISSR 7	6/29/2010	398.2	7.7	21.2	217.1	3088
ISSR 8	3/6/2009	xx	xx	xx	xx	xx
ISSR 8	4/4/2009	xx	xx	xx	xx	439
ISSR 8	5/17/2009	xx	xx	xx	260.1	668
ISSR 8	6/17/2009	492.2	7.68	21.6	269.9	1567
ISSR 8	7/17/2009	510.2	7.52	20.8	284.5	4371
ISSR 8	8/30/2009	505.8	7.01	24.1	276.9	6652

ISSR 8	9/14/2009	xx	xx	xx	xx	xx
ISSR 8	9/16/2009	xx	xx	xx	xx	8487
ISSR 8	9/27/2009	546.3	7.58	20.6	305.9	7211
ISSR 8	10/25/2009	576.7	7.75	22.6	325.4	4227
ISSR 8	11/15/2009	585.5	8.13	21.9	315.9	1908
ISSR 8	12/9/2009	499.9	8.33	18.9	xx	612
ISSR 8	12/18/2009	502.1	8.38	20.4	xx	592
ISSR 8	1/21/2010	502.6	8.21	21	274.9	687
ISSR 8	2/25/2010	526.2	8.41	19.7	xx	507
ISSR 8	3/30/2010	528.3	8.18	22.2	xx	519
ISSR 8	4/30/2010	468.3	8.33	21.2	xx	571
ISSR 8	5/30/2010	495.8	8.19	23	xx	1111
ISSR 8	6/29/2010	499.2	7.81	21.2	268.4	3088
ISSR 9	3/6/2009	xx	xx	xx	xx	xx
ISSR 9	4/4/2009	xx	xx	xx	xx	457
ISSR 9	5/17/2009	xx	xx	xx	xx	668
ISSR 9	6/17/2009	467.5	7.69	21.6	xx	1567
ISSR 9	7/17/2009	467.2	8.18	21.4	xx	4371
ISSR 9	8/30/2009	467.4	6.78	24.3	xx	6652
ISSR 9	9/14/2009	xx	xx	xx	xx	xx
ISSR 9	9/16/2009	470.6	7.91	24.2	xx	8487
ISSR 9	9/27/2009	478.5	7.82	20.7	xx	7211
ISSR 9	10/25/2009	519.1	7.91	23.1	xx	4227
ISSR 9	11/15/2009	589.3	8.1	22.4	xx	1908
ISSR 9	12/9/2009	xx	xx	xx	xx	612
ISSR 9	12/18/2009	532.7	8.39	19	xx	592
ISSR 9	1/21/2010	511.3	8.25	21.1	xx	687
ISSR 9	2/25/2010	500.5	8.45	19.3	xx	507
ISSR 9	3/30/2010	507.3	8.28	22.3	xx	519
ISSR 9	4/30/2010	509.1	8.36	21.5	xx	571
ISSR 9	5/30/2010	498.2	8.21	21.4	xx	1111
ISSR 9	6/29/2010	491	7.8	21.6	xx	3088

Table B2.4. Effective rainfall, PDSI and monthly rainfall for the Austin, TX area.

Month	Effective rainfall	PDSI	Monthly rainfall
1/1/2000	4.94	1.34	2.49
2/1/2000	-1.76	0.65	1.41
3/1/2000	2.66	2.07	2.75
4/1/2000	-1.91	2.11	1.92
5/1/2000	2.58	2.24	5.91
6/1/2000	0.15	2.65	6.36
7/1/2000	5.21	5.75	0.43
8/1/2000	-4.46	6.54	0.22
9/1/2000	-1.02	-0.16	3.23
10/1/2000	-3.02	-0.45	8.03
11/1/2000	-1.45	-0.52	9.47
12/1/2000	-1.77	-1.00	3.66
1/1/2001	-1.51	-1.10	4
2/1/2001	-2.48	-1.69	2.01
3/1/2001	-1.27	-1.57	7.16
4/1/2001	-1.27	-1.66	1.81
5/1/2001	-2.04	-2.42	4.2
6/1/2001	-5.29	-3.34	1.85
7/1/2001	-9.65	-3.09	0.53
8/1/2001	-3.20	-2.48	3.47
9/1/2001	-5.74	-3.08	1.84
10/1/2001	-8.11	-3.23	3
11/1/2001	-2.76	-3.61	6.09
12/1/2001	-1.76	-3.97	3.86
1/1/2002	-1.76	-4.49	0.83
2/1/2002	-1.49	-5.26	1.04
3/1/2002	-0.78	-4.91	1.28
4/1/2002	-1.08	-4.44	0.83
5/1/2002	-2.66	-4.94	2.06
6/1/2002	-3.71	-5.85	3.25
7/1/2002	-7.58	-6.37	5.42
8/1/2002	-8.18	-6.51	0.65
9/1/2002	-7.74	0.58	3.9
10/1/2002	-1.49	1.71	9.96
11/1/2002	0.35	2.31	2.54
12/1/2002	-1.57	2.86	4.76
1/1/2003	-1.37	3.16	1.43
2/1/2003	-0.17	3.66	4.33
3/1/2003	-1.25	3.45	1.15

4/1/2003	-3.37	2.96	0.29
5/1/2003	-4.46	2.44	2.03
6/1/2003	-6.17	2.39	5.11
7/1/2003	-6.65	3.03	1.61
8/1/2003	-5.80	2.18	2.43
9/1/2003	-8.80	3.09	3.28
10/1/2003	2.62		2.29
11/1/2003	4.94	1.34	0.74
12/1/2003	-1.76	0.65	0.67
1/1/2004	2.66	2.07	4.58
2/1/2004	-1.91	2.11	4.69
3/1/2004	2.58	2.24	2.07
4/1/2004	0.15	2.65	3.24
5/1/2004	5.21	5.75	2.18
6/1/2004	-4.46	6.54	10.53
7/1/2004	-1.02	-0.16	2.76
8/1/2004	-3.02	-0.45	5.63
9/1/2004	-1.45	-0.52	0.74
10/1/2004	-1.77	-1.00	8.28
11/1/2004	-1.51	-1.10	8.37
12/1/2004	-2.48	-1.69	0.76
1/1/2005	-1.27	-1.57	1.98
2/1/2005	-1.27	-1.66	3.26
3/1/2005	-2.04	-2.42	2.95
4/1/2005	-5.29	-3.34	1.29
5/1/2005	-9.65	-3.09	3.2
6/1/2005	-3.20	-2.48	0.58
7/1/2005	-5.74	-3.08	2.69
8/1/2005	-8.11	-3.23	7.95
9/1/2005	-2.76	-3.61	0.2
10/1/2005	-1.76	-3.97	1.51
11/1/2005	-1.76	-4.49	1.36
12/1/2005	-1.49	-5.26	0.18
1/1/2006	-0.78	-4.91	1.8
2/1/2006	-1.08	-4.44	0.89
3/1/2006	-2.66	-4.94	7.54
4/1/2006	-3.71	-5.85	2.89
5/1/2006	-7.58	-6.37	5.28
6/1/2006	-8.18	-6.51	3.18
7/1/2006	-7.74	0.58	0.48
8/1/2006	-1.49	1.71	0.22
9/1/2006	0.35	2.31	3

10/1/2006	-1.57	2.86	3.93
11/1/2006	-1.37	3.16	1.29
12/1/2006	-0.17	3.66	4.2
1/1/2007	-1.25	3.45	6.92
2/1/2007	-3.37	2.96	0.14
3/1/2007	-4.46	2.44	5.95
4/1/2007	-6.17	2.39	2.25
5/1/2007	-6.65	3.03	7.01
6/1/2007	-5.80	2.18	5.41
7/1/2007	-8.80	3.09	9.84
8/1/2007	2.62		2.5
9/1/2007	4.94	1.34	3.97
10/1/2007	-1.76	0.65	1.13
11/1/2007	2.66	2.07	1.16
12/1/2007	-1.91	2.11	0.67
1/1/2008	2.58	2.24	0.82
2/1/2008	0.15	2.65	0.51
3/1/2008	5.21	5.75	2.86
4/1/2008	-4.46	6.54	3.52
5/1/2008	-1.02	-0.16	1.7
6/1/2008	-3.02	-0.45	0.74
7/1/2008	-1.45	-0.52	0.38
8/1/2008	-1.77	-1.00	2.39
9/1/2008	-1.51	-1.10	0.02
10/1/2008	-2.48	-1.69	2.01
11/1/2008	-1.27	-1.57	0.72
12/1/2008	-1.27	-1.66	0.74
1/1/2009	-2.04	-2.42	1.47
2/1/2009	-5.29	-3.34	3.04
3/1/2009	-9.65	-3.09	2.78
4/1/2009	-3.20	-2.48	1.77
5/1/2009	-5.74	-3.08	1.36
6/1/2009	-8.11	-3.23	0
7/1/2009	-2.76	-3.61	1.59
8/1/2009	-1.76	-3.97	2.64
9/1/2009	-1.76	-4.49	3.81
10/1/2009	-1.49	-5.26	0.56
11/1/2009	-0.78	-4.91	0.31
12/1/2009	-1.08	-4.44	0.74
1/1/2010	-2.66	-4.94	1.22
2/1/2010	-3.71	-5.85	0.31
3/1/2010	xx	-6.37	0.69

4/1/2010	xx	-6.51	0.1
5/1/2010	xx	0.58	0.41
6/1/2010	xx	1.71	1.03
7/1/2010	xx	2.31	0.65
8/1/2010	xx	2.86	0

Table B2.5. Major anions and cations for charge balances.

Site	Date	Alk	Cl	NO_3	SO_4	F	Br	Σ-anions
ISSR 3	4/26/09	225.0	8.1	12.3	9.1	0.22	0.06	-4.41
ISSR 3	5/17/09	217.6	7.4	13.2	8.6	0.21	0.06	-4.27
ISSR 3	6/17/09	251.1	7.8	12.8	8.6	0.23	0.06	-4.82
ISSR 3	7/17/09	217.6	8.9	13.9	8.8	0.29	0.07	-4.34
ISSR 3	8/30/09	246.2	8.1	14.3	8.8	0.23	0.07	-4.79
ISSR 3	9/16/09	242.1	10.3	17.4	9.8	0.27	0.05	-4.86
ISSR 3	10/25/09	264.0	9.2	13.6	9.5	0.23	0.06	-5.12
ISSR 3	11/15/09	241.4	8.6	13.8	9.5	0.22	0.06	-4.73
ISSR 3	1/21/2010	250.8	9.0	13.1	9.7	0.24	0.06	-4.89
ISSR 4	7/17/2009	284.3	10.4	13.8	9.4	0.32	0.07	-5.49
ISSR 4	8/30/2009	250.3	8.5	14.1	9.2	0.22	0.07	-4.87
ISSR 4	9/16/2009	242.5	10.2	17.3	9.8	0.25	0.06	-4.86
ISSR 4	1/23/2010	244.7	8.9	13.3	9.7	0.22	0.06	-4.79
ISSR 5	5/17/2009	251.6	7.7	13.3	8.5	0.23	0.06	-4.83
ISSR 5	8/30/2009	222.5	8.5	13.3	8.4	0.26	0.06	-4.38
ISSR 5	10/25/2009	269.6	8.8	13.7	9.5	0.22	0.06	-5.20
ISSR 5	1/23/2010	262.1	8.6	13.7	9.9	0.21	0.06	-5.08
ISST	8/30/2009	250.6	29.0	22.9	14.8	0.18	0.15	-5.77
ISST	9/16/2009	289.9	21.6	16.3	12.8	0.23	0.09	-6.04
ISST	9/27/2009	233.3	19.9	12.8	11.9	0.21	0.09	-4.98

ISST	10/25/2009	254.0	18.1	11.1	11.6	0.23	0.07	-5.23
ISST	11/15/2009	227.2	19.9	13.9	12.4	0.23	0.10	-4.91
ISST	12/18/2009	214.0	19.9	15.0	12.8	0.22	0.09	-4.72
ISST	1/21/2010	197.6	17.3	12.9	11.9	0.29	0.08	-4.32

Site	Date	Na	K	Ca	Mg	Si	Σ-cations	Charge balance
ISSR 3	4/26/09	2.9	2.2	79.1	4.2	3.9	4.75	3.73
ISSR 3	5/17/09	2.8	2.0	74.5	4.4	3.8	4.53	2.89
ISSR 3	6/17/09	2.8	2.1	77.5	4.6	4.0	4.70	-1.28
ISSR 3	7/17/09	2.9	2.0	81.2	4.7	4.2	4.92	6.29
ISSR 3	8/30/09	3.8	2.1	84.1	4.6	3.6	5.05	2.66
ISSR 3	9/16/09	3.9	2.3	88.9	4.1	3.8	5.28	4.06
ISSR 3	10/25/09	4.1	2.1	92.1	4.0	3.7	5.42	2.85
ISSR 3	11/15/09	4.0	2.2	90.2	4.2	3.9	5.36	6.16
ISSR 3	1/21/2010	3.5	1.2	88.0	4.1	3.7	5.18	2.87
ISSR 4	7/17/2009	3.5	1.1	86.3	4.5	3.8	5.13	-3.40
ISSR 4	8/30/2009	3.9	1.3	86.0	4.6	3.6	5.13	2.58
ISSR 4	9/16/2009	4.1	1.2	92.1	3.8	3.7	5.38	5.05
ISSR 4	1/23/2010	3.5	1.2	88.9	4.0	3.8	5.22	4.30
ISSR 5	5/17/2009	3.6	1.2	73.5	4.3	3.6	4.47	-3.96
ISSR 5	8/30/2009	3.7	1.0	75.9	4.7	3.5	4.61	2.57
ISSR 5	10/25/2009	4.2	1.1	93.6	4.3	3.2	5.46	2.50
ISSR 5	1/23/2010	3.5	1.3	89.6	4.2	3.8	5.27	1.87

ISST	8/30/2009	12.3	2.7	75.3	14.1	4.7	5.86	0.80
ISST	9/16/2009	14.2	2.2	79.7	13.8	5.1	6.15	0.94
ISST	9/27/2009	12.6	2.3	68.0	12.4	4.9	5.37	3.82
ISST	10/25/2009	12.7	2.2	69.7	11.7	4.9	5.40	1.61
ISST	11/15/2009	11.6	2.6	69.8	10.9	4.6	5.27	3.57
ISST	12/18/2009	11.1	2.7	64.3	10.2	4.3	4.90	1.88
ISST	1/21/2010	10.3	2.4	58.9	9.5	4.1	4.53	2.30

Table B2.6. Correlations of Mg/Ca and Sr/Ca as well as Sr/Ca and water flux. Significant correlations are marked with an asterisk.

Site	Sr/Ca vs Mg/Ca	Sr/Ca vs drip rate	Sr/Ca vs eff. rainfall	Sr/Ca vs PDSI
ISSR 3	r = -0.46, p< 0.001*	r^2 = 0.03, p = 0.13	r^2 = 0.01, p = 0.27	r^2 = 0.01, p = 0.22
ISSR 5	r = 0.01, p = 0.33	r^2 = 0.37, p < 0.01*	r^2 = 0.03, p = 0.21	r^2 = 0.37, p < 0.01*
ISSR 6	r = -0.24, p = 0.18	r^2 = 0.16, p = 0.07	r^2 = 0.14, p = 0.08	r^2 = 0.00, p = 0.49
ISSR 7	r =- 0.13, p = 0.32	r^2 = 0.10, p = 0.12	r^2 = 0.37, p < 0.01	r^2 = 0.01, p = 0.34
ISSR 8	r = -0.33, p = 0.10	r^2 = 0.14, p = 0.08	r^2 = 0.08, p = 0.14	r^2 = 0.37, p < 0.01
ISSR 9	r = -0.57, p < 0.01*	r^2 = 0.04, p = 0.22	r^2 = 0.17, p = 0.06	r^2 = 0.01, p = 0.36
ISST	r = 0.80, p < 0.001*	r^2 = 0.06, p < 0.05*	r^2 = 0.01, p = 0.22	r^2 = 0.09, p < 0.01*
ISLM	r = 0.96, p < 0.001*	r^2 = 0.03, p = 0.13	r^2 = 0.09, p = 0.10	r^2 = 0.01, p = 0.32

Table B2.7. Correlations of Ba/Ca and Sr/Ca and Ba/Ca and water flux. Significant correlations are marked with an asterisk.

Site	Ba/Ca vs Mg/Ca	Ba/Ca vs Sr/Ca	Ba/Ca vs drip rate	Ba/Ca vs eff. rainfall	Ba/Ca vs PDSI
ISSR 3	$r = 0.10$, $p = 0.26$	$r = 0.07$, $p = 0.34$	$r^2 = 0.06$, $p = 0.06$	$r^2 = 0.03$, $p = 0.13$	$r^2 = 0.01$, $p = 0.31$
ISSR 5	$r = 0.46$, $p < 0.05$*	$r = 0.78$, $p < 0.001$*	$r^2 = 0.17$, $p < 0.05$*	$r^2 = 0.12$, $p = 0.06$	$r^2 = 0.53$, $p < 0.001$*
ISSR 6	$r = 0.04$, $p = 0.44$	$r = 0.21$, $p = 0.21$	$r^2 = 0.08$, $p = 0.15$	$r^2 = 0.02$, $p = 0.29$	$r^2 = 0.21$, $p < 0.05$*
ISSR 7	$r = 0.61$, $p < 0.005$*	$r = 0.35$, $p = 0.08$	$r^2 = 0.04$, $p = 0.24$	$r^2 = 0.001$, $p = 0.45$	$r^2 = 0.55$, $p < 0.001$*
ISSR 8	$r = 0.51$, $p < 0.05$*	$r = 0.50$, $p < 0.05$*	$r^2 = 0.03$, $p = 0.53$	$r^2 = 0.01$, $p = 0.40$	$r^2 = 0.21$, $p < 0.05$*
ISSR 9	$r = 0.44$, $p < 0.05$*	$r = 0.20$, $p = 0.22$	$r^2 = 0.28$, $p < 0.05$*	$r^2 = 0.04$, $p = 0.25$	$r^2 = 0.66$, $p < 0.001$*

Table B2.8. Correlations of N and K and water flux. Significant correlations are marked with an asterisk.

Site	Na vs. drip rate	Na vs. eff. rainfall	Na vs. PDSI	K vs. drip rate	K vs. eff. rainfall	K vs. PDSI
ISSR 3	$r^2 = 0.12$, $p < 0.02$*	$r^2 = 0.18$, $p < 0.005$*	$r^2 = 0.24$, $p < 0.001$*	$r^2 = 0.006$, $p = 0.32$	$r^2 = 0.003$, $p = 0.36$	$r^2 = 0.44$, $p < 0.001$*
ISSR 5	$r^2 = 0.29$, $p < 0.005$*	$r^2 = 0.01$, $p = 0.36$	$r^2 = 0.002$, $p = 0.42$	$r^2 = 0.28$, $p < 0.005$*	$r^2 = 0.006$, $p = 0.36$	$r^2 = 0.08$, $p = 0.09$
ISSR 6	$r^2 = 0.003$, $p = 0.41$	$r^2 = 0.02$, $p = 0.28$	$r^2 = 0.004$, $p = 0.39$	$r^2 = 0.00$, $p = 0.48$	$r^2 = 0.03$, $p = 0.25$	$r^2 = 0.17$, $p = 0.25$
ISSR 7	$r^2 = 0.17$, $p < 0.05$*	$r^2 = 0.01$, $p = 0.33$	$r^2 = 0.24$, $p < 0.01$*	$r^2 = 0.003$, $p = 0.41$	$r^2 = 0.03$, $p = 0.27$	$r^2 = 0.27$, $p < 0.05$*
ISSR 8	$r^2 = 0.20$, $p < 0.05$*	$r^2 = 0.14$, < 0.05*	$r^2 = 0.01$, $p = 0.35$	$r^2 = 0.17$, $p < 0.05$*	$r^2 = 0.02$, $p = 0.32$	$r^2 = 0.17$, $p < 0.05$*
ISSR 9	$r^2 = 0.33$, $p < 0.005$*	$r^2 = 0.05$, $p = 0.16$	$r^2 = 0.07$, $p = 0.11$	$r^2 = 0.10$, $p = 0.11$	$r^2 = 0.05$, $p = 0.19$	$r^2 = 0.36$, $p < 0.01$*

Appendix B3: Physical parameters, geochemical parameters, and correlations of cave air, cave drip water, and calcite at Westcave

Table B3.1. Drip rate, calcite growth rate, Ca, Mg, Sr, and Ba.

Site	Date	drip rate (ml/sec)	calcite growth (mg/day)	Ca (ppm)	Mg (ppm)	Sr (ppm)	Ba (ppm)
WC1	7/3/2009	n/a	n/a	109.3	34.0	0.322	0.075
WC1	8/28/2009	5.3e-3	n/a	105.4	33.8	0.319	0.072
WC1	9/15/2009	2.5e-3	n/a	104.5	34.1	0.322	0.072
WC1	10/5/2009	7.0e-3	28.8	111.7	35.0	0.331	0.073
WC1	10/29/2009	7.9e-3	20.5	111.6	29.8	0.300	0.071
WC1	12/7/2009	6.5e-3	12.7	105.7	31.4	0.286	0.057
WC1	1/21/2010	5.5e-3	8.4	108.4	32.2	0.295	0.064
WC1	1/21/2010	5.5e-3	8.4				
WC1	2/20/2010	2.0e-3	8.5	110.3	29.3	0.284	0.061
WC1	3/28/2010	1.5e-3	9.2	111.2	30.4	0.287	0.063
WC1	4/27/2010	1.6e-3	12.5	112.5	31.7	0.299	0.068
WC1	5/31/2010	1.7e-3	15.1	107.0	32.6	0.296	0.069
WC1	7/6/2010	4.2e-3	23.5	109.5	33.0	0.300	0.070
WC1	7/28/2010	7.3e-3	27.2	110.1	32.8	0.306	0.071
WC1	8/26/2010	8.3e-3	32.4	111.9	33.2	0.305	0.072
WC1	9/26/2010	6.7e-3	32.2	110.1	33.0	0.304	0.068
WC3	7/3/2009	8.7e-4	n/a	80.4	36.0	0.296	0.060
WC3	8/28/2009	1.5e-5	28.1	100.9	36.1	0.345	0.076
WC3	10/5/2009	1.1e-3	18.2	98.1	36.1	0.334	0.073
WC3	10/29/2009	1.3e-3	20.3	89.6	46.4	0.311	0.066
WC3	12/7/2009	8.7e-4	13.0	88.2	33.3	0.288	0.049
WC3	1/21/2010	9.3e-4	6.4	85.5	32.7	0.279	0.047
WC3	2/20/2010	1.2e-3	7.3	86.7	37.7	0.283	0.049
WC3	3/28/2010	1.0e-3	8.3	95.5	37.1	0.312	0.054
WC3	4/27/2010	1.1e-3	9.4	98.5	35.7	0.333	0.066
WC3	7/6/2010	9.9e-4	11.2	88.9	36.7	0.309	0.064
WC3	7/28/2010	1.5e-3	14.2	101.7	35.6	0.349	0.079
WC3	8/26/2010	9.9e-4	19.0	101.0	35.8	0.338	0.076
WC3	9/26/2010	1.2e-3	18.6	104.7	36.8	0.342	0.071
WC4	8/28/2009	6.0e-4	24.4	90.8	41.5	0.324	0.065
WC4	9/15/2009	1.8e-3	n/a	106.4	37.8	0.355	0.079

WC4	10/5/2009	3.2e-3	11.3	101.5	36.7	0.347	0.075
WC4	10/29/2009	3.0e-3	12.2	98.4	38.4	0.331	0.072
WC4	12/7/2009	2.4e-3	11.8	97.9	36.0	0.306	0.055
WC4	1/21/2010	2.7e-3	2.6	89.4	36.4	0.289	0.052
WC4	2/20/2010	3.1e-3	3.3	93.3	36.5	0.295	0.052
WC4	3/28/2010	2.4e-3	8.6	94.4	36.9	0.298	0.053
WC4	4/27/2010	2.4e-3	10.4	100.0	38.2	0.322	0.064
WC4	5/31/2010	1.0e-3	12.6	89.8	38.3	0.294	0.057
WC4	7/6/2010	8.3e-4	10.9	84.3	40.4	0.255	0.047
WC4	7/28/2010	4.7e-4	4.6	76.5	37.0	0.257	0.047
WC4	8/26/2010	7.4e-4	5.0	84.8	38.5	0.284	0.055
WC4	9/26/2010	2.5e-3	15.0	103.0	37.0	0.338	0.071
WC5	8/28/2009	2.3e-3	n/a	94.8	37.3	0.345	0.068
WC5	9/15/2009	3.1e-3	n/a	105.9	37.2	0.374	0.078
WC5	10/5/2009	2.5e-3	14.5	104.6	37.5	0.375	0.076
WC5	10/29/2009	1.8e-3	9.7	101.0	38.9	0.369	0.073
WC5	1/21/2010	4.0e-4	4.4	97.3	40.0	0.340	0.057
WC5	2/20/2010	3.8e-4	7.4	93.4	37.8	0.336	0.055
WC5	3/28/2010	6.3e-4	4.2	97.7	38.6	0.336	0.058
WC5	4/27/2010	1.4e-3	10.2	102.8	38.8	0.343	0.065
WC5	5/31/2010	1.4e-3	10.9	88.6	38.7	0.318	0.062
WC5	7/6/2010	1.5e-3	31.9	86.3	38.4	0.290	0.055
WC6	8/28/2009	0.090	n/a	91.5	34.8	0.331	0.072
WC6	9/15/2009	0.038	n/a	81.1	34.5	0.330	0.070
WC6	10/5/2009	0.062	35.6	90.2	34.7	0.324	0.070
WC6	10/29/2009	0.099	31.2	93.1	33.8	0.324	0.069
WC6	12/7/2009	0.043	20.5	91.6	33.1	0.301	0.057
WC6	1/21/2010	0.048	8.0	89.5	32.3	0.295	0.055
WC6	2/20/2010	0.078	12.7	94.4	33.0	0.300	0.055
WC6	3/28/2010	0.076	14.5	97.0	34.0	0.310	0.059
WC6	4/27/2010	0.075	28.8	98.1	35.8	0.328	0.066
WC6	5/31/2010	0.034	35.1	75.4	36.4	0.321	0.065
WC6	7/6/2010	0.097	47.4	88.0	36.7	0.327	0.068
WC6	7/28/2010	0.099	61.2	82.4	34.7	0.323	0.067
WC6	8/26/2010	0.089	67.4	94.8	35.2	0.334	0.070
WC6	9/26/2010	0.090	55.1	95.4	34.3	0.327	0.068

WC7	8/28/2009	2.3e-3	n/a	76.2	46.1	1.081	0.093
WC7	9/15/2009	1.2e-3	n/a	76.6	45.2	1.041	0.086
WC7	10/5/2009	2.2e-3	9.4	75.0	45.2	1.020	0.082
WC7	10/29/2009	1.2e-3	6.0			0.655	0.053
WC7	12/7/2009	3.6e-4	4.0	74.1	45.8	0.878	0.055
WC7	1/21/2010	8.5e-4	3.8	69.7	43.6	0.836	0.053
WC7	2/20/2010	7.7e-4	2.9	66.8	40.7	0.810	0.055
WC7	3/28/2010	7.3e-4	4.9	75.1	46.8	0.935	0.061
WC7	4/27/2010	3.3e-4	5.8	74.9	47.7	0.981	0.072
WC7	5/31/2010	6.1e-4	5.0	73.9	47.2	1.063	0.087
WC7	7/6/2010	6.1e-4	9.4	73.1	47.3	1.073	0.091

Table B3.2. Mg/Ca, Sr/Ca, and Ba/Ca values.

Site	Date	Mg/Ca (mmol/mol)	Sr/Ca (mmol/mol)	Ba/Ca (mmol/mol)
WC1	7/3/2009	513.4	1.34	0.20
WC1	8/28/2009	529.3	1.38	0.20
WC1	9/15/2009	538.0	1.40	0.20
WC1	10/5/2009	516.9	1.35	0.19
WC1	10/29/2009	440.7	1.22	0.18
WC1	12/7/2009	490.2	1.23	0.15
WC1	1/21/2010	489.1	1.24	0.17
WC1	2/20/2010	438.2	1.17	0.16
WC1	3/28/2010	450.2	1.18	0.16
WC1	4/27/2010	465.1	1.21	0.17
WC1	5/31/2010	501.6	1.26	0.19
WC1	7/6/2010	497.2	1.25	0.18
WC1	7/28/2010	490.9	1.27	0.19
WC1	8/26/2010	489.0	1.24	0.18
WC1	9/26/2010	493.8	1.26	0.18
WC3	7/3/2009	738.9	1.68	0.21
WC3	8/28/2009	590.3	1.56	0.22
WC3	10/5/2009	607.4	1.55	0.21
WC3	10/29/2009	853.6	1.58	0.21
WC3	12/7/2009	622.1	1.49	0.16
WC3	1/21/2010	630.9	1.49	0.16
WC3	2/20/2010	716.4	1.49	0.16
WC3	3/28/2010	641.3	1.49	0.16
WC3	4/27/2010	597.8	1.55	0.19
WC3	7/6/2010	680.6	1.59	0.21
WC3	7/28/2010	576.8	1.57	0.22
WC3	8/26/2010	584.9	1.53	0.22
WC3	9/26/2010	580.2	1.49	0.20
WC4	8/28/2009	753.6	1.63	0.21
WC4	9/15/2009	586.1	1.52	0.21
WC4	10/5/2009	596.6	1.56	0.21
WC4	10/29/200	643.0	1.53	0.21

	9			
WC4	12/7/2009	607.0	1.43	0.16
WC4	1/21/2010	671.6	1.48	0.17
WC4	2/20/2010	644.5	1.44	0.16
WC4	3/28/2010	644.6	1.44	0.16
WC4	4/27/2010	630.5	1.47	0.18
WC4	5/31/2010	702.8	1.49	0.18
WC4	7/6/2010	789.8	1.38	0.16
WC4	7/28/2010	797.2	1.54	0.18
WC4	8/26/2010	747.6	1.53	0.18
WC4	9/26/2010	592.8	1.50	0.20
WC5	8/28/2009	650.0	1.66	0.20
WC5	9/15/2009	579.0	1.61	0.21
WC5	10/5/2009	592.2	1.64	0.21
WC5	10/29/2009	634.5	1.67	0.21
WC5	1/21/2010	677.6	1.59	0.17
WC5	2/20/2010	668.0	1.64	0.17
WC5	3/28/2010	651.4	1.57	0.17
WC5	4/27/2010	622.3	1.52	0.18
WC5	5/31/2010	720.2	1.64	0.20
WC5	7/6/2010	733.3	1.54	0.18
WC6	8/28/2009	627.2	1.65	0.22
WC6	9/15/2009	700.9	1.86	0.25
WC6	10/5/2009	633.8	1.64	0.22
WC6	10/29/2009	598.5	1.59	0.21
WC6	12/7/2009	596.5	1.50	0.18
WC6	1/21/2010	594.4	1.50	0.18
WC6	2/20/2010	576.0	1.45	0.17
WC6	3/28/2010	577.4	1.46	0.18
WC6	4/27/2010	602.4	1.53	0.19
WC6	5/31/2010	795.4	1.94	0.25
WC6	7/6/2010	688.1	1.70	0.22
WC6	7/28/2010	694.1	1.79	0.23
WC6	8/26/2010	612.4	1.61	0.21
WC6	9/26/2010	592.9	1.57	0.20
WC7	8/28/2009	997.1	6.49	0.35
WC7	9/15/2009	973.6	6.21	0.32

WC7	10/5/2009	993.1	6.21	0.32
WC7	10/29/2009		6.36	0.33
WC7	12/7/2009	1018.6	5.42	0.22
WC7	1/21/2010	1030.1	5.48	0.22
WC7	2/20/2010	1004.9	5.54	0.24
WC7	3/28/2010	1027.9	5.69	0.23
WC7	4/27/2010	1050.7	5.98	0.28
WC7	5/31/2010	1054.2	6.57	0.34
WC7	7/6/2010	1067.2	6.71	0.36

Table B3.3. Conductivity, pH, water temperature, alkalinity, and cave air CO_2 concentration for drip sites.

Site	Date	Conductivity (µS)	pH	Water temperature (Celsius)	Alkalinity (ppm)	Cave air CO_2 (ppm)
WC1	7/3/2009	xx	xx	xx	xx	xx
WC1	8/28/2009	747.7	7.96	30.5	xx	xx
WC1	9/15/2009	722.8	8.21	26.5	xx	457
WC1	10/5/2009	758	8.23	22.3	xx	477
WC1	10/29/2009	702.5	8.16	22.8	413.6	411
WC1	12/7/2009	726.2	8.16	16.3	434.3	488
WC1	1/21/2010	724.5	8.1	19.3	413.3	432
WC1	2/20/2010	710.1	8.42	17.5	xx	466
WC1	3/28/2010	718.4	8.31	24.6	xx	446
WC1	4/27/2010	729.3	8.49	19.1	xx	385
WC1	5/31/2010	706.3	8.44	22.5	xx	425
WC1	7/6/2010	732.7	8.42	25.3	xx	547
WC1	7/28/2010	xx	xx	xx	388.2	454
WC1	8/26/2010	773	8.14	23.8	446.8	497
WC1	9/26/2010	773.9	8.13	18.7	423.8	425
WC3	7/3/2009	xx	xx	xx	xx	xx
WC3	8/28/2009	747.7	7.96	30.5	xx	432
WC3	9/15/09	xx	xx	xx	xx	501
WC3	10/5/2009	xx	xx	xx	xx	467
WC3	10/29/2009	767.9	8.44	24.8	xx	415
WC3	12/7/2009	664.5	8.57	14.6	xx	510
WC3	1/21/2010	639.2	8.47	18.2	xx	442
WC3	2/20/2010	649.3	8.43	18.6	xx	452
WC3	3/28/2010	686.4	8.25	23.4	xx	475
WC3	4/27/2010	693.1	8.54	19.5	xx	394
WC3	5/31/2010	xx	8.56	24	xx	423
WC3	7/6/2010	674.4	8.55	26	xx	638
WC3	7/28/2010	xx	xx	xx	xx	443
WC3	8/26/2010	712.1	8.52	24	xx	462
WC3	9/26/2010	755.2	8.3	18.7	xx	454
WC4	8/28/2009	xx	xx	xx	xx	432
WC4	9/15/2009	xx	xx	xx	xx	501
WC4	10/5/2009	733.8	8.54	23.6	xx	467
WC4	10/29/2009	722.7	8.19	23.2	xx	415

WC4	12/7/2009	726.8	8.37	14.4	xx	510
WC4	1/21/2010	702.5	8.23	18.9	xx	442
WC4	2/20/2010	700	8.48	17.4	xx	452
WC4	3/28/2010	700.2	8.3	22.7	xx	475
WC4	4/27/2010	716.5	8.52	19.5	xx	394
WC4	5/31/2010	673.9	8.52	24.1	xx	423
WC4	7/6/2010	629.5	8.58	24.6	xx	638
WC4	7/28/2010	xx	xx	xx	xx	443
WC4	8/26/2010	462	8.52	24	xx	462
WC4	9/26/2010	759.1	8.35	19.3	xx	454
WC5	8/28/2009	709.2	8.21	27.8	xx	432
WC5	9/15/2009	743	8.31	25	xx	501
WC5	10/5/2009	732.8	8.65	21.7	xx	467
WC5	10/29/2009	706.9	8.42	23.4	xx	415
WC5	1/21/2010	xx	xx	xx	xx	442
WC5	2/20/2010	xx	xx	xx	xx	452
WC5	3/28/2010	xx	xx	xx	xx	475
WC5	4/27/2010	714.5	8.58	20.2	xx	394
WC5	5/31/2010	654.4	8.56	24.1	xx	423
WC5	7/6/2010	662	8.48	25.2	xx	638
WC6	8/28/2009	693.4	8.01	28.2	381.6	432
WC6	9/15/2009	652.1	8.73	22.3	374.5	501
WC6	10/5/2009	666.1	8.57	22.8	392.6	467
WC6	10/29/2009	668.2	8.22	23.4	385.8	415
WC6	12/7/2009	677.1	8.22	15.4	372.5	510
WC6	1/21/2010	660.5	8	17.6	389.4	442
WC6	2/20/2010	683.6	8.17	17.8	360.6	452
WC6	3/28/2010	696.1	8.14	16.3	xx	475
WC6	4/27/2010	700.2	8.28	15	xx	394
WC6	5/31/2010	616.8	8.16	23.5	358.7	423
WC6	7/6/2010	673.5	8.26	24.7	xx	638
WC6	7/28/2010	655.3	8.22	24.8	454.6	443
WC6	8/26/2010	728	8.15	23.6	419.9	462
WC6	9/26/2010	727.6	8.1	16.8	412.4	454
WC7	8/28/2009	xx	8.55	28.4	xx	432
WC7	9/15/2009	xx	xx	xx	xx	501
WC7	10/5/2009	697.8	8.52	22.7	xx	467
WC7	10/29/2009	841	8.53	23.9	xx	415
WC7	12/7/2009	xx	xx	xx	xx	510

WC7	1/21/2010	668.1	8.52	18.8	xx	442
WC7	2/20/2010	xx	xx	xx	xx	452
WC7	3/28/2010	xx	xx	xx	xx	475
WC7	4/27/2010	xx	xx	xx	xx	394
WC7	5/31/2010	xx	8.66	23.4	xx	423
WC7	7/6/2010	xx	xx	xx	xx	638

Table B3.4. Effective rainfall, PDSI and monthly rainfall for the Austin, TX area.

Month	Rainfall (in)	Effective rainfall (in)	PDSI	Average monthly surface air temperature (Celsius)
7/3/2009	2.48	-7.42	-5.85	30.6
7/28/2009	1.14	-5.99	-6.37	32.2
8/28/2009	0.20	-9.22	-6.51	32.1
9/15/2009	4.67	3.75	0.58	27.6
10/5/2009	3.79	6.70	1.71	25.7
10/29/2009	10.14	1.01	2.31	20.3
12/7/2009	5.18	0.80	2.86	14.4
1/21/2010	3.33	1.21	3.16	9.0
2/20/2010	2.51	-0.32	3.66	9.3
3/28/2010	4.37	-3.23	3.45	13.5
4/27/2010	1.33	-4.67	2.96	20.0
5/31/2010	1.91	-4.46	2.44	25.7
7/6/2010	5.75	-2.78	2.36	28.9
7/28/2010	1.04	-8.33	3.05	29.4
8/26/2010	0.57	2.51	2.20	31.5
9/26/2010	7.59	-7.42	3.10	27.9

Table B3.5. Major anions and cations for charge balances.

Site	Date	Alk	Cl	NO_3	SO_4	F	Br	anions
WC 1	10/26/2009	413.6	19.5	3.3	16.9	0.41	0.09	-7.93
WC 1	12/7/2009	434.3	18.7	1.8	17.5	0.38	0.09	-8.24
WC 6	9/15/2009	374.5	20.6	0.3	17.6	0.41	0.11	-7.30
WC 6	10/26/2009	385.8	20.6	1.2	17.9	0.41	0.11	-7.51
WC 6	1/21/2010	389.4	20.2	1.3	17.2	0.43	0.10	-7.53
WC 6	5/30/2010	358.7	21.7	0.8	18.2	0.42	0.11	-7.10

Site	Date	Na	K	Ca	Mg	Si	cations	Charge balance
WC 1	10/26/2009	10.6	1.0	111.6	29.8	5.9	8.93	5.92
WC 1	12/7/2009	10.8	1.0	105.7	31.4	6.1	8.80	3.25
WC 6	9/15/2009	13.9	1.1	79.6	34.5	5.5	7.83	3.54
WC 6	10/26/2009	13.5	1.2	90.4	33.8	6.0	8.34	5.23
WC 6	1/21/2010	11.0	1.0	86.8	32.9	5.6	7.95	2.65
WC 6	5/30/2010	12.1	1.1	76.0	36.4	7.3	7.87	5.14

Table B3.7. Statistical relationships between trace elements and average monthly surface air temperature. The +/- of β represents the direction of the relationship.

Site	Mg/Ca vs. average monthly surface air temperature	Sr/Ca vs. average monthly surface air temperature	Ba/Ca vs. average monthly surface air temperature
WC-1	$r^2 = 0.40$, $p = 0.01$ ($\beta = 0.63$)	$r^2 = 0.42$, $p < 0.05$ ($\beta = 0.65$)	$r^2 = 0.74$, $p < 0.0001$ ($\beta = 0.86$)
WC-3	$r^2 = 0.02$, $p = 0.32$	$r^2 = 0.43$, $p < 0.01$ ($\beta = 0.65$)	$r^2 = 0.82$, $p < 0.0001$ ($\beta = 0.91$)
WC-4	$r^2 = 0.29$, $p < 0.05$ ($\beta = 0.54$)	$r^2 = 0.26$, $p < 0.05$ ($\beta = 0.51$)	$r^2 = 0.30$, $p < 0.05$ ($\beta = 0.55$)
WC-5	$r^2 = 0.007$, $p = 0.47$	$r^2 = 0.01$, $p = 0.40$	$r^2 = 0.57$, $p < 0.01$ ($\beta = 0.76$)
WC-6	$r^2 = 0.25$, $p < 0.05$ ($\beta = 0.50$)	$r^2 = 0.43$, $p < 0.001$ ($\beta = 0.66$)	$r^2 = 0.72$, $p < 0.0001$ ($\beta = 0.85$)
WC-7	$r^2 = 0.01$, $p = 0.39$	$r^2 = 0.84$, $p = 0.001$ ($\beta = 0.91$)	$r^2 = 0.86$, $p < 0.0001$ ($\beta = 0.93$)

Table B3.8. Statistical relationships between trace elements and average water temperature. The +/- of β represents the direction of the relationship.

Site	Mg/Ca vs. average water temperature	Sr/Ca vs. average water temperature	Ba/Ca vs. average water temperature
WC-1	$r^2 = 0.21$, $p = 0.05$ ($\beta = +$)	$r^2 = 0.34$, $p < 0.05$ ($\beta = +$)	$r^2 = 0.71$, $p < 0.001$ ($\beta = +$)
WC-3	xx	$r^2 = 0.73$, $p < 0.001$ ($\beta = +$)	$r^2 = 0.60$, $p = 0.001$ ($\beta = +$)
WC-4	$r^2 = 0.36$, $p = 0.01$ ($\beta = +$)	$r^2 = 0.33$, $p < 0.05$ ($\beta = +$)	$r^2 = 0.23$, $p < 0.05$ ($\beta = +$)
WC-5	xx	xx	$r^2 = 0.47$, $p < 0.05$ ($\beta = +$)
WC-6	$r^2 = 0.30$, $p < 0.01$ ($\beta = +$)	$r^2 = 0.42$, $p < 0.01$ ($\beta = +$)	$r^2 = 0.61$, $p < 0.001$ ($\beta = +$)
WC-7	xx	$r^2 = 0.72$, $p < 0.001$ ($\beta = +$)	$r^2 = 0.75$, $p < 0.001$ ($\beta = +$)

Table B3.9. Statistical relationships between trace element ratios, drip rate, and effective precipitation. The +/- of β represents the direction of the relationship.

Site	Sr/Ca vs. drip rate	Sr/Ca vs. effective rainfall	Mg/Ca vs. drip rate	Mg/Ca vs. effective rainfall
WC-1	$r^2 = 0.03$, $p = 0.28$	$r^2 = 0.03$, $p = 0.28$	$r^2 = 0.02$, $p = 0.32$	$r^2 = 0.27$, $p < 0.05$ ($\beta = -0.52$)
WC-3	$r^2 = 0.30$, $p < 0.05$	$r^2 = 0.04$, $p = 0.27$	$r^2 = 0.04$, $p = 0.26$	$r^2 = 0.16$, $p = 0.09$
WC-4	$r^2 = 0.04$, $p = 0.24$	$r^2 = 0.07$, $p = 0.18$	$r^2 = 0.68$, $p < 0.001$ ($\beta = -0.82$)	$r^2 = 0.52$, $p < 0.005$ ($\beta = -0.72$)
WC-5	$r^2 = 0.07$, $p = 0.24$	$r^2 = 0.09$, $p = 0.40$	$r^2 = 0.33$, $p = 0.05$ ($\beta = -0.58$)	$r^2 = 0.006$, $p = 0.44$
WC-6	$r^2 = 0.06$, $p = 0.19$	$r^2 = 0.03$, $p = 0.28$	$r^2 = 0.11$, $p = 0.13$	$r^2 = 0.05$, $p = 0.28$
WC-7	$r^2 = 0.14$, $p = 0.13$	$r^2 = 0.005$, $p = 0.42$	$r^2 = 0.42$, $p < 0.05$ ($\beta = -0.65$)	$r^2 = 0.002$, $p = 0.46$

Site	Ba/Ca vs. drip rate	Ba/Ca vs. effective rainfall	Drip rate vs. effective rainfall
WC-1	$r^2 = 0.04$, $p = 0.25$	$r^2 = 0.23$, $p < 0.05$ ($\beta = -0.48$)	$r^2 = 0.05$, $p = 0.28$
WC-3	$r^2 = 0.00$, $p = 0.50$	$r^2 = 0.006$, $p = 0.40$	$r^2 = 0.32$, $p < 0.05$ ($\beta = -0.57$)
WC-4	$r^2 = 0.002$, $p = 0.45$	$r^2 = 0.03$, $p = 0.27$	$r^2 = 0.74$, $p < 0.001$ ($\beta = -0.48$)
WC-5	$r^2 = 0.84$, $p < 0.001$ ($\beta = 0.92$)	$r^2 = 0.04$, $p = 0.30$	$r^2 = 0.02$, $p = 0.30$
WC-6	$r^2 = 0.001$, $p = 0.46$	$r^2 = 0.01$, $p = 0.37$	$r^2 = 0.01$, $p = 0.35$
WC-7	$r^2 = 0.21$, $p = 0.09$	$r^2 = 0.003$, $p = 0.43$	$r^2 = 0.00$, $p = 0.48$

Table B3.10. Statistical relationships between trace element ratios and PDSI as well as between PDSI and drip rate. The +/- of β represents the direction of the relationship.

Site	Mg/Ca vs. PDSI	Sr/Ca vs. PDSI	Ba/Ca vs. PDSI	PDSI vs. drip rate
WC-1	$r^2 = 0.33$, $p < 0.05$ ($\beta = -0.57$)	$r^2 = 0.50$, $p < 0.005$ ($\beta = -0.71$)	$r^2 = 0.41$, $p < 0.005$ ($\beta = -0.64$)	$r^2 = 0.007$, $p = 0.39$
WC-3	$r^2 = 0.09$, $p = 0.17$	$r^2 = 0.69$, $p < 0.001$	$r^2 = 0.16$, $p = 0.09$	$r^2 = 0.50$, $p < 0.005$ ($\beta = 0.71$)
WC-4	$r^2 = 0.07$, $p = 0.19$	$r^2 = 0.48$, $p < 0.005$ ($\beta = -0.69$)	$r^2 = 0.25$, $p < 0.05$ ($\beta = -0.50$)	$r^2 = 0.34$, $p < 0.05$ ($\beta = 0.58$)
WC-5	$r^2 = 0.03$, $p = 0.33$	$r^2 = 0.16$, $p = 0.13$	$r^2 = 0.27$, $p = 0.06$	$r^2 = 0.45$, $p < 0.005$ ($\beta = -0.67$)
WC-6	$r^2 = 0.01$, $p = 0.35$	$r^2 = 0.05$, $p = 0.21$	$r^2 = 0.15$, $p = 0.09$	$r^2 = 0.01$, $p = 0.37$
WC-7	$r^2 = 0.17$, $p = 0.12$	$r^2 = 0.20$, $p = 0.08$	$r^2 = 0.27$, $p = 0.05$ ($\beta = -0.50$)	$r^2 = 0.52$, $p < 0.005$ ($\beta = -0.72$)

APPENDIX C- LAB CLEANING PROCEDURES, PLATE PROCEDURES, ALKALINITY PROCEDURES

PRE-CLEANING

Non-acid cleaning

Items that require non-acid cleaning include: glass vials, 15 ml plastic bottles for anion collection, plates, plate holders/jewel cases.
Procedure:

- Put small items into larger container, and fill with DIST and a cap full of micro, let sit overnight.
- Rinse three to four times with DIST, let sit overnight
- Rinse three times with DI, let sit overnight
- Drain, and set items out in drying hood

Acid cleaning

Items that require non-acid cleaning include: 30 ml plastic vials for Sr isotope collection, 15 ml plastic bottles for cation collection.
Procedure:

- Put small items into larger container, and fill with DIST and a cap full of micro, let sit overnight.
- Rinse three to four times with DIST, let sit overnight
- Drain, and add HNO3, let sit overnight
- Use a funnel and a pouring lid to pour acid back into its container
- Rinse three times with DI, let sit overnight
- Drain, and set items out in drying hood

Collection bottles

Collection bottles are specific to a site, and the caps and body of the bottle should be labeled with the site name. Take care not to swap caps between bottles. Clean using the following procedure:

- Pre-wash bottles in cave closest sink before bringing them into the clean lab. This consists of rinsing the bottles, and ensuring that there is no mud on the bottles.
- In the clean lab, put all the bottles in the sink and rinse thoroughly with DIST.
- Rinse each bottle three times with DIST, let sit overnight.
- Rinse each bottle three times with DI, let sit overnight.

- Set out to dry in the drying hood, with caps slightly offset.

PLATES

Sanding

- Take the glass squares to the sandblasting machine in the basement.
- Put ~five plates into the enclosure, and shut the lid. If the sandblasting machine does not make a hissing noise with the top closed, make sure that the compressed gas is turned on (or find Roger to help).
- Put your hands in the gloves, and turn on the sand with the foot peddle.
- With the plates stack, frost all the edges at once.
- One plate at a time, frost a single face of the plate until all the shine is gone.
- Make sure the frost is even on the face, and that there are no remaining sharp edges.

Washing

Pre-wash

- Take the sandblasted plates to the 4th floor rock-sawing lab, 4.134.
- Scrub them with the brush next to the sink, some micro from the squirt bottle, and distilled water from the tap.
- Transfer the plates from the "dirty" tupperware into the "clean" one.
- Make sure to rinse the sink out thoroughly when you are done.

Clean lab wash

- Take the plates in the "clean" tupperware into the clean lab.
- Use the large white non-acid bin marked "plate cleaning" and a CD rack.
- Set the CD rack in the bin and the plates in the rack so that they don't lie against each other.
- Follow the normal non-acid cleaning procedure - micro, distilled, DI water - make sure to rinse each plate and the rack separately between each cleaning step.
- Set the plates out to dry in the drying hood.

Weighing

- Weigh the standard plate five times at the beginning and end of your weighing session (be careful with this plate, we base the weights of all the other plates on the weight of this one).
- Weigh each new plate three times.
- Refer to Banner et al. (2007) for a more detailed weighing procedure.

In the cave

Placing

- At the drip site, place the plates sandblasted side up.
- The drip should land in the center of the plate.
- At slow sites, the plate should be slightly tilted so that the drip runs off the plate.
- At all other sites, the plates should be close to level; use a small bubble level to ensure that this is the case.

Collecting

- Pick up the plate carefully and rinse it with DI water, blotting one corner with a kimwipe to collect excess water.
- Set the plate calcite/sandblasted side up in the plate carrier labeled for that site.
- Pack the plate carrier carefully in the bucket/supply tote so that it won't bang around or get tilted.

Quality control

We collect two samples per cave for data quality assessment purposes, a blank and a replicate.

- For a replicate, simply fill two bottle kits at one site (usually a faster dripping site).
- For a blank, bring along a 250 ml or a one liter bottle of DI to the cave and use it to fill a bottle kit at a site in the cave.
    - For sites where a collection bottle is left out, uncap the DI and place it where no water will drip into it. Leave it for the same amount of time that your sample bottle is left uncapped.

Bibliography

Alley, W.M. 1984. The Palmer Drought Severity Index: Limitations and assumptions, Journal of Climate and Applied Meteorology, v. 23, 1100–1109.

Amundson, R.G., and Smith, V.S. 1988. Annual cycles of physical and biological properties in an uncultivated and irrigated soil in the San Joaquin Valley of California. Agriculture, Ecosystems, and Environment, v. 20, 195-208.

Baker, A., Fuller, L., Genty, D., Fairchild, I.J., Jex, C. and Smith, C.L. 2008. Annually laminated stalagmites: A review. International Journal of Speleology, v. 37, 193-206.

Baldini, J.U.L., McDermott, F., Fairchild, I.J. 2006. Spatial variability in cave drip water hydrochemistry: Implications for stalagmite paleoclimate records. Chemical Geology, v. 235, 290–304.

Banner, J. L., and Hanson, G. N. 1990. Calculation of simultaneous isotopic and trace-element variations during water-rock interaction with applications to carbonate diagenesis. Geochimica et Cosmochimica Acta, v. 54, 3123-3137.

Banner, J.L. 1995. Application of the trace element and isotope geochemistry of strontium to studies of carbonate diagenesis. Sedimentology, v. 42, 805-824.

Banner, J.L., Musgrove, M., Asmerom, Y., Edwards, R.L., Hoff, J.A. 1996. High resolution temporal record of Holocene ground-water chemistry: Tracing links between climate and hydrology. Geology, v. 24, p. 1049-1053.

Banner, J.L., Guilfoyle, A., James, E.W., Stern, L.A., Musgrove, M. 2007. Seasonal variations in modern speleothem calcite growth in central Texas, U.S.A. Journal of Sedimentary Research, v. 77, p. 615-622.

Banner, J. L., Jackson, C. S., Zong-Liang, Y., Hayhoe, K., Woodhouse, C., Gulden, L., Jacobs,K., North, G., Leung, R., Washington, W., Jiang, X., Casteel, R. 2010. Climate change impacts on Texas water: a white paper assessment of the past, present and future and recommendations for action. Texas Water Journal, v. 1, 1-24.

Beck, J.W., Edwards, R.L., Ito, E., Taylor, F.W., Recy, J., Rougetie, F., Joannot, P. and Henin, C. 1992. Sea-surface temperature from coral skeletal strontium/calcium ratios. Science, v.257, 644-647.

Beck, J.W., Recy, J., Taylor, F.W., Edwards, R.L., and Cabioch, G. 1997. Abrupt changes in early Holocene tropical sea surface temperature derived from coral record. Nature, v.385, 705-707.

Borken, W., Xu, Y. J., Brumme, R. and Lamersdorf, N. 1999. A climate change scenario for carbon dioxide and dissolved organic carbon fluxes from a temperate forest soil: Drought and rewetting effects. Soil Science Society of America, v. 63, 1848–1855.

Bryant, V.M. 1969. Late Full-Glacial and Post-Glacial pollen analysis of Texas sediments. Thesis. University of Texas, Austin, TX.

Bryant, V.M. 1977. A 16,000 year pollen record of vegetational change in central Texas. Palynology, v. 1, 143-156

Bryant, V.M., and Holloway, R.W. 1985. The Late Quaternary paleoenvironmental record of Texas. In V.M. Bryant and R.W. Holloway (Editors), Pollen Records of Late Quaternary North American Sediments. American Association of Stratigraphic Palynology, Dallas, p. 39-70.

Camper, H.A. 1991. Pollen analysis of Patscke Bog, Texas. Thesis. Texas A and M Univ., College Station, TX.

Caran, S.C., 2004a. Geology and hydrology of Westcave Preserve, Travis County, Texas. Unpublished data.

Caran, S.C., 2004b. Westcave Preserve Travis County, Texas. Unpublished data.

Cleaveland, M.K., Votteler, T.H., Stahle, D., Casteel, R.C., Banner, J.L. 2011, Extended chronology of drought in south-central and west Texas. Manuscript submitted for publication.

Cohen, J. 1988. Statistical Power Analysis for the Behavioral Sciences (second ed.), Lawrence Erlbaum Associates. New York, NY.

Cook, E.R., and Pederson, N. 2011. Uncertainty, Emergence, and Statistics in Dendrochronology Dendroclimatology Developments in Paleoenvironmental Research, v. 11, part 2,77-112.

Cooke, M.J., Stern, L.A., Banner, J.L., Mack, L.E., Stafford, T.W. Jr., Toomey III, R.S. 2003. Precise timing and rate of massive late Quaternary soil denudation. Geology, v.31, 853-856.

Correge, T., Delcroix, T., Recy, J., Beck, W., Cabioch, G., Le Cornec, F. 2000. Evidence for a stronger El Nino-Southern Oscillation (ENSO) events in a mid-Holocene massive coral. Paleoceanography,v. 15, 465-470.

Cowan, B. 2010. Temporal and spatial variability of cave-air carbon dioxide in central Texas, USA. Thesis. University of Texas, Austin.

Dalquest, W.W., Roth, E. and Judd, F. 1969. The mammal fauna from Sehulze Cave, Edwards County, Texas. Bulletin of the Florida State Museum, v. 13, 206-276.

Dansgaard, W., White, J.W.C., Johnson, S.J. 1989. The abrupt termination of the Younger Dryas climate event. Nature, v. 339, 532 – 534.

De Villiers, S., Shen, G.T., Nelson, B.K. 1993. The Sr/Ca-temperature relationship in coralline aragonite: Influence of variability in $Sr/Ca_{seawater}$ and skeletal growth parameters. Geochimica et Cosmochimica Acta, v. 58, 197-208.

Duran, L., and Jay L. B. 2010. Application of Sr isotopes to tracing vadose flows paths in the Edwards Aquifer and implications for reconstructing paleoclimate. Geological Society of America, Joint Annual Meeting, Denver, CO.

Edwards, N. T. 1975. Effects of temperature and moisture on carbon dioxide evolution in a mixed deciduous forest floor. Soil Science Society of America Proceedings, v. 39, 361–365.

Ellison, Christopher R. W.; Chapman, Mark R.; Hall, Ian R. 2006. Surface and Deep Ocean Interactions During the Cold Climate Event 8200 Years Ago. Science, v. 312**,** 1929–1932.

Ellwood, B.B. and Gose, W.A. 2006. Heinrich H1 and 8200 yr B.P. climate events recorded in Hall's Cave Texas. Geology, v. 34, 753.

Fairchild, I.J., Smith, C.L., Baker, A., Fuller, L., Spotl, C., Mattey, D., McDermott, F., EIMF. 2006. Modification and preservation of environmental signals in peleothems.Earth-Science Reviews, v. 75, 105–153.

Fairchild, I.J. and Treble, P.C. 2009. Trace elements in speleothems as recorders of environmental change, Quaternary Science Reviews, v. 28, 449-468.

Feng, W., Banner, J.L., Guilfoyle, A., Musgrove, M., James, E. 2011. Oxygen isotopic fractionation between drip water and speleothem calcite: A 10-year monitoring study, central Texas, USA. In prep.

Fieseler, R., Bittinger, C., Lucas, A. 1972. Brunton and Tape Survey: Hammett's Cave, Travis County, Texas. Texas Speleological Survey. Available from: www.utexas.edu/tmm/sponsored_sites/tss/CaveMaps/index.html

Gascoyne, M. 1983. Trace-element partition coefficients in the calcite-water system and their paleoclimatic significance in cave studies. Journal of Hydrology, v. 61, 213–222.

Godfrey, C., McKee, G., S., Oakes, H., .1973. General soil map of Texas, Texas Agricultural Experimental Station, Texas A&M University, in cooperation with the Soil Conservation Service, U.S. Department of Agriculture.

Goodfriend, G.A. and Ellis, G.L. 2000. Stable carbon isotope record of middle to late Holocene climate changes from land snail shells at Hinds Cave, Texas. Quaternary International, v. 67, 47-60.

Graham, R.W. 1976. Pleistocene and Holocene mammals, taphonomy, and paleoecology of the Friesenhahn Cave local fauna, Bexar County, Texas. Thesis. University of Texas, Austin, TX.

Guilfoyle, AL. 2006. Temporal and Spatial Controls on Cave Water and Speleothem Calcite Isotopic and Elemental Chemistry, Central Texas. Thesis. University of Texas, Austin.

Hall, E.R. 1981. Mammals of North America. Wiley, New York, 1, 2nd ed., 600 pp.

Hall, S.A. 1985. Quaternary pollen analysis and vegetational history of the southwestern overview. In: V.M. Bryant and R.W. Holloway (Editors), Pollen Records of Late Quaternary North American Sediments. Am. Assoc. Stratigr. Palynol., Dallas, pp. 95-124.

Hall, S.A. 1988. Environment and archaeology of the Central Osage Plains. Plains Anthropology, v. 33, 203-218.

Hall, S.A. 1990. Channel trenching and climatic change in the southern U.S. Great Plains. Geology, v. 18, 342-345.

Hall, S.A. 1991. Late glacial grassland at the Aubrey Clovis site, North Texas: the pollen evidence. Annual Meeting South central/Rocky Mount section. Geological Society of America. Abstracts with Programs, 23, p. 29.

Hall, S.A., 1992, Late Quaternary vegetation and climate of the northwest Gulf Coastal Plain. Annual Meeting South central section. Geological Society of America. Abstracts with Programs, 24, p. 13.

Hatfield, T.H. 1964. The Texas Drought of 1950-1956. Thesis. University of Texas at Austin.

Holliday, V.T. 1989. Middle Holocene drought on the Southern High Plains. Quaternary Research, v. 31, 74-82.

Huang, Y., Fairchild, I.J. 2001. Partitioning of Sr^{2+} and Mg^{2+} into calcite under karst analogue experimental conditions. Geochimica et Cosmochimica Acta, v. 65, 47–62.

Huebner, J.A. 1991. Late Prehistoric bison populations in central and southern Texas. Plains Anthropology, v. 36, 343-358.

IPCC [Intergovernmental Panel on Climate Change]. 2007. Climate Change 2007 – Impacts, Adaptation and Vulnerability. Contribution of Working Group II to the Fourth Assessment Report of the Intergovernmental Panel on Climate Change. Parry ML, Canziani OF, Palutikov PJ, van der Linden PJ, Hanson CE, editors. Cambridge: Cambridge University Press. 476 p.

Jasek, J. 2001. Map of Inner Space Caverns. Texas Speleological Society. Available from: http://www.utexas.edu/tmm/sponsored_sites/tss/CaveMaps/mapimages/innerspace.gif.

Kastning, EH. 1983. Geomorphology and Hydrogeology of the Edwards Plateau Karst, Central Texas. Dissertation. University of Texas, Austin.

Katz, A. 1973. The interaction of magnesium with calcite during crystal growth at 25–95 °C and one atmosphere. Geochimica et Cosmochimica Acta, v. 36, 481–496.

Kjelgaard, J.F., Heilman, J.L., McInnes, K.J., Owens, M.K., Kamps, R.H. 2008. Carbon dioxide exchange in a subtropical, mixed C3/C4 grassland on the Edwards Plateau, Texas. Agricultural and Forest Meteorology, v. 148, 953-963.

Kowalenko, C. G. and Ivarson, K. C. 1978. Effect of moisture content, temperature and nitrogen fertilization on carbon dioxide evolution from field soils. Soil Biology and Biochemistry, v. 10, 417–423.

LCRA. 2007. Heinz Branch Watershed to Westcave Preserve. Retrieved July 2011 from: http://maps.lcra.org/default.aspx?MapType=Watershed%20Posters.

Larkin, D.A. and Bomar, G.W. 1983. Climatic Atlas of Texas, Texas Department of Water Resources, Austin, TX.

Lorens, R.B. 1981. Sr, Cd, Mn, and Co distribution coefficients in calcite as a function of calcite precipitation rate. Geochimica et Cosmochimica Acta, v. 45, 553-561.

Lundelius Jl., E.L. 1967. Late Pleistocene and Holocene faunal history of central Texas. in: P.S. Martin and H.E. Wright (Editors), Pleistocene Extinctions: A Search for a Cause. Yale Univ. Press, New Haven, CN, pp. 287-319.

Morse, J.W., Bender, M.L. 1990. Partition coefficients in calcite- Examination of factors influencing the validity of experimental results and their application to natural systems. Chemical Geology, v. 82, 265-277.

Musgrove, M., 2000. Temporal links between climate and hydrology: Insights from central Texas cave deposits and groundwater. Dissertation. University of Texas, Austin.

Musgrove, M., Banner, J.L., Mack, L.M., Combs, D.M., James, E.W., Cheng, H., Edwards, R.L. 2001. Geochronology of late Pleistocene to Holocene speleothems from central Texas: Implications for regional paleoclimate. GSA Bulletin, v. 113, 1532-1543.

Musgrove, M. and Banner, J. L. 2004. Controls on the spatial and temporal variability of vadose dripwater geochemistry: Edwards Aquifer, central Texas, Geochimica et Cosmochimica Acta, v. 68, 1007-1020.

NOAA. 2010. Effective precipitation data source available from: http://www7.ncdc.noaa.gov/IPS/coop/coop.html;jsessionid=DAB4133A1AAEC3F714CE2B784021C5F9?_page=2&state=TX&foreign=false&stationID=413507&_target3=Next+%3E.

NOAA, 2010, Palmer Drought Severity Index. Data source available from: http://lwf.ncdc.noaa.gov/temp-and- precip/time-series/index.php?parameter=pdsi&month=8&year=2009&filter=1&state=41&div=0.

Nordt, L.C., Boutton, T.W., Hallmark, C.T., Waters, M.R. 1994. Late Quaternary vegetation and climate changes in central Texas based on the isotopic composition of organic carbon. Quaternary Research, v. 41, 109-120.

Palmer WC. 1965. Meteorological drought. Washington DC: Department of Commerce Weather Bureau. Research Paper No. 45.

Pape J. R., Banner J. L., Mack L. E. , Musgrove M., Guilfoyle A. 2010. Controls on oxygen isotope variability in precipitation and cave drip waters, central Texas, USA. Journal of Hydrology, v. 385, 203–215.

Parkhurst, D.L. and Appelo, C.A.J. 1999. User's guide to PHREEQC (Version 2)—A computer program for speciation, batch-reaction, one-dimensional transport, and inverse geochemical calculations: U.S. Geological Survey Water-Resources Investigations Report

Pierson, S.J., Banner, J.L., Musgrove, M., Mack, L. 2005. Delineating flowpaths in the unsaturated zone of a karst aquifer; Sr isotope constraints. Abstracts with Programs - Geological Society of America, v. 37, p. 435.

Plummer L. N. 1977. Defining reactions and mass transfer in part of the Floridan Aquifer. WaterResources Res, v. 13, 801–812.

Porter, S.C. 1983. Introduction, In: H.E. Wright and S.C. Porter (Editors), Late-Quaternary Environments of the United States: Volume 1, The Late Pleistocene. University of Minnesota.

Rastogi, M., Singh, S., and Pathak, H. 2002. Emission of carbon dioxide from soil. Current Science, v. 82.

Reddell, A.R., and Smith, J. 1961. Brunton and Tape Survey: Hammett's Cave, Travis County, Texas. Texas Speleological Survey. Available from: www.utexas.edu/tmm/sponsored_sites/tss/CaveMaps/index.html.

Riggio, R.R., Bomar, G.W., and Larkin, T.J. 1987. Texas Drought: Its Recent History (1931- 1985). Texas Water Commission, LP 87-04.

Roberts, M.S., Smart, P., Baker, A. 1998. Annual trace element variations in a Holocene speleothem. Earth and Planetary Science Letters, v. 154, 237–246.

Shen, C. C., Lee, T., Chen, C.Y., Wang, C.H., Dai, C.F., Li, L.A. 1996. The calibration of *D*[Sr/Ca] versus sea surface temperature relationship for *Porites* corals. Geochimica et Cosmochimica Acta, v. 60, 3849-3858.

Smart, P.L. & Friederich, H. 1987. Water movement and storage in the unsaturated zone of a maturely karstified aquifer, Mendip Hills, England, Proceedings of the

Environmental Problems in Karst Terrains and Their Solutions Conference, p. 57-87, NWWA, Bowling Green, KY.

Spaulding, W.G., Leopold, E.B. and Van Devender, T.R. 1983. Late Wisconsin paleoecology of the American Southwest. In: H.E. Wright and S.C. Porter (Editors), Late Quaternary Environments of the United States. I. The Pleistocene. Univ. Minnesota Press, Minneapolis, pp. 259-293.

Stoll, H.M., Klaas, C.M., Probert, I. 2002. Calcification rate and temperature effects on Sr partitioning in coccoliths of multiple species of coccolithophroids in culture. Global and Planetary Change, v. 34, 153-171.

Stahle, D.W. and Cleaveland, M.K. 1988. Texas Drought History Reconstructed and Analyzed from 1698 to 1980. Journal of Climate, v. 1, 59-74.

Tesoriero, A.J., Pankow, J.F. 1996. Solid solution partitioning of Sr^{2+}, Ba^{2+}, and Cd^{2+} to calcite. Geochimica et Cosmochimica Acta, v. 60, 1053-1063.

Toomey III, R.S. 1991. Climatic tolerances and the significance of Late Pleistocene "disharmonius" vertebrate assemblages. Annual Meeting of the Geological Society of America. Abstracts with programs, 23, p. 97.

Toomey III, R.S. 1992. Central Texas climates and environments, 25,000 yrs BP to present: the vertebrate evidence. Annual Meeting South central section. Geological Society of America. Abstracts with Programs, v. 24, p. 49.

Toomey, R.S., Blum, M.D., Valastro, S. 1993. Late Quaternary climates and environments of The Edwards Plateau, Texas. Global and Planetary Change, v. 7, 299-320.

USDA NRCS, U.S. Department of Agriculture National Resources Conservation Service (Internet). Portland (OR): Water and Climate Center of the Natural Resources Conservation Service. (cited 2011 August 01). Available from: http://www.wcc.nrcs.usda.gov/climate/prism.html

Veni, G. 1994. Geomorphology, Hydrogeology, Geochemistry and Evolution Of the Karstic Lower Glen Rose Aquifer, South-Central Texas. Dissertation. University of Texas, Austin.

Wiant, H. V. Jr. 1967. Influence of temperature on the rate of soil respiration. Journal of Forestry, v. 65, 489–490.

Wong, C. 2008. Geochemical evolution of karst vadose water and brush clearing

impacts on recharge in central Texas. Thesis. University of Texas, Austin.

Wong, C.I., Banner, J.L., Musgrove, M. 2011. Seasonal dripwater Mg/Ca and Sr/Ca variations driven by cave ventilation: Implications for modeling of speleothem paleoclimate records. Geochimica et Cosmochimica Acta, v. 74, 3514-3529.